



SCHOOL OF ELECTRICAL AND ELECTRONIC ENGINEERING  
ELECTRIC POWER SYSTEMS RESEARCH GROUP

---

# QUANTIFYING THE BENEFITS AND RISKS OF REAL-TIME THERMAL RATINGS IN ELECTRICAL NETWORKS

---

A THESIS PRESENTED FOR THE DEGREE OF DOCTOR OF PHILOSOPHY

DAVID MICHAEL GREENWOOD

JULY 2014

## Abstract

Real-Time Thermal Rating (RTTR) is a technology that allows the rating of electrical conductors to be estimated using real-time, local weather conditions. In many cases this leads to an increased rating with respect to conventional approaches. It also identifies some instances in which the conventional, static, rating is greater than the true rating, and is therefore potentially unsafe.

The work in this thesis comprises methodologies to improve the planning and implementation of RTTR. Techniques commonly employed in the wind energy industry have been modified for use with RTTR. Computational wind simulations were employed to allow the identification of determining conductor spans, to inform network designers of the rating potential of different conductor routes, to estimate the additional wind energy that could be accommodated through the enhanced line rating and to allow informed placement of the monitoring equipment required to implement RTTR. Furthermore, the wind simulation data were also used to allow more accurate estimation of conductor ratings during operation. Probabilistic methods have been devised to estimate the level of additional load that could be accommodated through RTTR, and quantify the risk in doing so. Finally, a method has been developed to calculate the benefit RTTR can provide to system wide reliability. State sampling and sequential Monte Carlo simulations were used to evaluate the probabilistic functions associated with the ratings, the load and failures on both the existing network and the RTTR system itself.

These methods combine to address fundamental barriers to the wide scale adoption and implementation of RTTR. The majority of existing research has focussed on improving technical solutions, which are of little benefit if it is not possible to quantify the benefits of RTTR before it is implemented. This work allows quantification not only of those benefits, but of the associated risks and uncertainties as well.

## Declaration

I hereby declare that this thesis is a record of work undertaken by myself, that it has not been the subject of any previous application for a degree, and that all sources of information have been duly acknowledged.

© Copyright 2014, David Greenwood

Parts of this thesis have been published by the author:

### CHAPTER 3

---

D. M. Greenwood, P. C. Taylor, “Unlocking the Benefits of Real-Time Thermal Ratings through Probabilistic Power Network Planning”, IET Generation, Transmission and Distribution, 2014, DOI: [10.1049/iet-gtd.2014.0043](https://doi.org/10.1049/iet-gtd.2014.0043)

*This paper is a postprint of a paper submitted to and accepted for publication in IET Generation, Transmission & Distribution and is subject to Institution of Engineering and Technology Copyright. The copy of record is available at IET Digital Library*

### CHAPTER 6

---

D. M. Greenwood, P. C. Taylor, “Investigating the Impact of Real-Time Thermal Ratings on Power Network Reliability”, IEEE Transactions on Power Systems, 2014, DOI: [10.1109/TPWRS.2014.2305872](https://doi.org/10.1109/TPWRS.2014.2305872)

*© 2014 IEEE. Personal use of this material is permitted. Permission from IEEE must be obtained for all other uses, in any current or future media, including reprinting/republishing this material for advertising or promotional purposes, creating new collective works, for resale or redistribution to servers or lists, or reuse of any copyrighted component of this work in other works.*

*Science is about what is; engineering is about what can be.*

-Neil Armstrong

*“Be proud of your mistakes. Well, proud may not be exactly the right word, but respect them, treasure them, be kind to them, learn from them. And, more than that, and more important than that, make them. Make mistakes. Make great mistakes, make wonderful mistakes, make glorious mistakes. Better to make a hundred mistakes than to stare at a blank piece of paper too scared to do anything wrong...”*

-Neil Gaiman

*“Wind in the wires  
It's the sigh of wild electricity  
I'm on the edge of a cliff  
Surpassing  
Comfort and security*

*But here comes a gale  
A crippling anger  
Sea birds are blown  
Into the rocks  
Grace is lost to thunder*

*Thunder  
Pressure  
Getting  
Lower*

*But see her waters break  
Rain falling to the sea  
Into a granite wave*

*A unit  
A family*

*It's just a sigh  
Just a sigh*

*This wild electricity  
Made static by industry  
Like a bird in an aviary  
Singing to the sky  
Just singing to be free*

*To be free”*

-Patrick Wolf, Wind in the Wires

## Acknowledgements

I would like to express my gratitude to my supervisors, Professor Phil Taylor and Dr Grant Ingram. Without their help, support, expertise, faith, sarcasm, occasional verbal abuse and frequent complementary lattes, this work would have been impossible. I would also like to acknowledge the support of my industrial partners, Alan Collinson, Geoff Murphy and Diyar Kadar from Scottish Power, and Sarah Brown, Andrew Tewkesbury and Janet Wilson from Astrium GEO-Information Services.

I must, of course, acknowledge my colleagues at both Durham and Newcastle, in particular Peter Davison, Seán Norris, Peter Wyllie, Guy Hutchinson, Pádraig Lyons, Simon Blake and Iván Castro León. Special thanks to Richard Williams and Michael Hilfer for their help with CFD. Thanks must also go to the CDT in Energy and Matthias Troffaes.

I would like to thank my parents for their unwavering support, my sister Elanor for provision of overwrought drama, tragedy and occasional light relief, my brother George, and various cats and dogs.

Special thanks to Nigel Mitchell for his heroic efforts in proof reading this thesis, along with his encouragement and friendship for the last 26 years.

Massive props (also love and thanks!) to Kate Dutson, without whom I would certainly not have completed this thesis and instead would, in all likelihood, have ended up in a gutter somewhere.

Finally, I would like to acknowledge the things and people that kept me sane: Adam Chatterley, Tom Hollins, Will Dale, Ben Wilkins, Andy Summerhill, Cliff Radenski, Brad Pearce and Eddy Larkin – Bros for the Woes. Everyone at Xaos Games (Craig and John especially), Magic: the Gathering, Dinosaur Comics, the Agricola iPhone App, Dirgey Music, the Decemberists, my Kindle, Durham University Games Society, Harry Dresden, the Sandman, Games with small wooden cubes, Skippy the Skip Guitar, Olivia Carpenter, David Lomax, Andy Tattersfield, Matt Johnston, James Cable, Ian Beckett, Oliver Nicholls and Oliver Carrdus.

## List of Publications

### JOURNAL PAPERS

D. M. Greenwood, P. C. Taylor, "Investigating the Impact of Real-Time Thermal Ratings on Power Network Reliability", IEEE Transactions on Power Systems, 2014, DOI: [10.1109/TPWRS.2014.2305872](https://doi.org/10.1109/TPWRS.2014.2305872)

D. M. Greenwood, J. P. Gentle, G. L. Ingram, P. J. Davison, K. S. Myers, I. J. West, J. W. Bush, M. C. M. Troffaes, "A Comparison of Real Time Thermal Rating Systems in the U.S. and the UK", IEEE Transactions on Power Delivery, 2014, DOI: [10.1109/TPWRD.2014.2299068](https://doi.org/10.1109/TPWRD.2014.2299068)

P. J. Tavner, D. M. Greenwood, M. W. G. Whittle, R. Gindle, S. Faulstich, B. Hahn, "Study of Effect of Weather and Location on Wind Turbine Failure Rates", Vol. 16 ( 2), Wind Energy, 2013

D. M. Greenwood, P. C. Taylor, "Unlocking the Benefits of Real-Time Thermal Ratings through Probabilistic Power Network Planning", IET Generation, Transmission and Distribution, 2014, DOI: [10.1049/iet-gtd.2014.0043](https://doi.org/10.1049/iet-gtd.2014.0043)

S. Blake, P. J. Davison, D. M. Greenwood, N. Wade, "LWEC Paper 11: Energy: Power Systems, Transmission and Distribution", J. Infrastructure Asset Management, 2014 (SUBMITTED)

### CONFERENCE PROCEEDINGS

D. M. Greenwood, G. L. Ingram, P. C. Taylor, A. Collinson and S. C. Brown, "Network Planning Case Study Utilising Real-Time Thermal Ratings and Computational Wind Modelling", CIRED 2013, Stockholm, Sweden, 2013

D. M. Greenwood, Ingram, G.L., Taylor, P.C., "Improving Real-Time Thermal Ratings Using Computational Wind Simulations," in 10th Wind Integration Workshop, Aarhus, Denmark, 2011

## Acronyms

Acronym	Definition
ABL	Atmospheric Boundary Layer
AC	Alternating Current
ACSR	Aluminium Conductor, Steel Reinforced
ARMA	Auto Regressive Moving Average
BC	Boundary Condition
CCC	Current Carrying Capacity
CDF	Cumulative Distribution Function
CERL	Central Electricity Research Laboratories
CFD	Computational Fluid Dynamics
CIGRÉ	Conseil international des grands réseaux électriques
COPT	Capacity Output Probability Table
DC	Direct Current
DG	Distributed Generation
DLR	Dynamic Line Rating
DNO	Distribution Network Operator
DSR	Demand Side Response
DTR	Dynamic Thermal Rating
EENS	Expected Energy Not Supplied
FACTS	Flexible AC Transmission System
IC	Initial Condition
IEC	International Electro technical Commission
IEEE	Institute of Electrical and Electronic Engineers
IT	Information Technology
LDC	Load Duration Curve
LES	Large Eddy Simulation
LiDAR	Light Detection and Ranging
LOEE	Loss of Energy Expectation
LOL	Loss of Load
LOLE	Loss of Load Expectation
MC	Monte Carlo
MTTF	Mean Time To Failure
MTTR	Mean Time To Repair
NERC	National Electricity Reliability Corporation

NMS	Network Management System
OHL	Overhead Line
OPF	Optimal Power Flow
PDF	Probability Density Function
PFSF	Power Flow Sensitivity Factors
PLC	Power Line Carrier
PMU	Phasor Measurement Units
PUC	Public Utilities Committee
RAM	Random Access Memory
RANS	Reynolds Averaged Navier Stokes
RBTS	Roy Billinton Test System
RNG	Re-Normalization Group
RTTR	Real-Time Thermal Ratings
VoLL	Value of Lost Load
VoLLE	Value of Lost Load Expectation

---

---

## Nomenclature

$a$	Vertical distance between conductor supports	[m]
$ARMS$	Average Root Mean Squared Error	
$C$	Energy Constraint	[KWh]
$C_{pi}$	Capacity State Probability	
$D$	Conductor Diameter	[m]
$E$	Energy	[J],[KWh]
$e$	Uncertainty	
$EEENS$	Expected Energy not Supplied	[KWh]
$f$	Failure Rate	[y <sup>-1</sup> ]
$Gr$	Grashof Number	
$I$	Current	[A]
$I_{ac}$	Alternating Current	[A]
$I_{dc}$	Direct Current	[A]
$K_s$	Roughness Height	[m]
$l$	Length	[m]
$L$	Load	
$LOL$	Loss of Load	
$LOLE$	Loss of Load Expectation	
$MTTF$	Mean time to failure	[h]
$MTTR$	Mean time to repair	[h]
$Nu$	Nusselt Number	
$Nu_{90}$	Nusselt Number for Perpendicular wind flow	
$Nu_{corr}$	Corrected Nusselt Number	
$p$	Pressure	[N.m <sup>-2</sup> ]
$P$	Power	[W]
$PO$	Power Output	
$Pr$	Prandtl Number	
$q_c$	Convective Heat Exchange	[W.m <sup>-1</sup> ]

---

$q_i$	Corona Heating	[W.m <sup>-1</sup> ]
$q_m$	Magnetic Heating	[W.m <sup>-1</sup> ]
$q_r$	Radiative Heat Loss	[W.m <sup>-1</sup> ]
$q_s$	Solar Heating	[W.m <sup>-1</sup> ]
$q_w$	Evaporative Cooling	[W.m <sup>-1</sup> ]
$r$	Conductor Rating	[A]
$R$	Resistance	[Ω]
$R_{ac}$	AC Resistance	[Ω]
$\bar{r}$	Mean conductor rating	[A]
$R_{dc}$	DC resistance	[Ω]
$Re$	Reynolds Number	
$r_e$	Rating adjusted for excursion time	[A]
$R_{gc}$	Gas Constant	
$r_i$	rating state, i	
$S$	Incident solar radiation	[W.m <sup>-2</sup> ]
$s$	Conductor Sag	[m]
$S_{i,Wd}$	Speedup characteristic at point I and wind direction Wd	
$T$	Temperature	[K],[°C]
$T_a$	Ambient Temperature	[K],[°C]
$T_c$	Conductor Core Temperature	[K],[°C]
$Tm$	Persistence Time	[h]
$T_s$	Conductor Surface Temperature	[K],[°C]
$u$	X Direction Wind Vector	[m.s <sup>-1</sup> ]
$\tilde{u}$	Estimated X Direction Wind Vector	[m.s <sup>-1</sup> ]
$u^+$	Dimensionless Velocity	
$v$	Y Direction Wind vector	[m.s <sup>-1</sup> ]
$V$	Voltage	[V]
$\tilde{v}$	Estimated Y Direction Wind Vector	[m.s <sup>-1</sup> ]
$w$	Mechanical Load	[N]

---

---

$\widetilde{W}_d$	Estimated Wind Direction	[°]
$\widetilde{W}_s$	Estimated Wind Speed	[m.s <sup>-1</sup> ]
$y^+$	Dimensionless Distance	
$z_h$	Wind Turbine Hub Height	[m]
$z_a$	Conductor Height	[m]
$\alpha$	Absorptivity of Conductor Surface	
$\varepsilon$	Emissivity	
$\theta$	Angle of Incidence	[°]
$\lambda$	Mean Thermal Conductivity	[W.m <sup>-1</sup> .K <sup>-1</sup> ]
$\lambda_f$	Thermal Conductivity of Air	[W.m <sup>-1</sup> .K <sup>-1</sup> ]
$\rho$	Density	[kg.m <sup>-3</sup> ]
$\rho_a$	Density of Air	[kg.m <sup>-3</sup> ]
$\sigma_B$	Stefan Boltzmann Constant	[W.M <sup>-2</sup> .K <sup>-4</sup> ]
$\tau$	Tension	[N]

---

# Table of Contents

<b>Chapter 1. Introduction .....</b>	<b>1</b>
1.1. Background.....	2
1.2. Smart Grids .....	3
1.3. Real-Time Thermal Ratings .....	4
1.4. Conductor Thermal Ratings .....	7
1.5. Barriers to Implementation .....	18
1.6. Research Objectives .....	19
1.7. Thesis Outline .....	19
<b>Chapter 2. RTTR: The State of the Art.....</b>	<b>21</b>
2.1. Introduction.....	22
2.2. Initial Research .....	22
2.3. Modern RTTR Technologies.....	23
2.4. Operational RTTR Schemes.....	28
2.5. RTTR Applications .....	29
2.6. Forecasting RTTR .....	30
2.7. Network Planning for RTTR.....	30
2.8. Conclusion .....	31
<b>Chapter 3. Probabilistic Security of Supply.....</b>	<b>33</b>
3.1. Introduction.....	34
3.2. Review of Network Security Standards .....	34
3.3. Meteorological Data Sources.....	37
3.4. Contribution of RTTR by Evaluating EENS.....	37
3.5. Proposed Probabilistic Method .....	43
3.6. Conclusions.....	54

---

<b>Chapter 4. Wind Simulations: Modelling Approach.....</b>	<b>56</b>
4.1. Introduction.....	57
4.2. Motivation.....	57
4.3. Background.....	58
4.4. Methodology.....	63
4.5. Simulation Scheme for RTTR.....	68
4.6. CFD Validation using Bolund Hill .....	68
4.7. Conclusion .....	74
<b>Chapter 5. Wind Simulations: Applications.....</b>	<b>75</b>
5.1. Introduction.....	76
5.2. Network Planning with a CFD Wind Model .....	76
5.3. Real-Time State Estimation .....	95
5.4. Conclusions.....	104
<b>Chapter 6. Impact on Network Reliability .....</b>	<b>106</b>
6.1. Introduction.....	107
6.2. Background.....	107
6.3. Methodology.....	111
6.4. Results .....	121
6.5. Discussion .....	126
6.6. Conclusion .....	128
<b>Chapter 7. Discussion .....</b>	<b>130</b>
7.1. Introduction.....	131
7.2. Discussion .....	131
7.3. Broader Implications.....	133
7.4. Further Research .....	139
7.5. Summary .....	147

<b>Chapter 8. Conclusions .....</b>	<b>148</b>
8.1. Overview .....	149
8.2. Key Findings.....	149
8.3. Fulfilment of Research Objectives.....	150
8.4. Conclusion .....	153
<b>References.....</b>	<b>155</b>
<b>Appendix 1: CIGRÉ Ratings Code.....</b>	<b>171</b>
<b>Appendix 2: Table of Confidence Values.....</b>	<b>175</b>
<b>Appendix 3: Risk and Confidence Analysis Method .....</b>	<b>176</b>

## List of Figures

Figure 1.1: The unutilised headroom that can be exploited through the use of RTTR, compared to the seasonal ratings .....	5
Figure 1.2: The typical structure of an aluminium conductor, steel reinforced. ....	8
Figure 1.3: The variation in rating as a consequence of wind speed, wind direction, ambient temperature and solar irradiance.....	14
Figure 1.4: a curve of correlation term against excursion time.....	16
Figure 1.5: General case of a suspended conductor [24] .....	18
Figure 2.1: A comparison of calculated and measured conductor temperature for the trial site [13].. ....	26
Figure 3.1: The typical scenario considered in this chapter; a load connected by a dual circuit, supported by RTTR.....	38
Figure 3.2: The method used to determine the capacity model.....	40
Figure 3.3: The Load Duration Curve used in this study, showing how energy not supplied is evaluated [91] .....	41
Figure 3.4: The mean contribution values for the four sites considered in this study. ....	42
Figure 3.5: An illustration of the key problem in overhead line ratings. ....	44
Figure 3.6: A simple example of a Monte Carlo simulation. ....	45
Figure 3.7: The solution to the problem illustrated in Figure 3.6, showing the effect of the number of samples, $n$ .....	46
Figure 3.8: A flow chart showing the steps to evaluate confidence using Monte Carlo simulation .....	47
Figure 3.9: Plot of confidence of not exceeding ratings against contribution to security, with $T_m$ varying from 1 hour to 168 hours.....	48
Figure 3.10: Effect of data resolution on confidence levels for $T_m=3$ hours .	49
Figure 3.11: Probability density, risk density and cumulative risk plots for excursions above static seasonal ratings.....	51
Figure 3.12: Risk associated with varying contributions to security .....	52
Figure 3.13: The Risk assumed by P27 compared with the real Risk of excursion .....	53
Figure 4.1: The effect of wind speed and direction on the rating of a 132kV Lynx conductor in 10°C ambient conditions.....	57
Figure 4.2: An illustration of mesh structure, with small cells close to the boundary and larger cells at higher altitudes. ....	65
Figure 4.3: A typical velocity inlet profile for a CFD wind study.....	66

---

Figure 4.4: Sand grains on a smooth wall, and their effect on the first element height [117].....	67
Figure 4.5: Contours of Bolund hill showing the location of the ten weather masts. Masts M0 and M9 were outside the simulation domain [136] .....	69
Figure 4.6: The layout of the computational domain, showing the inlet/outlet surfaces, mesh structure and topography .....	70
Figure 4.7: Speed-up characteristics compared to measured results for 239° inlet condition. The position is equivalent to the Easting in Figure 4.5.....	72
Figure 5.1: Example of a contour plot of speed up characteristics.....	78
Figure 5.2: A flow chart illustrating the methodology for calculating average line ratings and hence identifying thermal bottlenecks and selecting new conductor routes. ....	79
Figure 5.3 : Wind direction correction factors for conductor rating.....	80
Figure 5.4: Example of mean wind direction relative to conductor location	81
Figure 5.5: A flow chart describing the method for quantifying wind farm size, constraints and energy yields .....	84
Figure 5.6: Simplified wind turbine power curve .....	85
Figure 5.7: Average point correlation with the other points in the domain.	88
Figure 5.8: Rating correlation against distance between two points .....	89
Figure 5.9: A map of the case study area showing the route corridors for potential overhead lines. ....	90
Figure 5.10: Map of annual average conductor rating as a proportion of seasonal ratings. The locations of the approved route corridors are shown on the plot. ....	91
Figure 5.11: Energy throughput map for a 120MW Wind Generator (MWh) .....	92
Figure 5.12: A map of constraints to wind generation as a proportion of the annual energy yield of a 140MW wind farm .....	93
Figure 5.13: Time series of conductor rating and line current due to the wind farm. The two follow similar trends, meaning constraints are rarely required.....	94
Figure 5.14: The complete methodology used to apply CFD results to state estimation, broken down into offline and online processes. ....	97
Figure 5.15: A map of the trial site area, showing local features and the location of the meteorological stations and conductors .....	97
Figure 5.16: The CFD set up used for the state estimation case study. The surface is shaded with contours of elevation.....	98
Figure 5.17: Wind flow results for 290° inlet condition .....	99
Figure 5.18: A Comparison of measured and simulated wind speeds .....	101
Figure 5.19: Comparison of CFD rating estimation and measured values	102

---

---

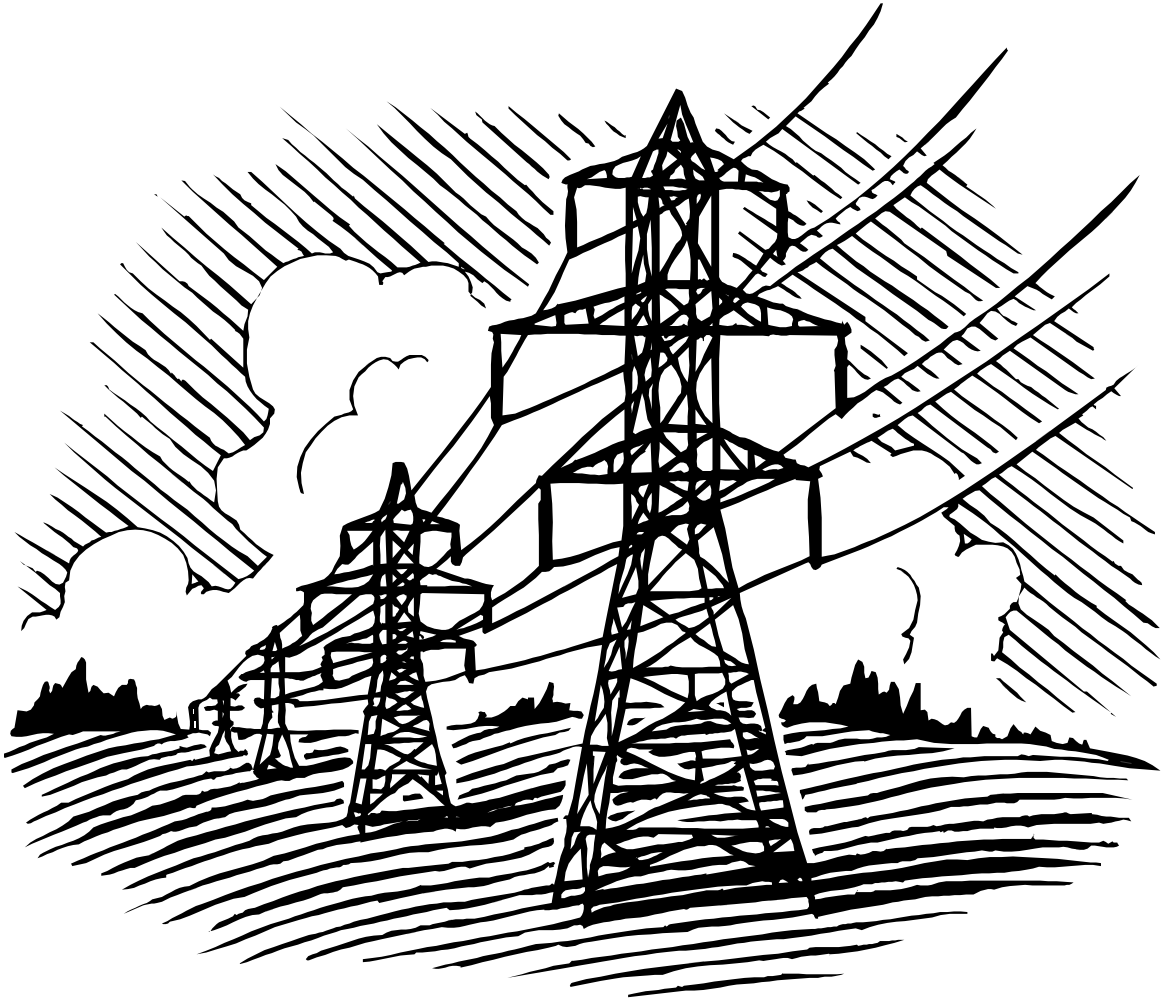
Figure 5.20: Terrain geometry compared to line rating using CFD interpolation (middle) and inverse distance interpolation (bottom) .....	104
Figure 6.1: Diagram of the test network .....	112
Figure 6.2: Plot of correlation between conductor ratings against distance between conductors .....	116
Figure 6.3: 7 sets of rating data with pre specified correlations. ....	117
Figure 6.4: Probability distribution of error in rating estimation.....	119
Figure 6.5: A Flow chart showing the complete methodology, broken into setup and simulation steps .....	120
Figure 6.6: An illustration of reliability model behaviour.....	121
Figure 6.7: LOLE in hours per year for RTTR and static ratings at different network loading conditions .....	122
Figure 6.8: The impact of correlation between ratings on network reliability. ....	123
Figure 6.9: LOLE in hours per year for RTTR with and without uncertainty. ....	124
Figure 6.10: LOLE in hours per year for the (a) 14 and (b) 24 bus network with and without RTTR .....	125
Figure 7.1: The difference between a uniform and non-uniform inlet boundary condition.....	140
Figure 7.2: The effect of surface roughness on wind flow.....	141

---

## List of Tables

Table 1.1: Environmental condition sensitivity analysis (parameter variation versus rating variation) [12] .....	12
Table 3.1: The weather data used to calculate line ratings for use in this study.....	37
Table 3.2: A new table 2 for P2/6 showing the contribution to security of RTTR as a percentage of the static rating of the conductor .....	42
Table 3.3: The solution to the MC example in Figure 3.6, for different numbers of samples, $n$ .....	45
Table 3.4: Typical repair times for overhead line faults.....	49
Table 4.1: Terrain classes and the corresponding surface roughness values from the LiDAR data.....	64
Table 4.2: Details of the CFD meshes created for the study and the number of simulations run .....	68
Table 4.3: Average errors in the speed up case at 5m height.....	72
Table 4.4: Average Wind Speed and Direction Errors .....	72
Table 4.5: Average Wind Speed and direction errors for measurements taken at 5m or higher.....	73
Table 5.1: Average errors in wind speed and direction estimation using the CFD Method .....	100
Table 5.2: The absolute average error in rating prediction using the CFD method and using inverse distance interpolation.....	103
Table 6.1: Average Root Mean Square errors of the load and rating distributions.....	115
Table 6.2: The impact of network size on simulation time.....	126

# Chapter 1. Introduction



## 1.1. BACKGROUND

The electricity industry is currently facing the largest upheaval since privatisation [1]. As a result of environmental and political pressure, electricity generation, along with many other industries, is being forced to decarbonise [2, 3]. This is leading to a paradigm shift in how networks are configured and how they are operated. This is an enormous challenge to an industry which, for most of its existence, has been used to a ‘business as usual’ approach, focussing primarily on keeping the lights on. It is also an opportunity to improve the way electrical networks are operated, and to get better value out of the existing infrastructure.

Conventionally, electrical networks are designed to be top down; the generation at the high voltage levels, with power flowing down through the system to the customers at the lower voltages. Distributed Generation (DG), particularly renewable energy, has caused this to change. Renewable energy projects must be built where the energy is abundant. This is often in relatively isolated locations, where the generation has to connect to the lower voltage distribution network. This DG can lead to bi-directional power flows, with areas of network that were traditionally loads becoming net generators.

In conventional power systems, the generators are dispatchable; the system operator can tell them when to generate, allowing supply to be balanced against demand. Many renewable energy sources, such as wind turbines and solar panels, are not fully dispatchable. Instead they are dependent on the local conditions; when the wind blows or the sun shines, they will generate electricity. This means the system operator must now dispatch the conventional generation to balance with both the load and the intermittent generation connected to the network. This intermittency is considered to be a serious flaw by some critics [4], but in reality it is an additional challenge and steps can be taken to mitigate its impact.

The second impact of CO<sub>2</sub> reduction targets is that tasks traditionally performed using fossil fuels are expected to be electrified. Transport and

heating will increasingly be moved onto the electricity system, leading to an increase in overall demand and a change in the pattern of energy consumption.

The conventional way to tackle these challenges would be by reinforcing and upgrading the network; adding more or higher rated overhead lines, transformers and underground cables to ensure the network is capable of facilitating the increased power flows without compromising its reliability. In some cases this may be the most appropriate solution, but in many cases it would be costly and time consuming [5, 6]. Upgrading assets, or building new ones, results in a lock in, where the new asset will be expected to solve the problem for 30-40 years. Much of the load and generation growth is a result of consumers and entrepreneurs, rather than central planning. This means it is less predictable than traditional load and consequently harder to plan for.

Networks are conventionally planned conservatively, reliability is primarily provided through asset based redundancy. This deterministic approach, which assigns fixed values for many parameters which are continually fluctuating, may not be well suited to solving the problems networks are facing now, and will face in the future. They could result in a situation where some areas of network are over engineered and inefficient, and others are not sufficient to meet the necessary challenges for the requisite time scales.

The work in this thesis focuses on distribution networks, in which one does not have to consider whole system demand and generation balance. However, many of the methods presented could equally be applied to transmission networks.

## 1.2. SMART GRIDS

Power networks were also designed to operate with as little intervention from operators as possible. While monitoring equipment is used on some network components, the majority of existing assets are installed and

expected to supply customers without any online control. Smart Grids represent a different approach, using active monitoring and control, IT and communications, active customer participation and management of distributed generation and distributed energy storage [7, 8].

The Smart Grid has many aims: to improve the utilisation of the existing network, to reduce the cost to customers by increasing their awareness, to facilitate the connection of renewable energy, to increase the flexibility of network operation [9], to allow the large scale integration of electric vehicles and other low carbon technologies. To achieve these goals requires secure communications, intelligent control, predictive capabilities, controllable loads, energy storage, monitoring and state estimation.

The work presented in this thesis focusses on just one aspect of the wide suite of smart grid technologies under development, Real-Time Thermal Ratings (RTTR).

### 1.3. REAL-TIME THERMAL RATINGS

Real-Time Thermal Ratings (RTTR) comes from the observation that the first limit of a current carrying conductor is its temperature. Conventionally conductors are given a rating based on a low probability of exceeding a certain design temperature, which is derived from a conservative set of weather conditions[10, 11]. These values were calculated in the 1980s when anything other than static seasonal rating would have been impractical to implement outside of simple applications in specific, favourable circumstances. In reality a conductor's current carrying capacity is continually fluctuating, which leads to unexploited capacity the majority of the time [12]. Figure 1.1 shows an example of this, calculated using real weather data from the UK.

Figure 1.1 shows the maximum and minimum daily rating of an overhead conductor compared with its seasonal rating throughout the year. It is clear that the majority of the time there is additional current carrying capacity that is not being utilised. Furthermore on rare occasions the actual rating of

a conductor falls below the seasonal rating. Through employing RTTR the additional capacity can be exploited, and the risks introduced by low rating events can be mitigated. In a review of conductor uprating methods conducted by CIGRÉ, RTTR was considered to be capable of delivering small increases in capacity at low cost [13].

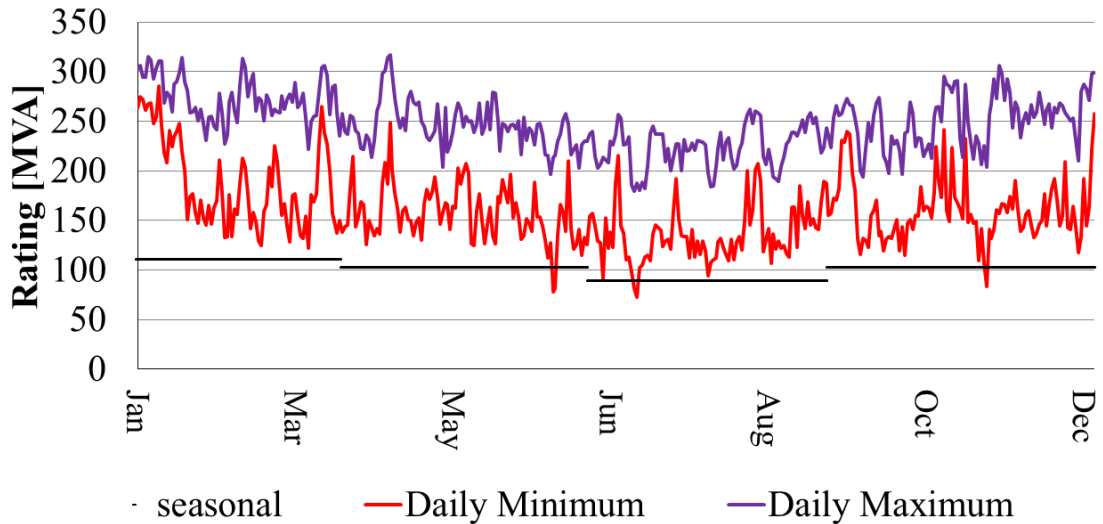


**Figure 1.1: The unutilised headroom that can be exploited through the use of RTTR, compared to the seasonal ratings**

RTTR allows this additional capacity to be exploited through active monitoring and state estimation. Real-time data is used to calculate the current carrying capacity of the line. This information can then be used to inform decisions by either control algorithms or engineers. It is worth noting that RTTR is, at its core, the use of active monitoring and thermal state estimation. The thermal and electrical properties of the conductor remain the same; the additional capacity is already there, but cannot safely be exploited without this monitoring. Similarly, periods of low current carrying capacity are also already present; RTTR simply allows them to be identified, potentially leading to safer operation.

While all electrical conductors can take advantage of RTTR, overhead lines show the greatest potential [12], as such they provided the focus for the work presented in this thesis. Underground cables and power transformers

have cyclic ratings that allow them to operate above their static rating for a given time period [14, 15], allowing overhead conductors to take advantage of RTTR even if other components in the network appear to be a limiting factor. Furthermore, because networks are designed to contain redundancy in the case of planned and unplanned outages, the additional capacity provided by RTTR will likely only be relied upon in contingency or other extreme load events.

A potential disadvantage of RTTR is that higher utilisation could result in higher transmission losses. By increasing utilisation the current, and hence the associated losses, will increase. This will represent an additional operating loss when compared to network reinforcement, because the losses do not scale linearly with utilisation. Furthermore, the increased current will cause the line temperature to increase, thereby increasing its resistance and hence further increasing the losses. In spite of this, the increase in losses is likely to be outweighed by the benefits of RTTR, especially if they are considered in a life cycle rather than purely operational, context.

The term Real-Time Thermal Ratings is used in preference to other terms such as Dynamic Line Rating (DLR) and Dynamic Thermal Rating (DTR). This is because the conductor rating is not being considered dynamically; the steady state rating is calculated based on real time weather observations. It is defined as being the current that can pass through a conductor for an extended period of time, without causing the conductor to exceed its design temperature [11]. In reality, the conductor will take time to change temperature when the weather conditions change, leading to more potential capacity. However, attempting to exploit this additional capacity through the thermal dynamics of the line could increase the likelihood of overheating the line and damaging components or infringing safety requirements. Consequently, it was considered prudent to set the steady state thermal rating using real-time data, hence the term Real-Time Thermal Rating.

## 1.4. CONDUCTOR THERMAL RATINGS

This section describes the fundamental concepts behind RTTR. In order to assign overhead conductors a rating in real time, it is necessary to understand the physical properties which define its rating. The heat transfer processes at work in overhead conductors are described, a sensitivity analysis is performed and the process for determining the actual conductor rating is described.

### 1.4.1. CURRENT CARRYING CAPACITY OF OVERHEAD CONDUCTORS

Generally, the maximum current that can be carried by a conductor is defined by a maximum permissible temperature, beyond which the conductor could be subject to excessive sag or long-term annealing [16]. A conductor is subject to a heat balance between the heating due to the Joule effect,  $I^2R$ , the heating due to solar radiation,  $q_s$ , and heat losses by convection,  $q_c$ , and radiation,  $q_r$ .

This heat balance is expressed in equation (1) below:

$$I^2R + q_s = q_c + q_r \quad (1)$$

or

$$I = \sqrt{\frac{q_c + q_r - q_s}{R}} \quad (2)$$

This describes a steady state energy balance, where  $I$  is the maximum permissible current at a design temperature  $t_d$ . The heat loss terms,  $q_r$  and  $q_c$  are dependent on the conductor temperature, as is the resistance  $R$ . It is worth noting that the full energy balance also contains terms for magnetic heating,  $q_m$ , corona heating,  $q_i$ , and evaporative cooling,  $q_w$ . The corona and evaporative terms are generally ignored since their effects are negligible [17], and the magnetic component is accounted for by a scaling parameter. The full equation is provided here for completeness:

$$I^2R + q_s + q_m + q_i = q_c + q_r + q_w \quad (3)$$

Different sets of equations have been developed to describe this heat balance. The most commonly used are those developed by the IEEE [18], CIGRÉ [17] and the IEC [19]. These models are all approximations, but experiments show that they all provide a comparably accurate representation of the real system [20, 21]. The work in this thesis was performed using the CIGRÉ overhead line model, because of the body of work that has been carried out by CIGRÉ on enhanced line ratings [13, 22, 23]; this model is described in detail in sections 1.4.1.2-1.4.1.6.

#### 1.4.1.1. CONDUCTOR STRUCTURE

Overhead conductors are not a single wire; instead they are made up of bundles of conductors. The most common of these, particularly in high voltage systems, is the ACSR (Aluminium Conductor, Steel Reinforced). This consists of a central strand of steel, wrapped in aluminium conductors. The steel provides strength, supporting the aluminium without stretching it, while aluminium has a high conductivity to weight ratio. Figure 1.2 shows an example of an ACSR structure, though many configurations exist.

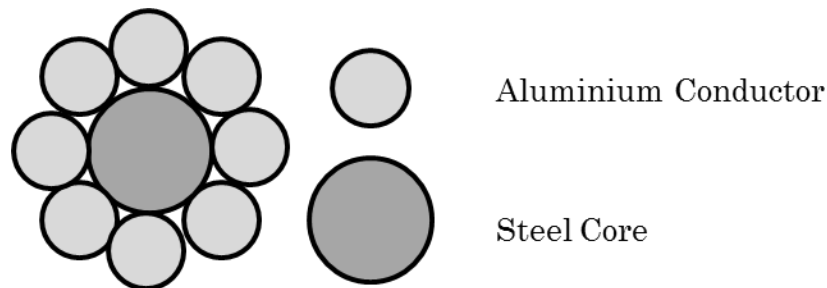


**Figure 1.2: The typical structure of an aluminium conductor, steel reinforced.**

#### 1.4.1.2. CALCULATION OF CURRENT HEATING EFFECTS

This theory works on the basis that the power input must be the same for both ac and dc currents for the same average temperature of the conductor. The dc current that will result in a certain temperature being reached is calculated and the empirical formulae are then used to convert this to the equivalent AC current [10], which will be lower due to the magnetic effects. The AC current is important in steel cored conductors, since magnetic heating can be significant here due to the longitudinal magnetic flux produced in the steel core.

$$q_j = I_{dc}^2 R_{dc} [1 + \alpha(T_{av} - 20)] \quad (4)$$

The AC and DC power inputs must be the same for the same average temperature of the conductor, hence:

$$I_{ac}^2 R_{ac} = I_{dc}^2 R_{dc} \quad (5)$$

For aluminium-steel conductors with 3 layers of aluminium wires:

$$I_{ac} = \frac{I_{dc}}{\sqrt{1.012 + 2.319 \cdot 10^{-5} \cdot I_{dc}}} \quad (6)$$

And for an aluminium-steel conductor with 1 or 2 layers of aluminium wires and a nominal cross sectional area of 175mm:

$$I_{ac} = \frac{I_{dc}}{\sqrt{1.0045 + 0.09 \cdot 10^{-6} \cdot I_{dc}}} \quad (7)$$

#### 1.4.1.3. RADIAL TEMPERATURE DISTRIBUTION

Conductors do not operate at a uniform temperature; the surface temperature,  $T_s$ , where heat transfer takes place, is at a slightly lower temperature than the core of the conductor [16]. This is important because the resistance depends on the average temperature,  $T_{av}$ , while the sag depends on the core temperature,  $T_c$ . The radial temperature difference can be written as [17]:

$$T_c - T_s = \frac{q_T}{2\pi\lambda} \left[ \frac{1}{2} - \frac{D_2^2}{D^2 - D_2^2} \left( \ln \frac{D}{D_2} \right) \right] \quad (8)$$

The difference between core and surface temperatures is usually between 0.5°C and 7°C, so it is generally sufficient to assume  $T_{av} = T_s$  [17].

#### 1.4.1.4. SOLAR HEATING

The other significant source of heating for overhead conductors is incident solar radiation. This heating is given by:

$$q_s = \alpha S D \quad (9)$$

Where  $\alpha$  is the absorptivity of the conductor,  $S$  is the incident solar radiation and  $D$  is the conductor diameter.

#### 1.4.1.5. CONVECTIVE COOLING

Convective cooling is the heat transfer from the conductor to the adjacent fluid (in this case air). There are two heat transfer mechanisms to consider: free and forced convection. In free convection, the conductor heats the adjacent air, which reduces the density of the heated air. This creates a natural convection current, causing the hot air to flow away from the conductor. Forced convection takes place when the air is already in motion; for overhead conductor ratings, this means the wind is blowing over the line. The convective heat loss is given by:

$$q_c = \pi \lambda_f (T_s - T_a) Nu \quad (10)$$

Where  $Nu$  is the Nusselt number and  $\lambda_f$  is the thermal conductivity of air. The Nusselt number is calculated differently for free and forced convection. For forced convection, the Nusselt number is given by:

$$Nu = B_1 (Re)^n \quad (11)$$

$$Re = \frac{\rho_a \cdot D \cdot Ws}{\mu} \quad (12)$$

where  $B_1$  and  $n$  are constants dependant on the Reynolds number and the conductor surface roughness. The conductor diameter,  $D$ , is taken to be the overall diameter, in spite of the fact that the structure of the conductor means the actual surface area available for heat transfer is 40-45% greater than a smooth cylinder of the same diameter. This is because the boundary layer detaches itself between the conductor strands, forming stagnation zones at the indices [17].

Wind direction plays an important role in the effectiveness of forced convection. The cooling effect is greatest when the wind is perpendicular to the conductor and least when the wind is parallel to the conductor. This is accounted for by an empirical angle correction. In equations (13)-(15),  $\theta$  represents the direction of the wind with respect to the conductor, where

$\theta=0$  represents wind flow parallel to the conductor and  $\theta=90$  represents wind flow perpendicular to the conductor.

$$Nu_{\delta} = Nu_{\delta=90}[A_1 + B_2(\sin \theta)^{m_1}] \quad (13)$$

where:

$$A_1 = 0.42, B_2 = 0.68 \text{ and } m_1 = 1.08 \text{ for } 0^\circ < \theta < 24^\circ \quad (14)$$

$$A_1 = 0.42, B_2 = 0.58 \text{ and } m_1 = 0.90 \text{ for } 24^\circ < \theta < 90^\circ \quad (15)$$

For low wind speeds ( $Ws < 0.5\text{m/s}$ ), wind direction is of little consequence and the corrected Nusselt number,  $Nu_{cor}$  is unlikely to go below:

$$Nu_{cor} = 0.55 Nu_{\theta=90} \quad (16)$$

The Nusselt number for free convection depends on the product of the Prandtl,  $Pr$ , and Grashof,  $Gr$ , numbers:

$$Nu = A_2(Gr.Pr)^{m_2} \quad (17)$$

Finally, for low wind speeds ( $Ws < 0.5\text{m/s}$ ), neither free nor forced convection is dominant. Three convection values are calculated, and the largest is then selected.

1. Since there is no preferred wind direction at these low wind speeds, an angle of attack of  $45^\circ$  is assumed, and forced convection is calculated using equations (13) and (10).
2. The second value is calculated using equations (14) and (10).
3. The free convection is calculated using equation (17).

#### 1.4.1.6. RADIATIVE COOLING

Radiative cooling generally represents a small fraction of the overall heat loss, especially when forced convection is taking place. It is considered sufficiently accurate to write [17]:

$$q_r = \pi D \epsilon \sigma_B [(T_s + 273)^4 - (T_a + 273)^4] \quad (18)$$

### 1.4.2. SENSITIVITY ANALYSIS

The previous section explained how a conductor's rating is affected by four external factors: wind speed, wind direction, ambient temperature and solar radiation. However, they are not equal contributors. A sensitivity analysis was performed by [12]; using credible midpoint values for each parameter and varying them by  $\pm 50\%$ , the authors concluded that wind speed had the greatest impact on conductor rating, followed by wind direction, ambient temperature and finally solar radiation. Their results are presented here in Table 1.1.

However this sensitivity analysis was not deemed comprehensive enough. It is unclear how the authors ensured a representative set of values for the other parameters was used in each case. Moreover, the decision to use 'credible midrange values' is highly subjective; A more comprehensive approach would be to ensure the full credible range of values is represented in the analysis.

**Table 1.1: Environmental condition sensitivity analysis (parameter variation versus rating variation) [12]**

<i>Parameter (credible mid-range value)</i>	<i>Ws (8m/s)</i>	<i>Wd (<math>\frac{\pi}{4}</math> rad)</i>	<i>Ta (15°C)</i>	<i>S (500W/m<sup>2</sup>)</i>
<b>Variation from mid-range value</b>				
-50%	-23.86%	-11.38%	+10.80%	+0.72%
-25%	-10.73%	-4.97%	+5.52%	+0.36%
-10%	-4.07%	-1.85%	+2.24%	+0.15%
+10%	+3.84%	+1.66%	-2.29%	-0.15%
+25%	+9.22%	+3.82%	-5.81%	-0.36%
+50%	+17.40%	+6.54%	-11.96%	-0.73%

A new sensitivity analysis was performed using the same weather data as the original analysis [12], which was available courtesy of the UK Met Office. For each weather parameter, the 1<sup>st</sup> through 99<sup>th</sup> percentile of each parameter was used as a fixed value. Monte Carlo simulation<sup>1</sup> was used, with non-parametric probability distributions representing the other weather parameters to ensure that a representative set of values was used

<sup>1</sup> Monte Carlo simulation is explained in detail in section 3.5.1

in each case, and that the variation due to other parameters could be captured in each case.

Figure 1.3 shows the results of this new sensitivity analysis. The curve shows the mean rating for each fixed value, while the error bars show one standard deviation of the variation arising from the effects of changes in the other weather parameters. This approach assumes the weather parameters vary independently. The spacing of the error bars illustrates how likely the parameters are to be in each state, for example solar radiation is much more likely to be low, and ambient temperature is more likely to be at an average value of around 10°C than particularly high or low.

Again, it is clear that wind speed has the greatest impact on overhead conductor rating. Wind direction and ambient temperature lead to a similar level of variation, though the impact of temperature is more linear. The effect of solar radiation is very small compared to the variation associated with the other parameters.

It is worth noting that this analysis assumed that the weather conditions are independent from one another, which may not be the case in reality. For example, zero solar radiation is unlikely to occur simultaneously with zero wind speed. Wind speed and direction have fewer error bars than the other curves because in the weather data they were measured at discrete intervals.

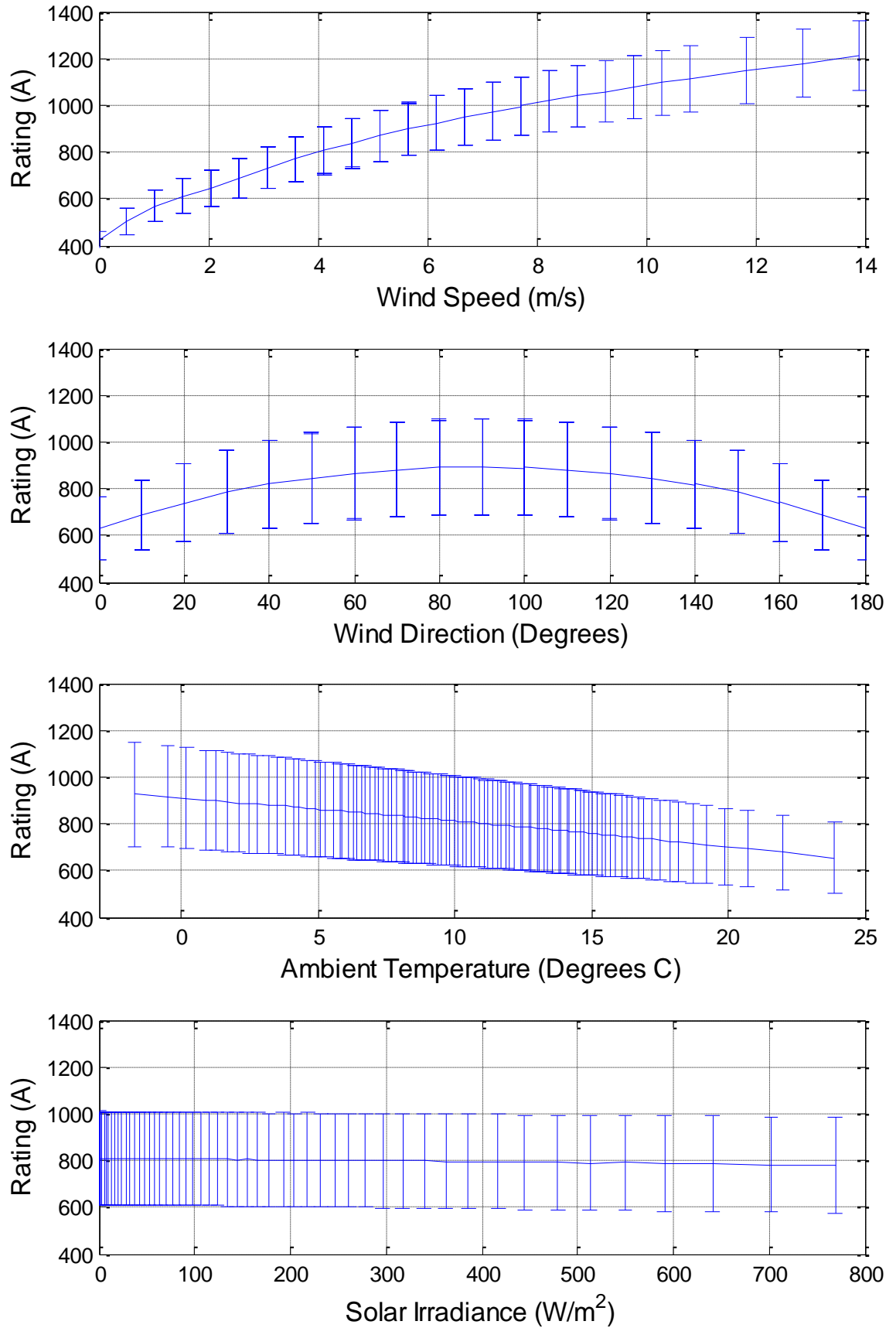


Figure 1.3: The variation in rating as a consequence of wind speed, wind direction, ambient temperature and solar irradiance.

### 1.4.3. CONDUCTOR RATING CALCULATION

The models described in section 1.4.1 allow the calculation of the maximum current flowing through a line given a design temperature and a specific set of environmental conditions. They do not dictate the rating that should be assigned to the conductor.

Common practice is to assign a conductor a rating based on a set of conservative weather conditions. In UK distribution networks this is a wind speed of 0.5m/s at 0° (parallel to the line), 0 solar radiation and ambient temperatures of 2°C, 9°C and 20°C for winter, spring/autumn and summer respectively [11].

The UK is unusual, in that the line rating is calculated such that the current carrying capacity of the conductor will be below the calculated rating for a predetermined proportion of time [11]. This concept of ‘excursion time’ was devised following research at CERL [10]. In general, single circuits are allowed an excursion time of 0%, while multi-circuits are allowed an excursion time of 3% [11].

Figure 1.4 shows the curve used to determine the rating of a conductor. This curve was obtained by experiment at CERL, and is used to assign conductor ratings based on a predetermined value for  $T_e$ . The process is straightforward; first the nominal rating of the conductor is determined using the environmental conditions described earlier. Next, the desired excursion time,  $T_e$ , is looked up on the graph. The rating is then calculated by multiplying the original rating by the correlation term or:

$$r_e = r \cdot CT \quad (19)$$

Since it is not possible to attain a value for  $T_e=0$ , the value is read off for  $T_e=0.001$  instead.

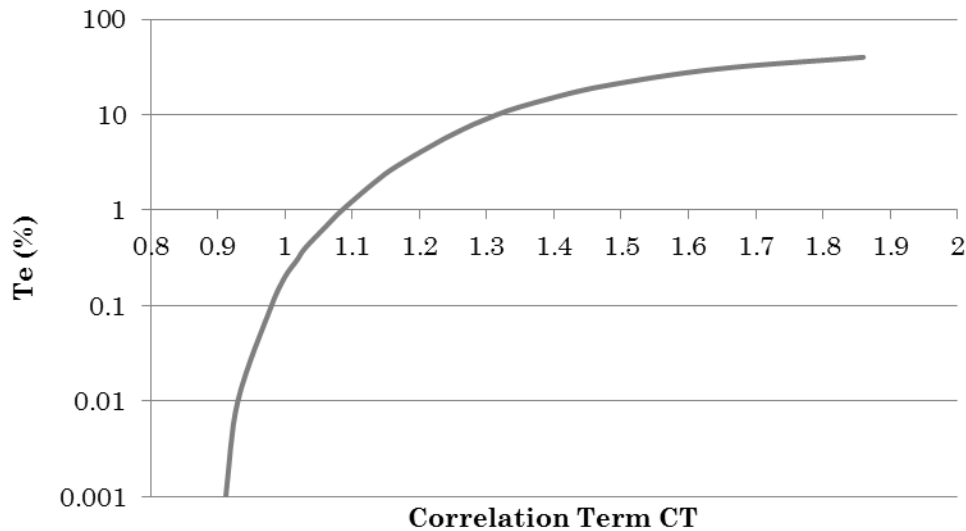


**Figure 1.4: a curve of correlation term against excursion time.**

#### 1.4.4. CONDUCTOR THERMAL LIMITS

##### 1.4.4.1. CONDUCTOR SAG

While the fundamental limit on conductor rating is temperature, often this maximum temperature is governed by conductor sag. As conductor temperature increases the materials in the OHL expand, causing the line to hang lower. Excessive sag can lead to the conductor touching nearby vegetation, or even the ground. Alternatively, it could lead to a flashover, where the electrical insulation provided by the air gap breaks down and current flows through a normally insulating medium. Not only is this dangerous, it can also lead to circuits tripping and potentially large numbers of customers being disconnected. Though line sag has long been understood [24], it remains a defining factor in overhead line and circuit design.

Conductor sag is fundamentally dependant on the following equations [24].

Relation between Sag, S, load, w, and tension,  $\tau$ :

$$s = \frac{wl^2}{8T} \quad (20)$$

Relation between Sag, Span length,  $l$ , and Length of conductor:

$$Length = \left( l + \frac{8s^2}{3l} \right) \quad (21)$$

Or

$$Length = \left( l + \frac{w^2 l^3}{24\tau^2} \right) \quad (22)$$

Relation between Tension, Load and Temperature for any given span length:

$$\left( \frac{C_1 w_2 l}{\tau_2} \right)^2 - \tau_2 = \left( \frac{C_1 w_1 l}{\tau_1} \right)^2 - \tau_1 + C_2 T \quad (23)$$

The subscripts 1 and 2 denote initial and final conditions respectively.

Sloping Spans:

$$y = \frac{l}{2} - \frac{a\tau}{w_v l} \quad (24)$$

$$\text{Vertical reaction at higher support} = w_v(l - y) \quad (25)$$

$$\text{Vertical reaction at lower support} = w_v y \quad (26)$$

Equations (20)-(26) and Figure 1.5 enable initial sag and tension calculations to be carried out. The maximum permissible sag, and therefore line temperature, varies from line to line, depending on the specific siting of the conductor.

#### 1.4.4.2. EFFECT OF TEMPERATURE ON CONDUCTOR PROPERTIES

Over a conductor's operational lifetime, it may be subject to annealing and loss of tensile strength, and these factors may be exacerbated by operating at an elevated temperature [25]. Though the steel and aluminium which make up the conductor are unlikely to experience annealing at less than 250°C, the zinc coating may suffer some damage. The loss of tensile strength during operation is difficult to quantify, however it can be observed that it is a function of both the temperatures at which the line is operated, and the duration for which the line is operated at these temperatures [25].

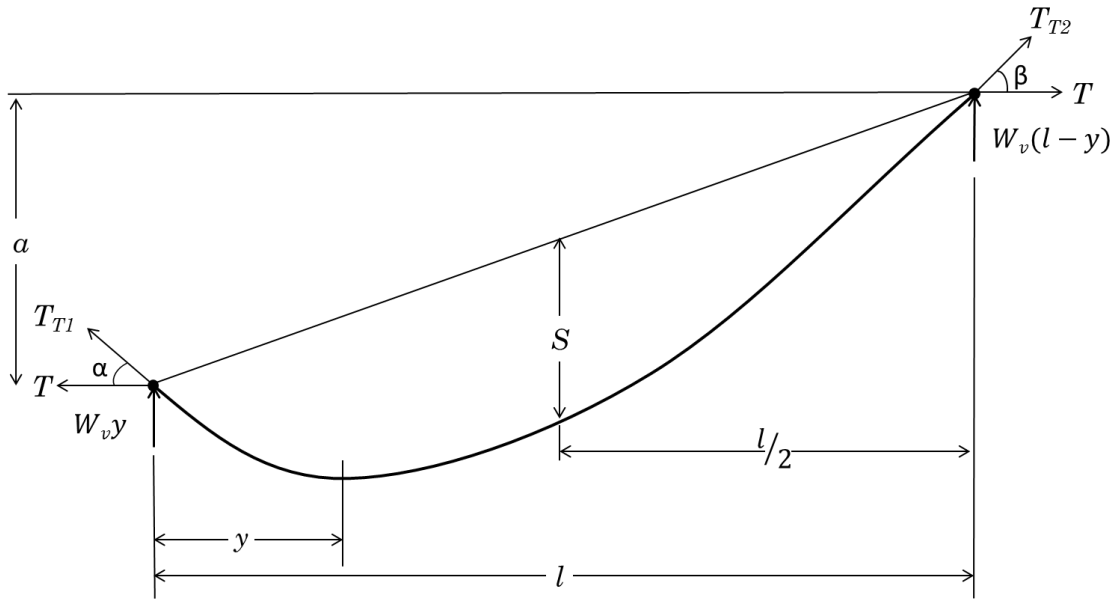


**Figure 1.5: General case of a suspended conductor [24]**

## 1.5. BARRIERS TO IMPLEMENTATION

Though RTTR has been the subject of considerable research, there are still barriers preventing its wide scale implementation. The regulatory framework does not currently exist to aid the wide scale uptake of RTTR - though there is an allowance for short-term and emergency ratings, which take advantage of the thermal inertia of the conductor. Furthermore, DNOs and system operators are risk averse, and a technology such as RTTR, which could be perceived to increase the risk within the network, does not dovetail well with this philosophy.

The vast majority of research into RTTR has been in improving and validating technical solutions. While this is clearly essential to the successful implementation of the technology, it is also necessary to consider which other challenges represent barriers to implementation. While it may seem counter intuitive to propose network planning methods for a technology that is, by its very nature, stochastic and variable, it is in fact essential to do so. Without adequate planning methods it would not be possible to quantify the impact of RTTR on network reliability, DG connections or security of supply. If these cannot be quantified at the planning stage, it is impossible for network operators to make informed

decisions about which technologies to deploy and their likely implications, and where to build network reinforcements or upgrade existing assets.

## 1.6. RESEARCH OBJECTIVES

The primary aim of the research presented in this thesis is to provide new methods to allow RTTR to be considered in power systems at the network planning and design stages. The main research objectives are:

1. Devise a method for assessing the impact of RTTR on distribution network security of supply, allowing both the benefits and risks to be quantified, to allow network operators to make informed decisions about network capacity.
2. Develop methods to allow wind simulations, which are widely used in the wind energy industry, to be applied to quantify the benefits of RTTR at the planning stage, and provide additional information to weather based RTTR systems during operation.
3. Design a means of quantification of the reliability of a network utilising RTTR, and provide indicative results using standard test networks.

## 1.7. THESIS OUTLINE

The rest of this thesis is structured as follows: In Chapter 2, the literature describing the state of the art of Real-Time Thermal Ratings is explored and described. This is broken down into the historical context, available technologies, operational projects, applications, planning and forecasting. This review is then used to identify the gaps in the existing knowledge that can be tackled by this thesis. Further specific, technical literature reviews are provided in the relevant subsequent chapters.

Chapter 3 describes the effect of RTTR on security of supply. A probabilistic methodology is presented that allows quantification of both the level of load that can be accommodated by RTTR and the level of risk within the network. This method is compared to the method currently used in the UK distribution network security of supply standard to quantify the benefits of

intermittent generation Example results are presented, using representative data for the UK.

Chapter 4 describes the computational wind model used to predict the effects of terrain geometry on wind flow. A validation study is presented to demonstrate that the simulations are equivalent to other state of the art work.

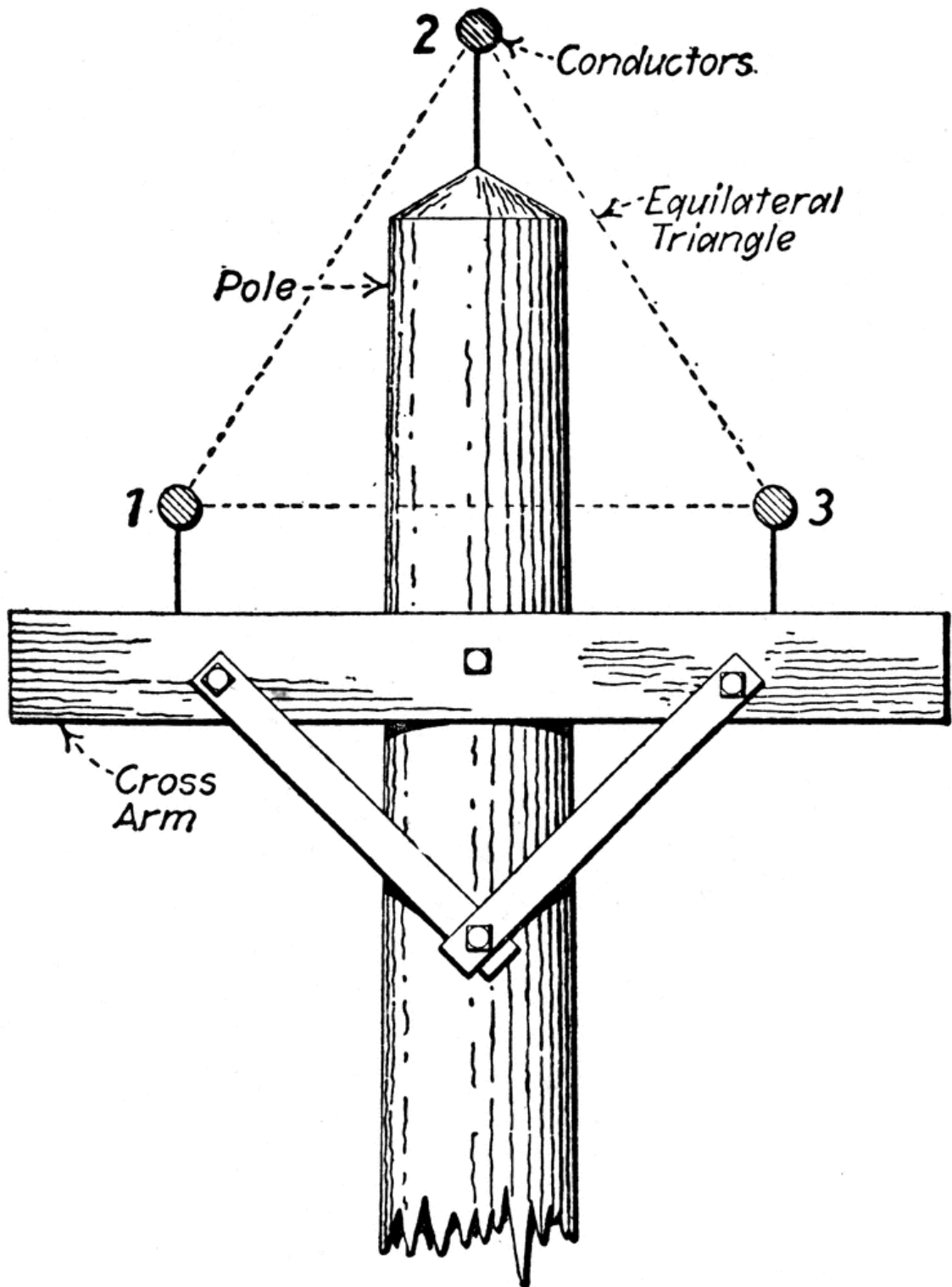
The applications of this model are discussed in Chapter 5. Methodologies are described for critical span identification, additional wind farm energy output prediction, optimal conductor siting, weather station siting and improved online wind estimation. Case studies are presented for both offline planning and operation.

Chapter 6 presents a method for assessing the impact of RTTR on power network reliability, using sequential Monte Carlo simulations coupled with models for RTTR reliability and uncertainty analysis. The impact of the correlation between conductor ratings and varying levels of load are considered, and systems of varying sizes are simulated to ensure the methodology is scalable in terms of computational time.

Chapter 7 presents critical discussion of the findings and the broader implications of the research, evaluating the benefits provided and the opportunities for further research in this field.

Finally, Chapter 8 summarises the key findings with respect to the research objectives set out in Chapter 1.

Chapter 2. RTRR: The State of the Art



## 2.1. INTRODUCTION

Before new research can be carried out, it is essential to take stock of the current state of knowledge. This literature review describes the state of the art in RTTR technology and provides critical discussion; shortcomings and gaps in the state of knowledge are identified. The literature relating to specific, technical aspects of the resulting research is provided in the relevant chapters.

## 2.2. INITIAL RESEARCH

The impact of varying weather conditions on conductor ratings is not a new concept; as section 1.4 discussed, it is fundamental in determining the currently imposed static ratings. As early as 1943, engineers were attempting to maximise the capacity of overhead conductors while maintaining safe operation [26]. This section describes early research into RTTR, and discusses its merits and shortcomings.

An early attempt at raising line ratings used temperature based methods, but did not propose this as a practical method for implementation [27]; the inability to measure each conductor in real time lead to attempts to employ statistical models for increasing conductor ratings . These methods yielded only small increases in conductor rating, and did so at a high level of risk. Given the stringent need for security of supply within power systems, methods with such a high level of uncertainty were not deemed appropriate.

A review of the state of the state of the art in RTTR from 1987 is presented in [28]. The authors suggest that the benefits of RTTR are considerable, quoting increases in line rating of up to 300%, though typically closer to 30-50%. However, due to the practicalities of implementation the actual benefit is likely to be considerably smaller. Various difficulties are identified, including the variation in wind direction along a line and the effect of nearby terrain features such as trees. This view is reinforced by [29], which suggests that not only are there significant benefits to be reaped from RTTR, but that the rating approach at the time was not as conservative as it

appeared, given the possibility that the wind could be blowing parallel to the line, and hence providing a reduced cooling effect.

An attempt to increase line ratings using measurements from a nearby weather station is presented in [30]. The authors claim that a similar statistical approximation of the line rating is possible using weather data from 20 miles away to that using temperature data measured on the line itself. However, significant errors were identified in both the estimated ratings, and the measurement devices on the line. It was found that ‘critical span’ (the line with the lowest rating in the system), was not constant, though in summer and winter trials, a single line was identified as the critical span for over 50% of the time. It was, however, a different line in each season.

The work in [31] is an attempt to calculate conductor temperatures using current and weather measurements along with the thermal time constant of the conductor. The thermal time constant is important for the operational use of RTTR since it dictates how often the rating must be calculated.

### 2.3. MODERN RTTR TECHNOLOGIES

A review of the state of the art in RTTR in 2011 is presented in [32]. The paper divides the available technologies into Sag-Based, Tension-Based, Temperature-Based and Current Based. The first three technologies measure the parameter on each line in real time, and this is used to calculate the line rating. Current based technologies measure the current in the line and estimate the environmental parameters to calculate the rating. This reduces the number of measurements and communications required to operate the system.

#### 2.3.1. SAG AND TENSION MONITORING

Since conductor sag is often the defining factor in a conductor’s rating, several methods and devices have been developed to measure the sag directly, using GPS [33-35], LiDAR (Light Detection and Ranging) [36], and Power Line Carrier Sag (PLC-SAG) [37]. The GPS methods can infer the

line sag to within 0.4m with a 90% confidence [33]. No published error figures were available for the LiDAR or PLC-SAG methods.

Though measuring line sag may seem like an obvious course of action, it alone does not allow the network operator to know the true ampacity of the conductor [38]. The sag is a function of the line temperature, which is subject to the energy balance presented in equation (1). If the line has not yet expanded into a steady state condition, the energy balance is not satisfied, and consequently the current carrying capacity of the line is unknown. Therefore some estimate of the local weather conditions, or the rate of thermal expansion, is required for sag measurement to allow accurate estimation of conductor rating.

As described in section 1.4.4.1, conductor sag is related to tension; hence tension monitoring can be used to calculate line sag. Again, weather values are required to calculate ampacity [39]. Several tension monitors have been developed, some of which also make weather measurements [40].

The Ampacimon device [38, 41, 42] is a sag monitoring system which uses vibration measurements to calculate the fundamental frequency of a conductor, and hence the line sag. The original design used effective ambient conditions to estimate conductor ratings, but more recent models feature temperature, wind and solar radiation sensors.

Although measuring the lines directly can yield accurate current carrying capacity estimates, this approach relies on monitoring individual spans. Consequently, if meaningful estimates are to be acquired, then either every span or the determining spans must be measured. The former approach is likely to be prohibitively expensive, while the latter requires knowledge of which spans are likely to contain bottlenecks; this is particularly challenging without measurements already in place, especially given that the determining span is likely to vary [30].

### 2.3.2. WEATHER MONITORING

Since conductor ampacity is dependent on the local conditions, precise and accurate weather monitoring can yield direct calculation of conductor current carrying capacity. However, weather conditions, particularly wind speed and direction, are highly variable on small space and time scales [43]. Consequently it is possible that a local weather measurement may not be able to produce accurate estimates of the rating of nearby conductors, and indeed the wind speed and direction may vary sufficiently that even along the length of a single span, the rating cannot be accurately estimated.

Work at Durham University [12, 44, 45] focussed on a weather based system and employed a thermal state estimation algorithm to calculate the rating at any point in the network. The model performed well in a validation in December 2009, with average errors of between -2.2 and 1.4°C at five different measurement points within an 11km section of network. The weather parameters were estimated using a simple interpolation, with some adjustment of wind speed to account for ground roughness. Monte Carlo simulations were used to provide some uncertainty quantification during the state estimation process.

The validations were initially carried out during the winter months. As part of this project, the validation was re-run using data from the summer months, resulting in an average error of 3.0°C [46]. Figure 2.1 shows the conductor temperature estimation from both the original study, and the summer validation. The outliers are primarily the result of missing data at the measurement stations [44].

Similar work has been carried out at the Idaho National Lab (INL) [46, 47]. The INL researchers used a computational wind model to alleviate some of the difficulties associated with using only weather measurements. The simulation package used was developed for the wind energy industry, and focusses on turbine siting and energy yield prediction [48]. The INL study used a much larger test area, and obtained an average temperature estimation error of 1.1°C.

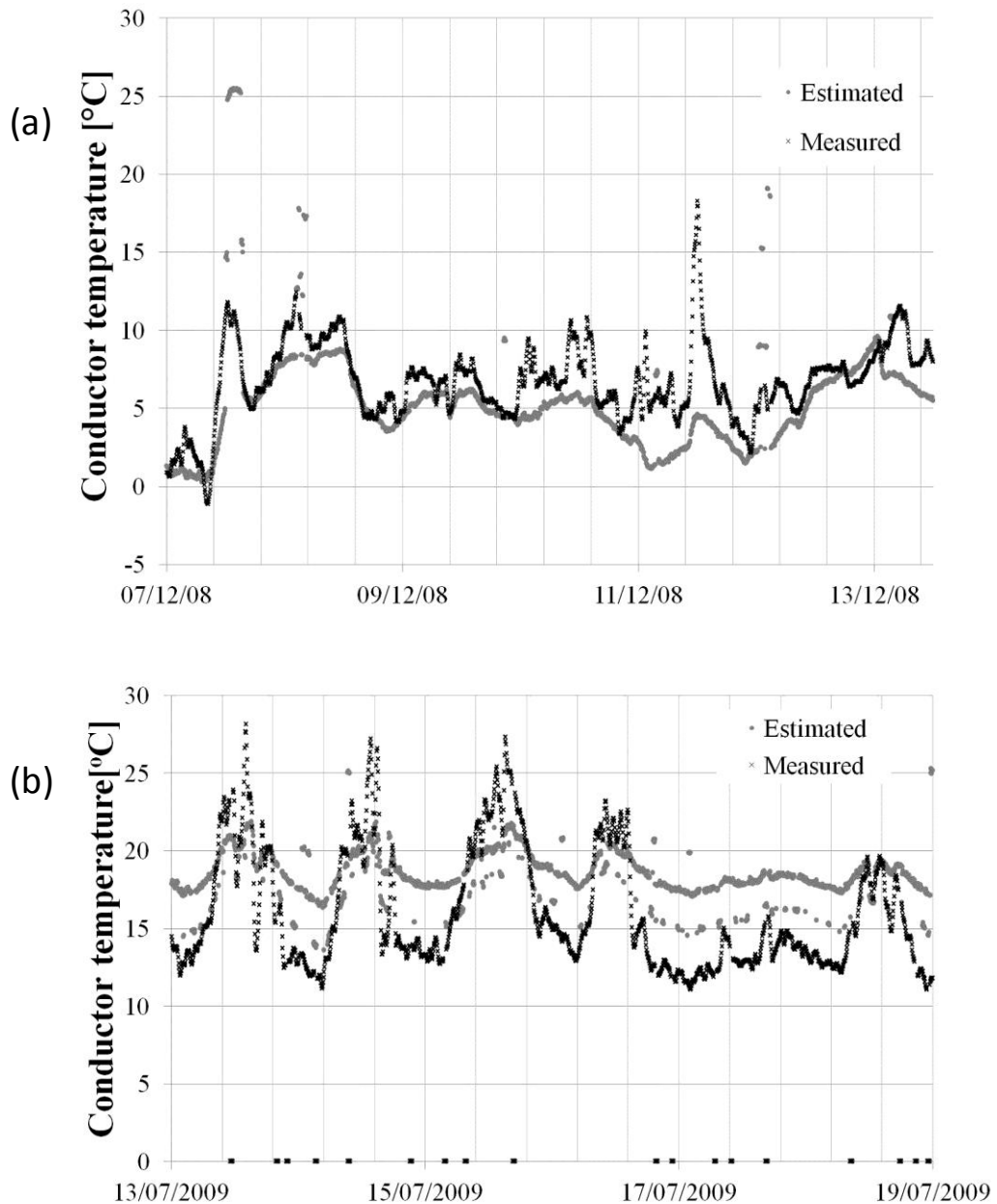


**Figure 2.1:** A comparison of calculated and measured conductor temperature for the trial site [13]. (a) shows the comparison in winter 2008/2009 when the original study was performed, while (b) shows results using data from summer 2009, where the agreement between the estimated and measured values is worse than in the original study.

One area of interest in weather based RTTR is the impact of the time resolution of the meteorological data. A study by *Hosek* [49] suggests that, given the thermal time constant of an overhead line, the data should have a sampling rate not less than one sample every 10 minutes. The results indicate that line temperatures can exceed their design temperature for

almost 1.6% of the time when using hourly sampling, compared with 0.01% using 10 minute sampling.

### 2.3.3. TEMPERATURE MONITORING

Temperature is the fundamental limit on conductor ratings, since sag, and damage through annealing and other processes, are dependent on temperature. Consequently, measuring the line temperature can be used to inform RTTR schemes. Various sensors are available for this purpose: the power donut [50] measures both conductor temperature and current, Smart Wires produce a FACTS (Flexible AC Transmissions System) device which monitors conductor temperature [51] and could conceivably be used for RTTR. RITHERM Equipments produce a Surface Acoustic Wave (SAW) transducer for conductor temperature monitoring [52].

As with sag and tension monitoring, conductor temperature measurements need to be combined with an estimation or observation of environmental conditions [53] to allow prediction of conductor rating.

### 2.3.4. PHASOR MEASUREMENT UNITS

There have been attempts to implement RTTR using Phasor Measurement Units (PMUs) [54, 55]. By placing the PMUs at either end of the line and knowing its length at a reference temperature, it is possible to calculate the average temperature of the line. However, since the line is limited by its hottest point, rather than the average temperature this method cannot fully exploit the headroom available in the system.

### 2.3.5. SUMMARY

This section has examined the different technical solutions for implementing RTTR, and examined the pros and cons in each case. Weather monitoring allows wide areas to be covered with relatively little monitoring equipment, but is less accurate than line monitoring solutions. Conversely, line monitoring solutions offer accurate estimates at precise locations. PMU based solutions are unlikely to be realisable, since they can only estimate the average line temperature, and hence cannot identify determining spans, nor calculate the current carrying capacity at these spans.

## 2.4. OPERATIONAL RTTR SCHEMES

There are several RTTR schemes already in operation. These are primarily proofs of concept, and as such are on simple sections of network. However, Schneider-Electric currently offer a commercial Dynamic Line Rating system [56]. The system uses a single weather station to estimate the rating of the line. It is currently in use on two trial schemes, and increases the line capacity by 30% or more.

Details of the deployment of a Dynamic Line Rating (DLR) scheme based on conductor temperature measurements and an RTTR system based on measurement of meteorological parameters are described by [57]. The schemes were implemented to reduce the curtailment of distributed generators on the network. The DLR scheme increases the rating of one line whose temperature is monitored. Conversely, the RTTR scheme attempts to increase the rating of every line in the network based on state estimation.

An RTTR scheme has been in place since 2008 on the Central Networks distribution network [58-61]. The system operates using weather data, and was validated using power donuts on the line. The system is used to allow a wind farm to export more power down an otherwise constrained line. An RTTR system was installed on the Orkney Smart Grid, off the coast of Scotland to relieve constraints on heavily loaded lines [57]. The scheme also aimed to release capacity to allow additional non-firm generation to connect to the network.

Transmission networks in the UK can take advantage of Met Office Rating Enhancement (MORE), which uses day-ahead weather forecasts to allow conservative increases of 5-11% [62].

These schemes are all installed on existing areas of network. RTTR could also be considered at the network design stage and when planning new assets. Additionally, [32] suggests the need for a planning tool to properly implement RTTR.

## 2.5. RTTR APPLICATIONS

RTTR is a technology with broad implications: if power lines move from having a fixed rating to a higher variable rating, what are the best ways to reap the benefits? The most widely explored application for RTTR is connecting additional wind generation to the distribution network. Since both wind generation and RTTR are heavily influenced by wind speed, it stands to reason that in times of high wind generation, the rating of nearby overhead conductors will be enhanced. This could allow more wind generation to be connected than the static ratings of the network would imply.

When injecting additional power into the network, it is important to understand which conductors will be affected, and hence where enhanced conductor ratings will be most beneficial. Work in [63, 64] uses Power Flow Sensitivity Factors (PFSF) to accommodate additional generation based on the thermal state of the network. Single and multiple DG schemes are considered, with different control schemes leading to varying levels of additional generation and consequently revenue. A similar approach is taken by [65], but an Optimal Power Flow (OPF) is used instead of PFSF. The Central Networks project described in section 2.4 found that by using RTTR they were able to connect 20-50% more wind generation [58]. Much of the focus of the Ampacimon project has also been on wind integration[38, 42]. A project on the Orkney Smart Grid implemented an RTTR scheme, which led to a reduction in wind generation curtailment from 38.5% to 9.7% of energy yield [57].

There has been little research into what impact RTTR could have on networks aside from integration of DG. Some work has been done in reducing power flow congestion, which potentially improves network reliability and availability [66]. RTTR could potentially allow additional load to be connected to distribution networks without new overhead lines being constructed, or could defer the need for new lines. It has been demonstrated that DG can provide a benefit in this way [67]. Work by *Blake*

*et al.*[68] suggests that RTTR could allow additional load to connect to areas of network where, in contingency situations, the power flow may exceed the static line ratings. In a case study it was found that RTTR could provide sufficient current carrying capacity to ensure security of supply over 99.6% of the time.

## 2.6. FORECASTING RTTR

Although RTTR provides an increase in rating on an instantaneous basis, forecast ratings data would allow system operators to make better informed decisions. The majority of the work carried out in this area used pre-existing weather forecasts to inform conductor rating algorithms [41, 69, 70]. Different time horizons are considered, with [41] forecasting up to 48 hours in advance with a 98% confidence value; this yields only small increases in rating. In [69], MC simulation is used to evaluate the forecast, providing error bounds based on the weather forecast errors over time horizons of up to 24 hours. All of these approaches introduce the issue of using weather forecasts at some distance from the conductors.

Forecasting is more widely applied to wind power generation [71]. An attempt to couple wind power forecasts and RTTR is presented in [72]; unfortunately the line ratings are represented by a probability distribution, which is considered independent to the wind power forecast.

## 2.7. NETWORK PLANNING FOR RTTR

The research described in this section has focussed on the operational aspects of an RTTR system. Though this is clearly essential for the technology's success, it is not the only topic which must be investigated. Network operators need to be able to quantify the benefit of a new technology before it is deployed; otherwise its impact on the network cannot be accounted for in any planning decisions. The success of RTTR depends on how the system is actually deployed, where sensors are placed, what kind of equipment is used and how much extra capacity is attributed to RTTR.

Very little work has been done in this area. There have been some studies which focus on planning new wind farm connections. Studies have focussed on alleviating network congestion in areas where wind generation threatens to overload transmission lines. Two such studies have taken place in Northern Ireland [73] and the Humber Estuary [74]. Probabilistic methods were used in the Humber case to assess the cost of constraint under static and RTTR scenarios. The Northern Irish study [73] used historical data to infer that an increase in static rating could be used to accommodate wind generation. Both of these studies sought to solve specific problems rather than present general methods for network planning with RTTR.

There is more literature available on the design and planning of Smart Grids. It is suggested that because Smart Grids as a whole are complex systems, it is prudent to break them into smaller, understandable subsystems [75], while maintaining a holistic understanding of the system.

The planning and design approaches presently used in electrical networks are deterministic; the variables are given fixed values. In a Smart Grid setting, many of the parameters are varying, and would be better represented by some form of probabilistic model [76].

## 2.8. CONCLUSION

This chapter has reviewed literature concerning RTTR: The available technologies, operational schemes, the applications, and the state of forecasting and planning for RTTR. The majority of research in RTTR has focussed on the technical solutions; trying to make sure that the current carrying capacity can be estimated precisely and accurately. This is clearly important, but good technical solutions alone cannot and will not lead to the wide scale adoption of RTTR.

The review of RTTR technologies found that there are a variety of solutions available, each with its own advantages and disadvantages [77]. These limitations suggest that an optimal RTTR deployment would not rely on any one technology. Instead a combination of weather monitors to estimate the

majority of ratings, and line sensors in critical locations, or locations that cannot be well represented by weather monitoring at a remote location, would provide the best overall solution.

Forecasting is widely considered to be one of the cornerstones of a successful RTTR deployment. Although the state of the technology at present is lacking there is research being conducted in this area.

Much of the research is concerned with integration of higher levels of DG, particularly wind generation. Though this is the area where the benefit provided by RTTR is the most exploitable, other applications were identified. RTTR could provide a benefit to network reliability, allow additional load to be connected to otherwise congested areas of network, and defer or remove the need for investment in otherwise mandatory reinforcement projects.

There is an absence in the literature of network planning methods and solutions to facilitate the adoption of RTTR. Without these, network operators will be able to quantify neither the risks nor the benefits of implementing an RTTR system on their network. Consequently, the archival value of this thesis will be to develop these methods. One of the advantages of this approach is that it is not necessary to work on a specific RTTR technology. Since all of the technologies seek to exploit the same additional capacity, all can be considered under a broad set of planning methods. That being said, planning methods could be used to assess which RTTR technology is most appropriate for a particular situation, determine where to place measurement equipment, and which measurement equipment would be most appropriate for a given location.



### 3.1. INTRODUCTION

The primary aim of the work presented in this thesis is to allow the benefits and risks of using RTTR to be quantified at the planning and design stage. One of these potential benefits is allowing additional demand to connect to sections of network that would, according to conventional network design philosophies, require asset reinforcement to support it. This chapter evaluates how to connect additional demand using the Expected Energy Not Supplied (EENS) by a Perfect Circuit method, and proposes an alternative probabilistic method. In a probabilistic method, variables are treated as probability distributions rather than fixed values.

Power network operators are primarily concerned with providing reliable networks. If RTTR was implemented without adequately quantifying the risk to customers, then it could increase risk and be rejected, or be adopted with inadequate regulation and provide little benefit. However, a properly planned and analysed RTTR deployment could actually reduce operating risk, by allowing network operators to see when the line rating is below the static rating and hence take corrective action. The archival value of this work is, not only does it quantify the risks associated with using RTTR to allow varying additional load to connect to distribution networks; it also quantifies the level of risk that is already present in the system. This is coupled with an examination of the existing network design standard in the UK, which this work demonstrates is not fit for purpose for use with RTTR, or indeed any non-deterministic network asset, in its current form.

### 3.2. REVIEW OF NETWORK SECURITY STANDARDS

This section discusses the standards governing security of supply to demand groups in distribution networks. Network security is dominated internationally by the  $N-k$  principle. A network with  $N$  components must be able to service all customers even if  $k$  components are unavailable. In the UK, standard P2/6 governs security of supply during distribution network planning, prescribing the required level of security for different sizes of demand group. During operation, distribution companies are penalised by

the regulator per customer interruption and customer minute lost. While P2/6 is a deterministic standard, assuming all variables have fixed values, there is an exception for the way intermittent generation is treated.

Outside the UK, network planning and security standards at the distribution level are less universal, often being enforced differently by individual distribution companies. In China standards govern transmission level generation adequacy but have little impact on distribution level security of supply [78]. In the USA security standards are set on a state by state basis, with various bodies being involved including NERC (National Electricity Reliability Corporation) [79], PUCs (Public Utilities Commissions) and the utilities themselves. Though transmission level reliability is subject to stringent N-1 and N-2 security, distribution does not have a prescriptive security standard like P2/6. Some PUCs enforce financial penalties to distribution network operators if customers are disconnected, but this is not ubiquitous.

Deterministic, *N-1* style network security criteria can lead to situations where a network is over secure in some circumstances and under secure in others [80]. An Example of this is the use of dual circuits on the same towers to provide redundancy; although this provides sufficient redundancy according to network design standards, in reality there is a significant probability of any failure on one circuit affecting the other [81]. Another example is the assumption that rating values are infallible, when in reality components will be unable to work at this level for some proportion of the time. However, network operators are much more comfortable with these inflexible rules than with a probabilistic method, which can seem complicated and difficult to apply [82].

The impetus is on the industry to change. These variable quantities, which could appear problematic to the existing system, can actually offer benefits to network security. Many authors [83-87] have investigated the advantages Distributed Generation (DG) can provide to network operators. The main benefit discussed is investment deferral; since overhead power lines have a

lifetime cost of around £4m/km [88], the potential savings are significant. Installing DG can defer the need to install new conductors by supplying local loads directly. Intermittent generators, such as wind generation, provide a benefit that cannot be easily quantified. The current standard essentially allows them to add their average output, or capacity factor, to network security calculations [89]. This approach does not take adequate account of the variability of the system and will, like the deterministic criteria of which it is a product, lead to some occasions when the network is overly secure as a result of inefficient design and others when there is a risk of customer disconnection, damage to equipment and infringement of safety standards. While overly secure network design could be seen as desirable, it leads to an increased cost of energy, delays in connecting new loads or generators, and increases the carbon footprint of the power network.

Smart grids, and RTTR in particular, are similar to distributed generation in terms of supplementing network security. The potential benefits of RTTR are much higher than those arising from DG, due to the high average uplift in overhead line ratings [12]. DG is already rated to a fraction of the line rating, and is then further reduced by its low contribution. Conversely RTTR could increase the whole rating by 70% or more. This means the risk introduced by using an inappropriate value for DG is a fraction of that if an inappropriate value is selected for RTTR.

Power system security standards in the UK and elsewhere are inherently deterministic, relying on  $N-k$  criteria to secure customer connections. These standards were developed in a time when implementing a probabilistic or risk based standard would have been impractical due to the lack of appropriate measurement, control, IT and communication systems, and prohibitive computational cost. However with the technologies now available, a risk-based energy security standard is a realistic prospect, and initial evidence suggests it could lead to a reduction in planning and operational costs, without compromising security of supply [90].

### 3.3. METEOROLOGICAL DATA SOURCES

For the studies presented in this thesis, real weather data from 4 sites in the UK were used. Hourly average wind speed, wind direction, solar irradiance and ambient temperature data were available at an hourly resolution for a period of one year. The data was provided by the UK Met Office. There were times when the weather data was not available; the completeness of each data set is shown in Table 3.1, along with the mean wind speeds and temperatures for each site.

**Table 3.1: The weather data used to calculate line ratings for use in this study**

<i>Site</i>	<i>Missing Values</i>	<i>Completeness (%)</i>	<i>Mean Wind Speed (m/s)</i>	<i>Mean Temperature (°C)</i>
<b>Heathrow</b>	296	96.6	3.9	11.8
<b>Glasgow</b>	436	95.0	3.9	9.4
<b>Woodford</b>	538	93.9	3.7	10.2
<b>Valley</b>	28	99.6	6.2	10.9

Valley is both the most complete data set, and has the highest mean wind speed. Given that wind speed has the greatest impact on conductor rating [12], this implies that an overhead line at Valley would have a higher rating than the other sites. The sites are spread across the UK, in a mixture of coastal and inland areas.

### 3.4. CONTRIBUTION OF RTTR BY EVALUATING EENS

A distributed generator can add capacity to the network by directly supplying loads connected to the same substation. This alleviates some of the load on the conductors supplying that substation, allowing more load to be connected. RTTR can offer a similar benefit, supplying additional customers by allowing more power to flow through the existing overhead lines. In either case, the network is designed such that the additional capacity will only be relied upon in a contingency.

The methods in this section, and the probabilistic methods in section 5, consider a simple arrangement of a load connected to the grid through two

overhead lines of the same static seasonal rating. By the N-1 principle, the load cannot exceed the static seasonal rating of one conductor. By deploying RTTR onto the conductors, their ratings can be increased and consequently more load can be connected. The objective is to calculate how much additional load can be connected without compromising security of supply.

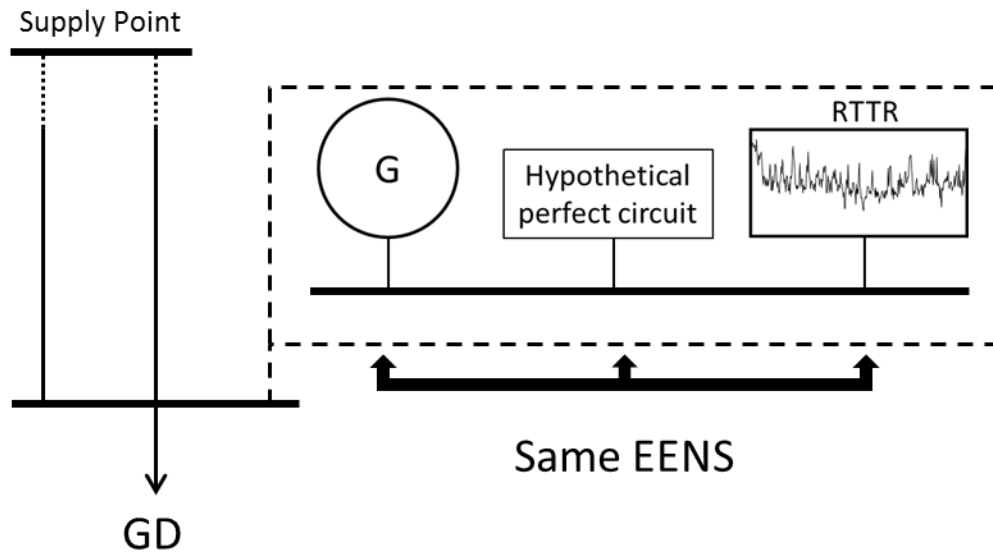


**Figure 3.1:** The typical scenario considered in this chapter; a load connected by a dual circuit, supported by RTTR. Generation and RTTR are compared with a hypothetical perfect circuit [91]. GD stands for group demand.

The additional capacity available is represented by a so called ‘perfect circuit’. This is an additional circuit connected to a load centre with 100% reliability, and the same Expected Energy Not Supplied (EENS) as the variable capacity source, as illustrated in Figure 3.1. This approach uses a single, constant value to represent a variable, probabilistic parameter; this is simple for a network operator to apply, but could lead to a risk of excursion, where the load current exceeds the line ratings, if the number is not selected carefully. The generation is modelled using a capacity outage probability table (COPT) and the load is represented by a load duration curve (LDC).

In the case of RTTR, contribution to security represents the additional percentage of a conductor’s static seasonal rating that can be relied upon in a contingency. This contribution corresponds to the additional load that could be securely accommodated.

### 3.4.1. CONCEPTS WITHIN THE ANALYSIS

The analysis in this chapter draws upon several concepts that may be defined in the security standard P2/6 [89]. These concepts are described here:

- Persistence Time – the time for which a parameter (in this case conductor rating) must remain above a threshold value to be allowed to contribute to network security of supply. Different persistence time requirements are in place depending on the size of a demand group.
- Excursion Time – the time for which the demand is above the conductor rating
- Repair Time – the time taken for an asset to be brought back into service following an outage

### 3.4.2. EXPECTED ENERGY NOT SUPPLIED BY A PERFECT CIRCUIT

In order to calculate the effective capacity of a conductor, the additional capacity due to RTTR is assumed analogous to intermittent generation [91]. The additional capacity is represented by a Capacity Outage Probability Table (COPT). The method necessitates calculating not just the probability of the line ratings exceeding a certain value, but the probability of them exceeding a certain value for a given length of time, referred to as the persistence time,  $T_m$ .

Figure 3.2 illustrates the method used to generate the COPT for the capacity model. The weather data from each site was used to calculate one year of sequential conductor ratings. This was compared to the static seasonal rating. The static seasonal was then increased to give a number of states from 5% extra capacity to 100% extra capacity. This is referred to as the rating level,  $R_i$ . The following steps are then undertaken:

- Identify each instance where the capacity is at least equal to  $R_i$  and continues to be for at least a Persistence Time,  $T_m$ .
- Count the number of times this occurs  $n_i$ , and the duration of each occurrence  $t_i$ .

- If  $T$  is the total time period of the study, then the probability that the capacity is at least  $r_i$ . Is given by:

$$CP_i = \sum_i \frac{n_i \cdot t_i}{T} \quad (27)$$

- This is then repeated for each rating level from 0%-100% additional capacity, and each minimum time  $T_m$  from 1 hour to 168 hours. Each capacity state is given by  $r_i$  and the cumulative probability by  $CP_i$

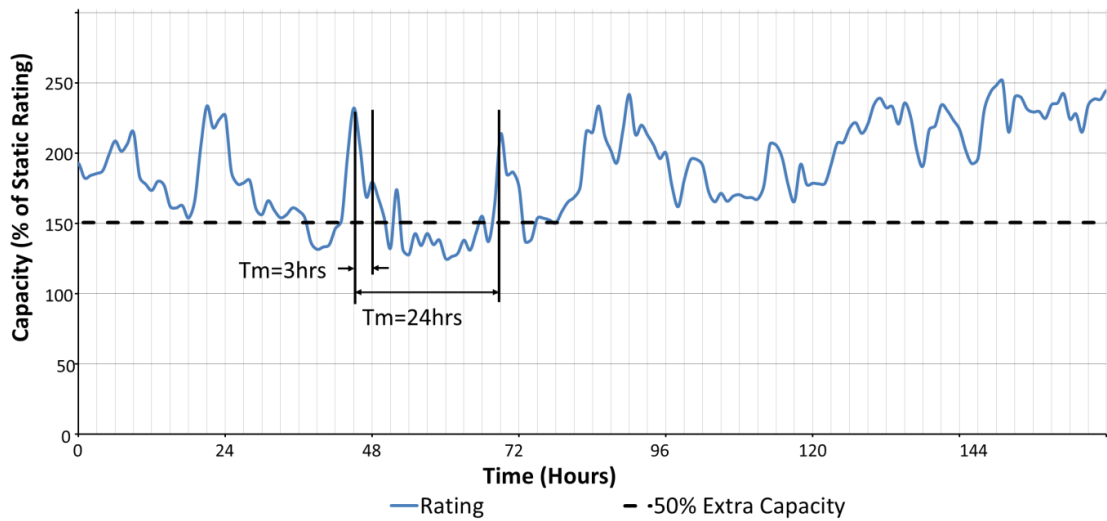


**Figure 3.2:** The method used to determine the capacity model. A time series of ratings data is compared to different fixed values above the static rating, to see if it meets the demand for varying persistence times,  $T_m$ . The figure shows one capacity state (50% extra capacity), and two values for  $T_m$ . For  $T_m=3\text{hrs}$ , the rating remains above the 50% value, and hence this interval would count towards the secure capacity probability. For the  $T_m=24\text{hr}$  interval, the rating falls below the capacity level, and hence the entire interval is discounted.

The individual state probabilities are then obtained from the cumulative probability. These states are then imposed on the LDC as illustrated in Figure 3.3.

The results from the capacity output probability table are used to calculate the effective contribution of the asset by evaluating the EENS:

- Each state of the COPT is superimposed on the LDC as shown in Figure 3.3. In this case it is necessary to determine a maximum possible rating. When using the LDC with a generator, 100% load is set to the maximum generator output. Since there is no set maximum

rating for an overhead line, 100% additional capacity was used as the maximum.

- The energy not supplied,  $E$ , is determined for each state as the area below the LDC and above the capacity available.
- This value is weighted by the probability of being in the capacity state.
- These weighted values of energy are summated over all capacity states (with the sum of probabilities for all capacity states being 1).
- From the concept of expectation:

$$EENS = \sum_{i=1}^n E_i P_i \quad (28)$$

The capacity of a perfect circuit that would give the same level of EENS is then calculated. This is defined as the effective rating of the circuit. This is used to calculate the contribution of RTTR by dividing by the total energy required by the maximum load considered.

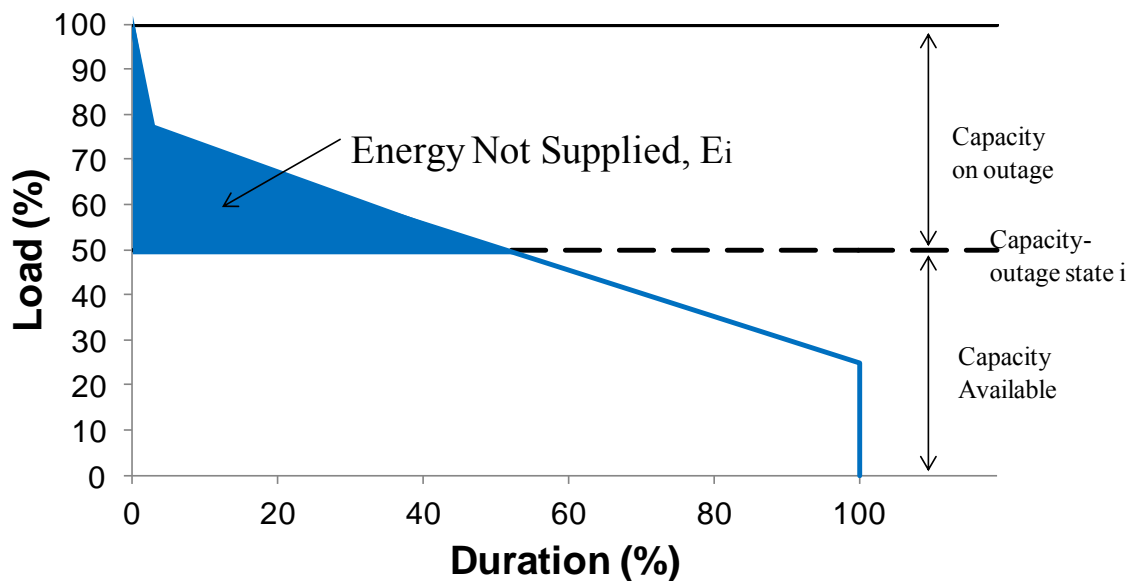


**Figure 3.3: The Load Duration Curve used in this study, showing how energy not supplied is evaluated [91]**

### 3.4.3. RESULTS

The contribution to security was evaluated for each of the four primary sites used for this study. Each case showed a similar pattern, with a high contribution to security decaying as  $T_m$  increased. As would be expected

from the high wind speeds, Valley offered the highest contribution to security in the short term. However, as  $T_m$  was increased Valley's contribution value decayed more quickly than that of the other sites. This could be attributed to the fact that a high average wind speed does not necessarily correspond to a consistently high one.

All of the contribution values were high compared to those attributed to wind generation[91]. However, this is in line with expectations given that wind farms typically have a capacity factor of 25-30% while RTTR offers average rating increases to overhead lines of 70-100% [12].

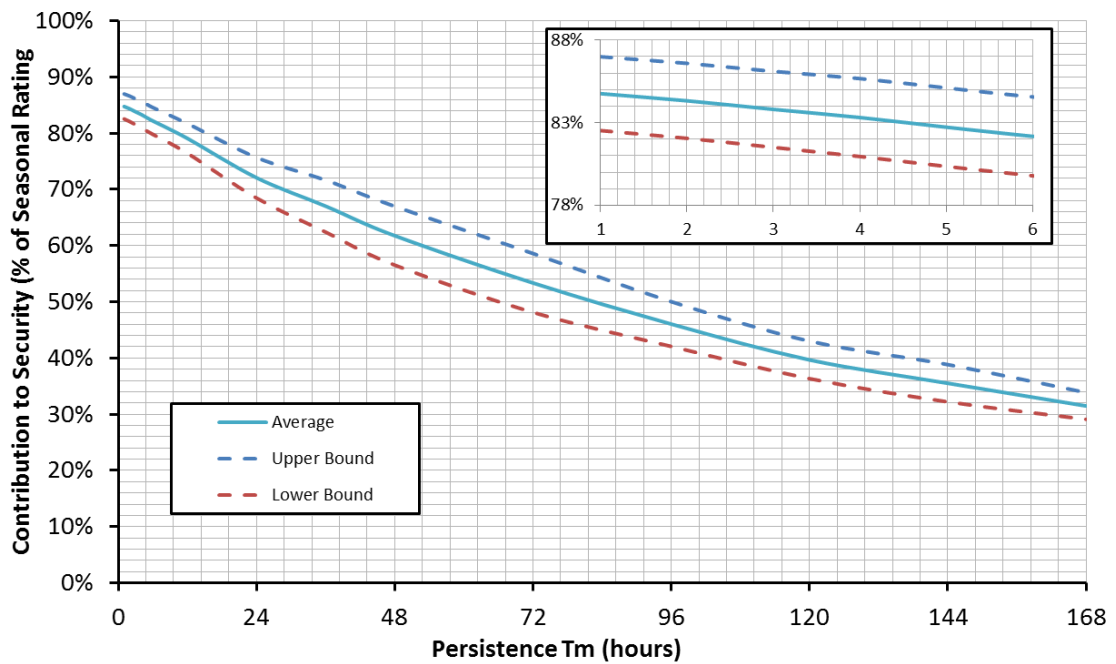


**Figure 3.4:** The mean contribution values for the four sites considered in this study. The upper and lower bounds were calculated as  $\pm 1$  standard deviation between the mean values at the four sites.

Figure 3.4 shows the average security contribution for the four sites. The upper and lower bounds show the results modified by one standard deviation. An equivalent to table 2 in P2/6 for RTTR is presented here:

**Table 3.2:** A new table 2 for P2/6 showing the contribution to security of RTTR as a percentage of the static rating of the conductor

Persistence Tm (Hours)	1	2	3	12	24	120	168
Contribution to Security (%)	83	82	81	76	68	36	29

Based on these results, it would be reasonable to conclude that RTTR can provide a significant benefit to security of supply. Increasing the maximum allowable load by 80% for just the cost of a few sensors and communications hardware seems like excellent value for money. Unfortunately, this method only allows the benefits to be quantified. Electrical networks are operated on a low risk basis, so it was prudent to investigate how increasing the load affects the risk of line ratings being exceeded – a method to quantify this risk is presented in section 3.5.

### 3.5. PROPOSED PROBABILISTIC METHOD

Though the methodology used to calculate the contribution to security in section 4 was inherently probabilistic, no account was made of the level of risk that would be introduced to the system were it implemented. Since the contribution from wind power, for which the methodology was originally conceived, is relatively small, the associated risk could be considered acceptable. However since RTTR provides a much larger contribution to system security, the risks should the technology be misrepresented are proportionally greater. As such it was prudent to investigate these risks before recommending such an approach be taken forward. The first step was to produce probability distributions for the load and the RTTR. These are shown in Figure 3.5.

Figure 3.5 also illustrates the risk associated with using RTTR to increase the load on a section of network. The risk region shows the small area under both curves in which it is possible to for the load to exceed the RTTR. As the load is increased the load PDF will expand to the right, increasing the probability of the load being greater than the conductor rating. Understanding this risk is essential to successfully incorporating RTTR into the industry standards.

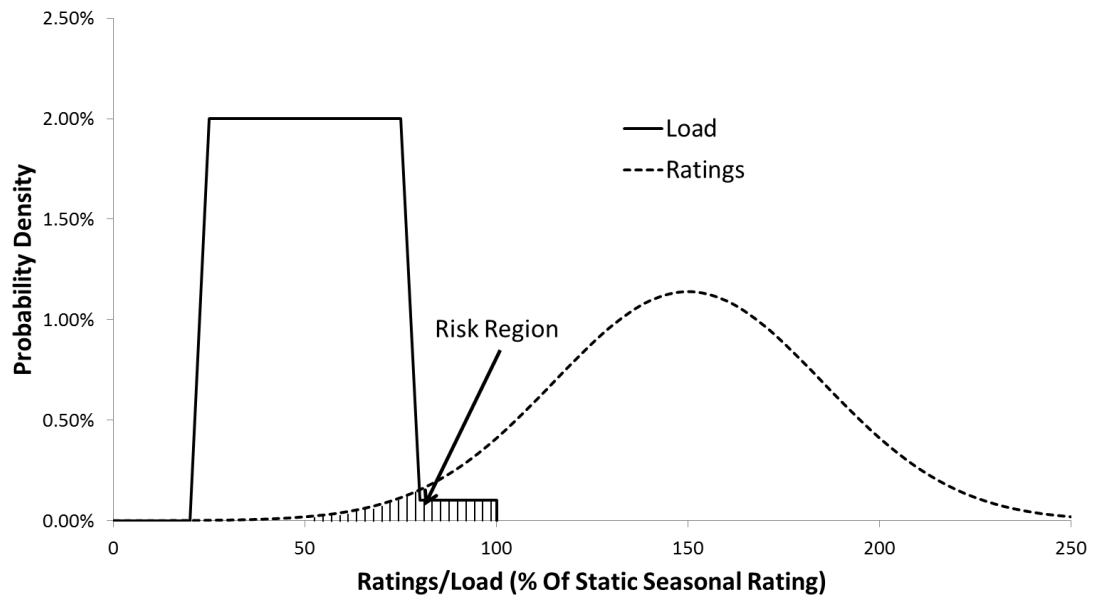


**Figure 3.5:** An illustration of the key problem in overhead line ratings. PDFs of line rating and load are shown, with the region where the two intersect being deemed the Risk Region. The rating curve is illustrative, rather than being based on real data, to ensure that the risk region is large enough to be easily visible.

It is worth noting that although it is unlikely that the highest ratings will be utilised due to external factors such as voltage constraints and protection settings, the rating will still be far above the maximum load. The benefit of RTTR does not lie in trying to unlock the low probability, high rating states, rather in taking advantage of the fact that there is generally a high probability of ratings being above the load.

### 3.5.1. MONTE CARLO SIMULATION

MC methods cover a broad range of computational algorithms for solving problems that involve one or more probabilistic variables. Though there is no set format for a MC simulation, most use some variation of the following procedure:

- Define the domain of possible inputs
- Generate random samples from the domain of possible inputs
- Perform deterministic calculations for each set of inputs
- Aggregate the results

A simple example of a MC simulation is shown in Figure 3.6. The parameter  $Z$  is the sum of two probabilistic variables,  $X$  and  $Y$ . Distributions are formed to represent  $X$  and  $Y$ ; these distributions are then sampled  $n$  times. For each pair of inputs, the calculation  $Z = X + Y$  is performed, giving  $n$  values for  $Z$ . Finally, the  $Z$  values can be fitted to a representative probability distribution.

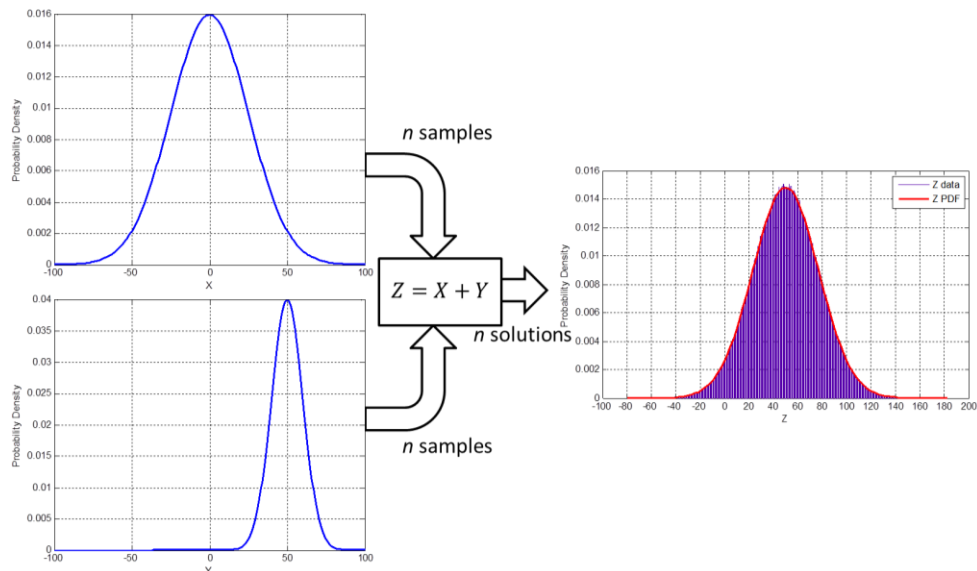


**Figure 3.6:** A simple example of a Monte Carlo simulation. The parameter  $Z$  is dependent on two probabilistic parameters  $X$  and  $Y$ . Through Monte Carlo simulation we are able to evaluate the distribution of  $Z$

**Table 3.3:** The solution to the MC example in Figure 3.6, for different numbers of samples,  $n$

$n$ Samples	$\mu$	$\sigma$
10	37.8	27.2
100	52.3	26.3
1000	48.9	27.4
1000000	50.0	26.907
<b>True Answer</b>	50	26.926

Because the MC simulation relies on randomly sampled input variables, the results will be slightly different each time the simulation is run. However, if the number of samples,  $n$  is large enough, then the simulation can be seen to converge.

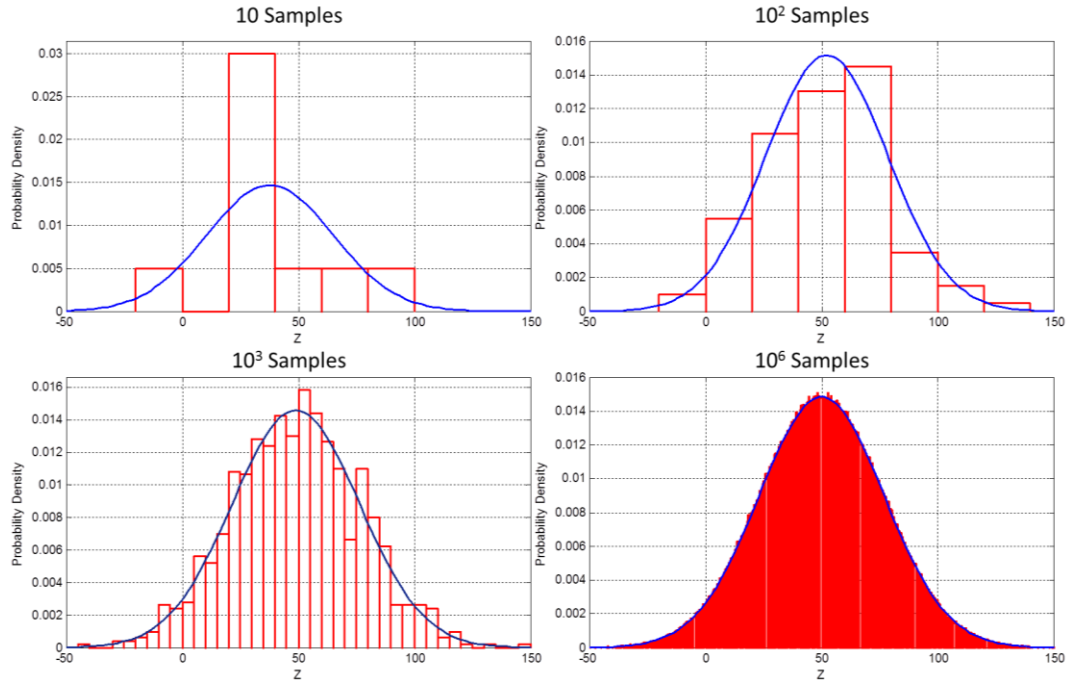


**Figure 3.7:** The solution to the problem illustrated in Figure 3.6, showing the effect of the number of samples,  $n$

The true answer was calculated using equation (29), which is true if  $X$  and  $Y$  are independent random variables that are normally distributed.

$$Z \sim N(\mu_X + \mu_Y, \sigma_X^2 + \sigma_Y^2) \quad (29)$$

Using MC methods is a trade-off between time and accuracy. Large numbers of samples lead to more accurate results at the cost of computational time.

A Monte Carlo approach was used to estimate the risk of the load exceeding the conductor rating. This involved taking a set of random samples from the load and ratings probability distributions, and comparing the two.

The probability of an excursion was then calculated using equation (30):

$$P_{excursion} = \frac{\sum_{i=0}^n \begin{cases} L > r, i = 1 \\ L < r, i = 0 \end{cases}}{n} \quad (30)$$

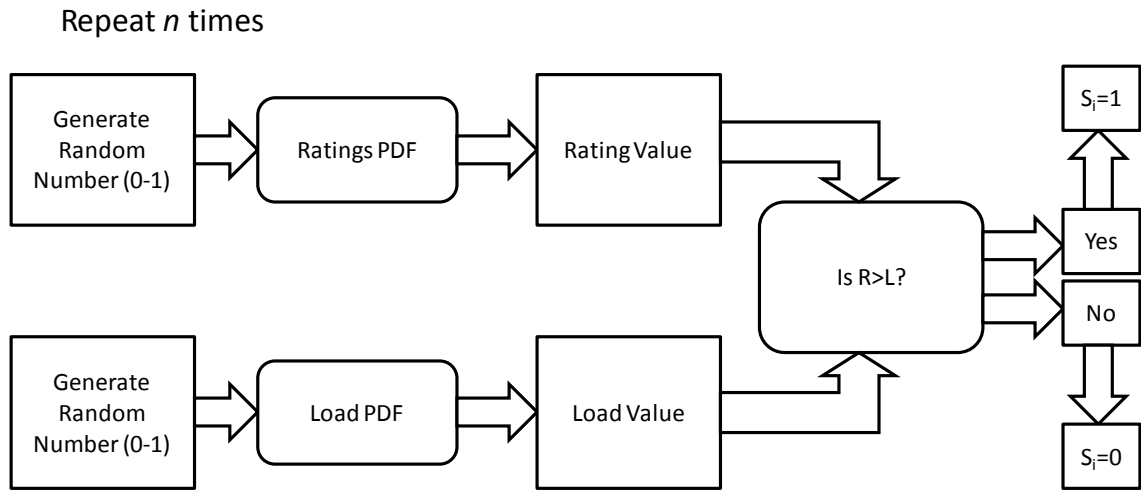


**Figure 3.8: A flow chart showing the steps to evaluate confidence using Monte Carlo simulation**

Where  $L$  is the load,  $r$  is the rating and  $n$  is the size of the sample set. Probability distributions were created for the ratings by fitting non parametric distributions to the CDF data calculated for section 3.4. Non-parametric distributions are models created directly from data rather than by using a conventional distribution and parameters such as mean and variance. This approach allows the persistence values to be considered in the probabilistic evaluation. The PDF calculated from the LDC (shown Figure 3.3) was used for the load. As the contribution to security was increased, the load PDF was increased linearly.

This method calculates the confidence of not exceeding the rating in the event of a contingency. Confidence is defined as the probability that the rating of a single conductor is greater than the load current.

### 3.5.2. RESULTS

Figure 3.9 shows the results of the probabilistic analysis. Confidence values vary from 98% for small contributions and low  $Tm$  to less than 5% for high contributions with  $Tm$  up to one week. This tells a network operator the probability that RTTR will be able to support the network in a given contingency, for varying levels of additional load. The true probability of the ratings being exceeded is the product of the probability of a contingency and the probability of an excursion. The confidence values corresponding to the contributions suggested by the Equivalent EENS method are very low; this

illustrates how inappropriate that method is for RTTR. The confidence values are provided in tabular form in Appendix 2.

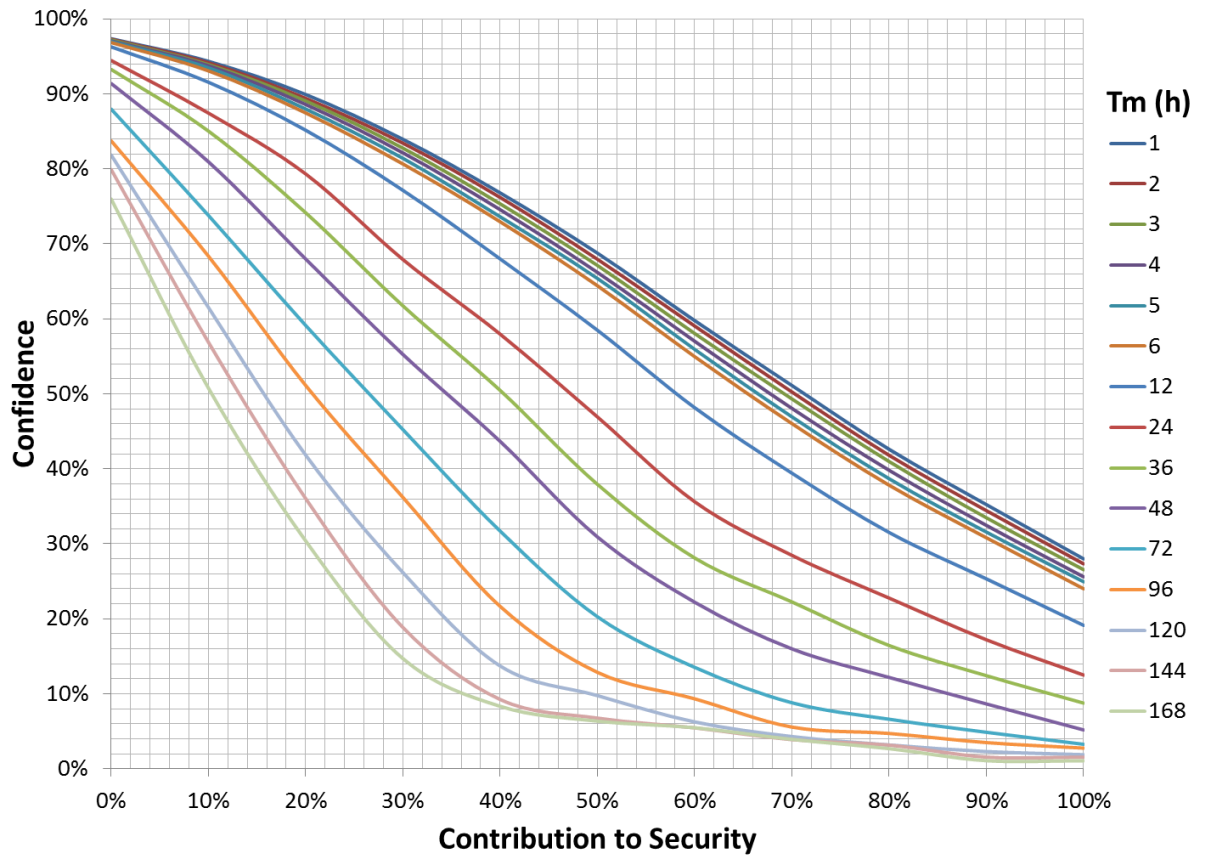


**Figure 3.9: Plot of confidence of not exceeding ratings against contribution to security, with  $T_m$  varying from 1 hour to 168 hours**

### 3.5.3. REPAIR TIMES

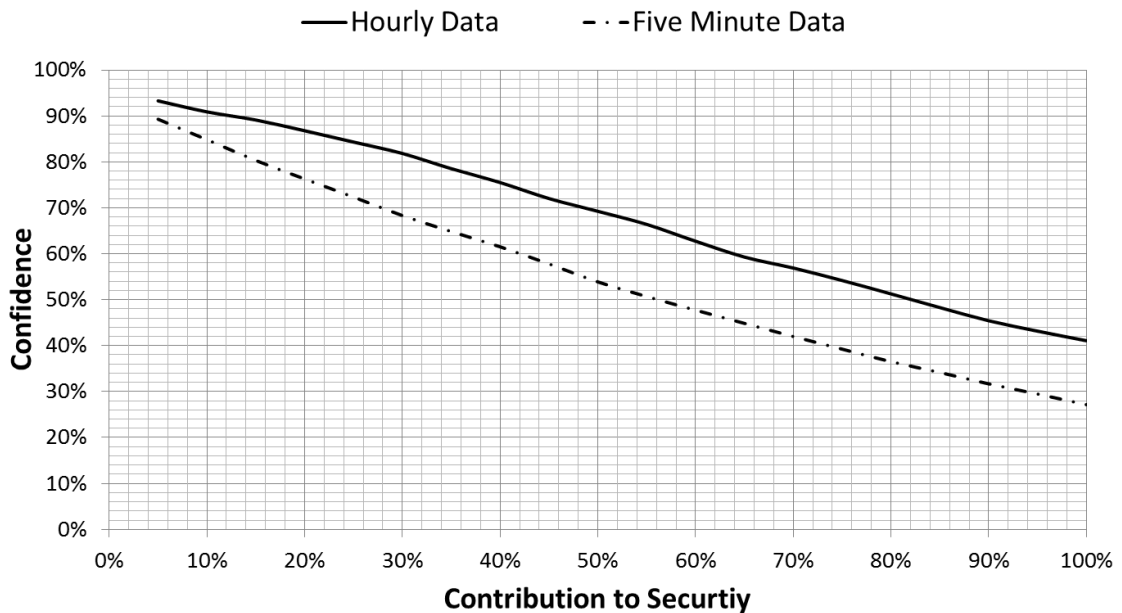
The persistence values are important for network operators because they provide information about not only how much capacity can be relied upon, but also how long it can be relied upon for. These times can be related to network repair times. Based on the distribution suggested by [92], Table 3.4 shows the percentage of faults that are restored within different durations. Data from the National Fault and Interruption Reporting Scheme (NaFIRS) was considered, but the data available was not appropriate or sufficient for the purposes of this work – the data was only available in an aggregated form, so it was not possible to calculate the necessary statistics.

**Table 3.4: Typical repair times for overhead line faults**

Time	5 mins	30 mins	1 hour	2 hours	3 hours	6 hours	12 hours	24 hours
% of Faults Repaired	0.00%	1.06%	9.07%	35.60%	57.79%	87.77%	98.34%	99.90%

The majority of faults are repaired within 6 hours, which corresponds to confidences of 83% and above for capacity increases up to 30%. Most outages in excess of 12 hours are a result of planned maintenance. In these cases, the outage is often planned such that the network can be restored quickly in the event of a contingency.

#### 3.5.4. IMPACT OF DATA TEMPORAL RESOLUTION


**Figure 3.10: Effect of data resolution on confidence levels for  $T_m=3$  hours**

The results presented have used data recorded at a temporal resolution of one hour. Since the time constant of an overhead line is 10-20 minutes [23, 93], the sampling theorem suggests that using 5 minute data would be more appropriate. The time constant of the overhead conductor is dependent on wind speed, with lower time constants at higher wind speeds. This is helpful from an RTTR perspective, since the rating is greater at higher wind speeds, so sudden changes in current are less likely to cause overloads in these cases.

Figure 3.10 shows the effect of data resolution on the proposed probabilistic method. Using 5 minute data reduces the confidence by around 5% for low contributions, and around 15% for high contributions; the author suggests this reduction be applied if using hourly data to estimate the contribution of RTTR.

### 3.5.5. DEFINITION AND QUANTIFICATION OF RISK

Knowing the likelihood of an excursion is not enough to understand the risk it poses to a network. Risk is defined as the product of likelihood and consequence. The likelihood in this case corresponds to the probability there is an outage leading to an excursion. The consequence represents the severity of the action that must be taken by network operators to avoid endangering the public and damaging equipment. For example, a small excursion, for only a short time, is unlikely to cause damage to equipment or endanger the public, since the conductor will not have time to heat up to its steady state temperature. However a large excursion is more likely to have severe consequences. For the purposes of this thesis, severity and duration of an excursion will be considered equal contributors to network risk. This leads to the definition of risk:

$$Risk = P(excursion).P(contingency).S_{excursion}.T_{excursion} \quad (31)$$

Where  $P$  is probability,  $S$  is severity and  $T$  is average excursion time. Figure 3.11 illustrates that the risk associated with using RTTR in network security is primarily associated with excursions of 5-30% above conductor rating. Larger excursions are unlikely to occur, while smaller excursions are unlikely to damage equipment, trip a circuit or cause overhead lines to breach clearance restrictions.

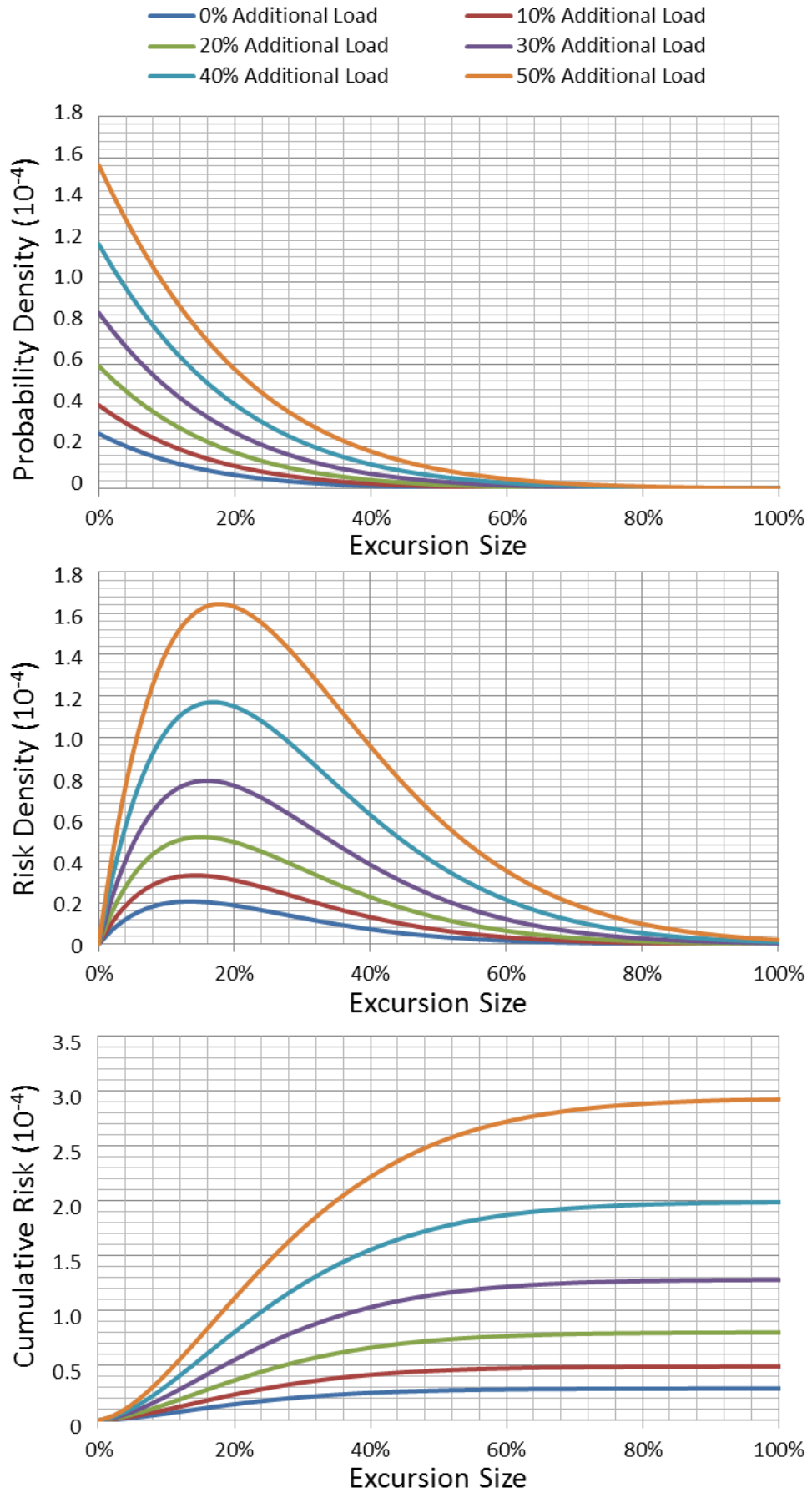
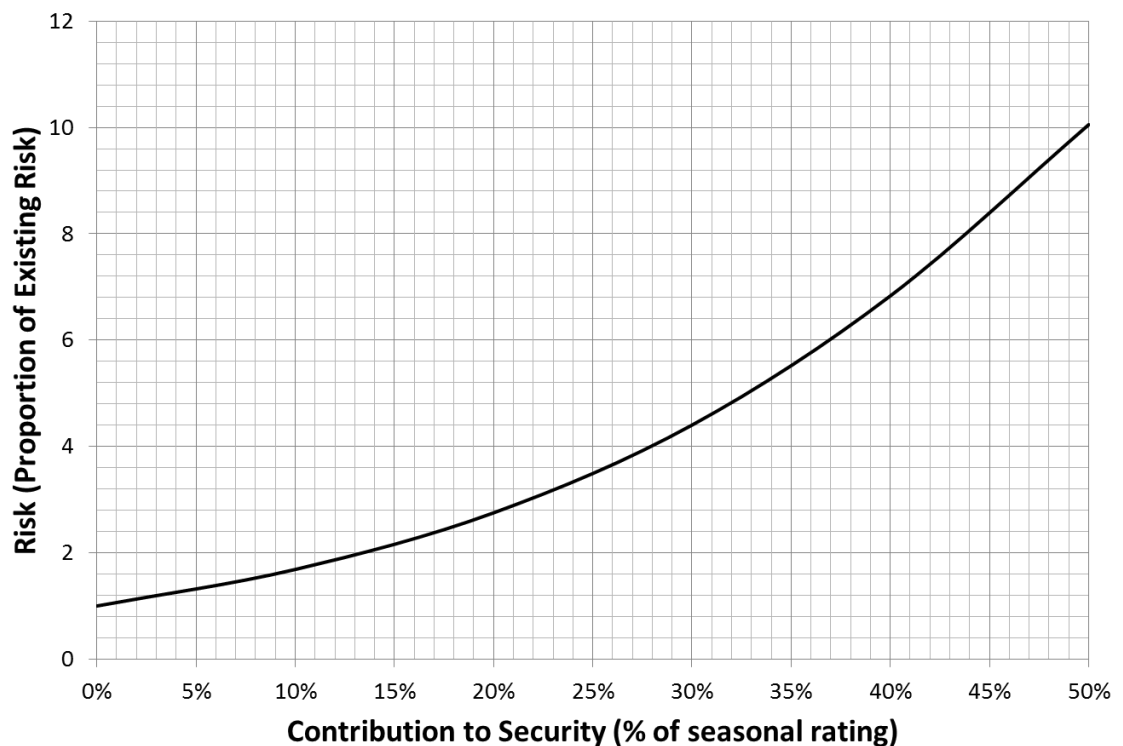


Figure 3.11: Probability density, risk density and cumulative risk plots for excursions above static seasonal ratings

The excursion probability distribution was generated by an MC evaluation of the difference between the load and the rating. Figure 3.11 shows the tail of the distribution associated with the load being greater than the rating. The risk density plot is the product of the excursion PDF and the consequences described in equation (31); the average excursion length was assessed using a similar method to that described in section 4.2, but calculating the average time for which the rating was below the load, using real load data, rather than the probability of it being above an arbitrary value.



**Figure 3.12: Risk associated with varying contributions to security. This curve was derived by plotting the final value of the cumulative risk curves shown in Figure 3.11**

It is important to understand how the level of risk varies as the contribution to network security increases. Figure 3.12 shows the total risk associated with increasing the maximum permissible load by up to 50% of the seasonal static rating. This was calculated by evaluating the cumulative risk for each additional load case and comparing it to with the risk associated with the static rating. The results indicate that adding an additional 50% load would lead to an increase in risk of approximately one order of magnitude. Smaller

increases in load yield much smaller increases in risk, with an additional 15% load corresponding to a doubling in the existing risk.

These increases in risk seem alarming, but there are a number of factors which mean that increasing the load through the use of RTTR is a very real possibility. First, the existing risk is incredibly low; the conservative design of networks means that the majority of the time equipment is operated far below its static rating. Secondly, the increase in risk can be offset by active monitoring and control. A doubling of risk seems much more acceptable when it is accompanied by the ability to perceive and take action against not only this new risk, but the existing risk as well. Excursions will only occur when peak load and low RTTR coincide with a contingency. If DSR were used to reduce the peak loads [94], the risk would be reduced. Additionally, if energy storage or DG was available during low rating events, the risk could again be reduced. Normally open points at lower voltage levels could also be closed to alleviate the increased power flows. All of this is made possible by the increased observability of the network's ratings provided by RTTR.

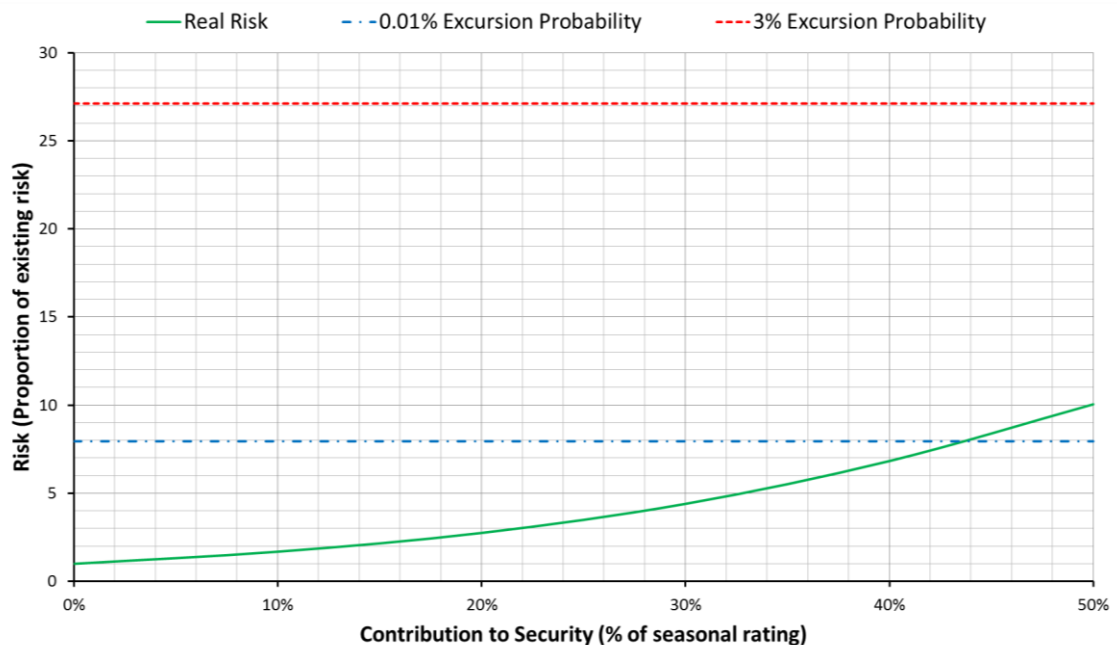


**Figure 3.13: The total risk associated with connecting different levels of demand to a network using RTTR. The risk deemed acceptable by the UK line rating standard, P27 [11], are also shown to provide additional context to the calculated risks.**

Additionally, it is interesting to observe that the P27 standard sets the rating with a degree of risk, but does so assuming that the conductor is always being utilized at 100% of its static rating [11, 95]. In other words, P27 only considers the rating to be variable, and does not consider its interaction with demand. The assumed risk associated with the P27 dual and single circuit ratings are plotted along with the actual risk in Figure 3.13. The excursion risk associated with connecting 50% additional load is comparable to the risk assumed for a single circuit by P27, and far lower than the risk assumed for a dual circuit by P27.

Details of the method and data flow for the methods presented in this chapter are illustrated by a flow chart in Appendix 3.

### 3.6. CONCLUSIONS

This chapter has described a new probabilistic method for power network planning, allowing additional load to be connected through the additional capacity provided by RTTR. This additional capacity can be accommodated at a quantified level of risk, ensuring safe and secure operation. Though increasing the level of load above the maximum load permitted by the  $n-1$  principle leads to an incremental increase in the risk of tripping a circuit or disconnecting customers, using RTTR to increase load should still be considered a valid option for connecting additional load without the need for new infrastructure. Because RTTR will increase the thermal visibility of the network, operators will be able to take corrective action to mitigate not only any additional risk introduced through the implementation of RTTR, but also on the risk that is already present in the system. An appropriately planned RTTR deployment could lead to increased network capacity and safer operation.

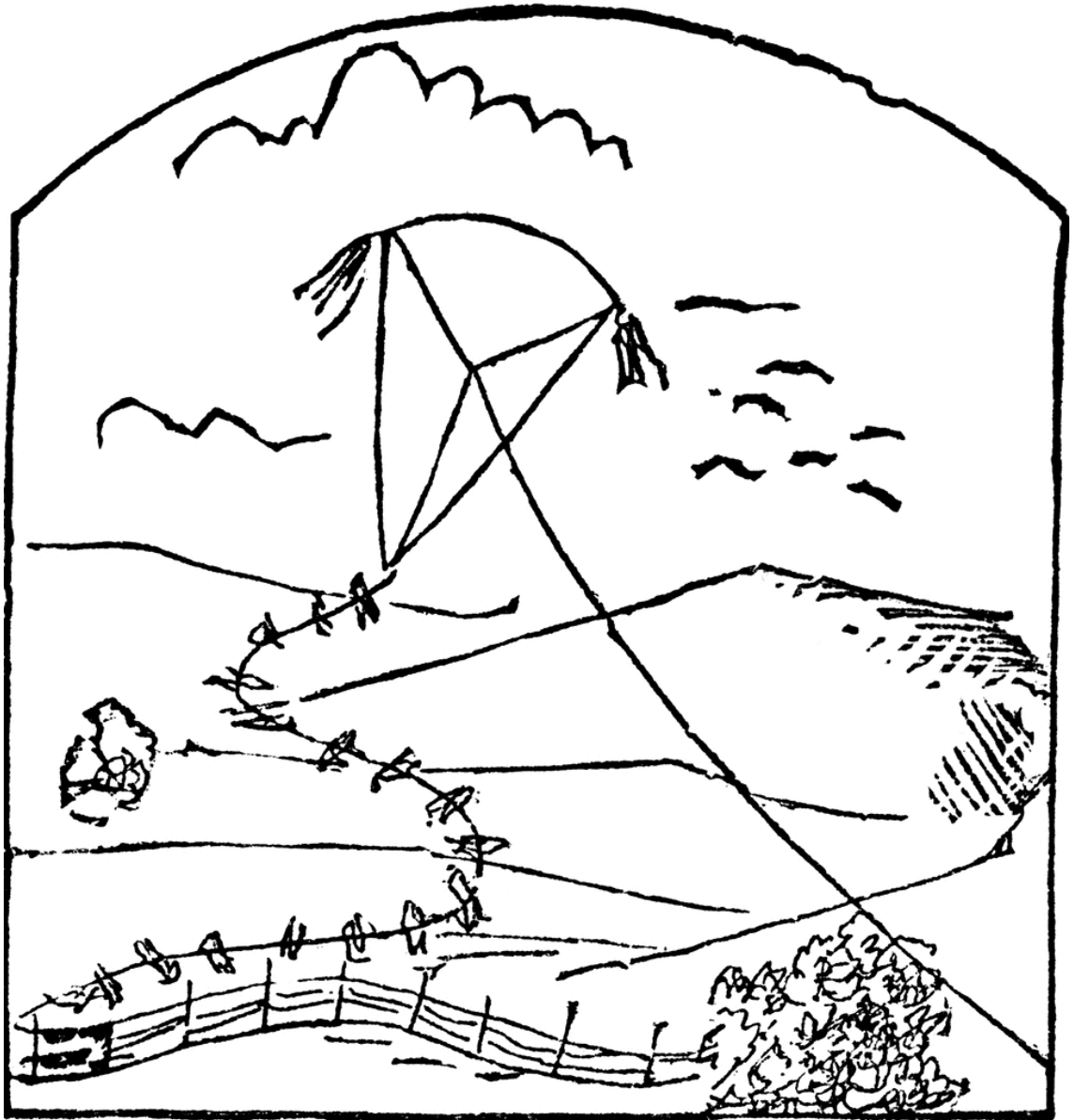
The method used Monte Carlo (MC) simulations to calculate the probability of line rating being sufficient to meet demand for varying load cases. Probability distributions of excursions above RTTR were derived to quantify the risk to security of supply, which was defined as the product of the probability, severity and duration of the excursion. Although the results in

this chapter use weather data from across the UK, any real RTTR deployment will be highly dependent on the local weather conditions, the alignment of the conductors relative to the prevailing wind direction, sheltering effects near to the line (such as trees or buildings) and anticipated load patterns. Consequently, confidence and risk values will vary on a per site basis.

Though initially the problem was approached from the perspective of the existing network planning framework in the UK, the method used to represent variable contributions to network security was found not to be fit for purpose. Representing variable quantities using single values and taking no account of the risk and uncertainty is unlikely to yield a successful RTTR implementation. Instead, the model proposed removes a fundamental barrier to the adoption of RTTR. By allowing network operators to see the benefits and the associated risks arising from adoption of RTTR at the network planning stage, this work can build confidence in the technology and demonstrate, at the network planning stage, that RTTR is a real alternative to costly network reinforcement. Intelligent, rigorously planned RTTR schemes have the potential to save billions of pounds that could otherwise be required for network reinforcement, and can unlock the additional capacity in a fraction of the time that would be required to build new infrastructure. The confidence values determined through this research suggest that RTTR is well suited to provide additional network capacity in the event of faults, most of which are resolved within a few hours.

Finally, although this thesis has only discussed this method within the context of RTTR, the probabilistic planning method put forward here could be used with other variable network technologies. The state of charge of energy storage, the variable impact of Demand Side Response and the variable output of distributed generation could all be accounted for using the method presented in this thesis. This could pave the way to a single, probabilistic framework for the planning of smart grids.

## Chapter 4. Wind Simulations: Modelling Approach



## 4.1. INTRODUCTION

This chapter describes the method used to estimate wind flow using Computational Fluid Dynamics (CFD) simulations. The motivation and applications for undertaking this work are considered, the relevant literature is explored to ensure that the methodology used is valid and robust. Following this the method is described in detail, and an industry standard case study is presented to illustrate that the methodology uses best practice and produces accurate results.

## 4.2. MOTIVATION

The sensitivity analysis in section 0 and [12] show that wind speed has the greatest impact on conductor current carrying capacity by a significant margin. Wind direction also leads to significant variations in current carrying capacity, having a comparable impact to ambient temperature. Figure 4.1 shows the variation in current carrying capacity based on varying only these parameters, with solar radiation fixed at 0 and ambient temperature at 10°C. Wind speed and direction are variable on space scales varying from metres to kilometres, particularly in complex or hilly terrain [96]. Being able to properly account for this variation is important for both planning and operation of RTTR in power systems.

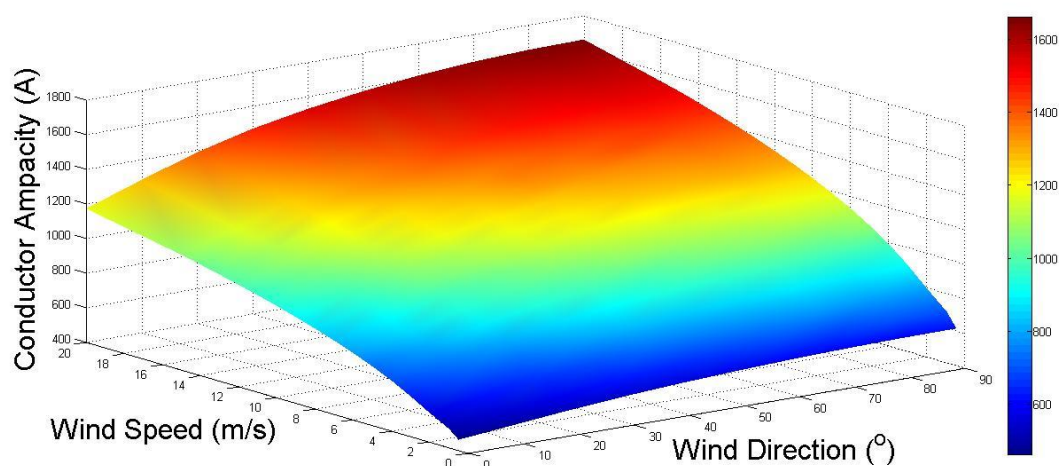


**Figure 4.1: The effect of wind speed and direction on the rating of a 132kV Lynx conductor in 10°C ambient conditions**

In the wind energy industry, micro scale numerical wind simulations are used to predict energy yields [97], site turbines within a wind farm [98, 99] and evaluate turbine wake effects [100]. This approach has been adapted to calculate the wind speeds and directions incident to overhead conductors.

### 4.3. BACKGROUND

Wind speed and direction can vary on small space and time scales. One of the difficulties in rating estimation is that wind flow patterns are dependent on the underlying terrain, roughness, orography, local sheltering and regional wind climatology [101]. These must be accounted for to allow accurate prediction of wind flow, and hence conductor rating.

Up to now, the main applications for wind models on this scale have been wind energy resource assessment [101] and pollutant dispersion [102]. Though these applications have some distinct features; wind resource assessment is concerned with finding locations with high average wind speeds [103] and pollutant dispersion simulations focus on urban terrains [104], while the majority of overhead lines are in rural areas. In spite of this, many of the general solutions are relevant to wind estimation for RTTR, where the interest is in wind speed and direction at specific times and locations.

#### 4.3.1. THE ATMOSPHERIC BOUNDARY LAYER

The wind flows that affect RTTR take place in the atmospheric boundary layer. This is the layer of air directly above the Earth's surface, which is directly influenced by the surface through its shape, roughness and temperature [105]. The forces that influence the ABL include frictional drag, evaporation and transpiration, heat transfer, pollutant emission and terrain induced flow modification [106]. This layer is close enough to the Earth's surface that effects that are important in the upper atmosphere, such as the Coriolis forces arising from the Earth's rotation, can be ignored. The ABL is commonly assumed to be neutrally stable, meaning the surface-boundary interaction is assumed to be a purely mechanical process [107], this means

that all of the aforementioned influences, save frictional drag and terrain induced flow modification, are ignored.

Like all fluid flows, wind flow is described by the Navier-Stokes equations for fluid motion:

$$\frac{\delta\rho}{\delta t} + \nabla \cdot (\rho\mathbf{u}) = 0 \quad (32)$$

$$\frac{\partial\mathbf{u}}{\partial t} + (\mathbf{u} \cdot \nabla)\mathbf{u} + \frac{1}{\rho}\nabla p = -\frac{1}{\rho}\nabla p + \mathbf{F} + \frac{\mu}{\rho}\nabla^2\mathbf{u} \quad (33)$$

$$\rho\left(\frac{\delta\varepsilon}{\delta t} + \mathbf{u} \cdot \nabla\varepsilon\right) - \nabla \cdot (K_H\nabla T) + p\nabla \cdot \mathbf{u} = 0 \quad (34)$$

Equation (32), (33) and (34) show the continuity, momentum and energy equations respectively. In these equations  $\mathbf{u}$  is a velocity vector field,  $p$  represents pressure,  $\rho$  is density,  $\mu$  is dynamic viscosity,  $t$  is time,  $T$  is temperature,  $\varepsilon$  is internal energy,  $\mathbf{F}$  is external force per unit mass,  $K_H$  is the heat conduction coefficient and  $\nabla = \frac{\partial}{\partial x} + \frac{\partial}{\partial y} + \frac{\partial}{\partial z}$ . The system is also represented by an equation of state; in this case the perfect gas law, in which  $R_{gc}$  is the gas constant:

$$\frac{p}{\rho} = R_{gc}T \quad (35)$$

Atmospheric boundary layer modelling is a complex field in its own right. Though the CFD modelling is a tool within this research, the methods used are described in some detail to illustrate that state of the art simulations were used to produce high quality results.

#### 4.3.2. TURBULENCE

As the wind speed increases, the structure of the flow breaks down and the flow becomes turbulent. Turbulent flow is characterised by its chaotic nature [108], as opposed to a laminar flow in which the fluid moves in a steady manner. Turbulent flow is difficult to model due to its unpredictable nature and the large number of complex shear forces –unaligned forces pushing one part of the fluid in one direction, and another part in the opposite direction– acting between eddies in the fluid. However, turbulence

has effects on how the flow behaves, so it must be accounted for in an accurate fluid flow model [108].

#### 4.3.3. REYNOLDS AVERAGING

No general solutions exist for the Navier-Stokes equations. Because many applications depend on being able to model fluid motion, approximations must be made so that meaningful solutions can be achieved. Reynolds decomposition removes the time-variant components of the Navier-Stokes equations. Equation (36) shows a quantity  $u$ , decomposed into  $\bar{u}$ , the time averaged component and  $u'$ , the fluctuating component.

$$u = \bar{u} + u' \tag{36}$$

These equations are then averaged, and since the average of a fluctuating component is zero, these components are removed. The resulting equations are known as the Reynolds-Averaged Navier Stokes (RANS) equations. They contain a non-linear stress term, referred to as the Reynolds Stress, which requires additional modelling to close the RANS equations for solving. Many different turbulence models have been created to allow the solution of this problem. These turbulence models provide approximate numerical solutions through the use of discretised computer code known as Computational Fluid Dynamics (CFD). It is worth noting that while CFD can also be used to solve laminar flows, all simulations presented in this thesis use full turbulence models.

#### 4.3.4. WIND FLOW SIMULATIONS USING CFD

CFD allows the differential equations governing fluid flow to be solved numerically. The problem is decomposed into many smaller problems using a grid, and the equations are discretised. If sufficient care is taken in the set up and solution, CFD can provide an answer that is a reasonable representation of reality [109].

In recent years CFD has increasingly been used by the wind energy industry for turbine siting and energy yield prediction [97-101]. This has proved most useful in rough or complex terrain, where other options such as

spatial interpolation and linear models [110] fail to predict nonlinear effects such as separated flow regions [99] (fluid flow usually follows the shape of the surface over which it is flowing, but in certain, complex cases it is unable to do so, and separates from the surface). A comprehensive review of the techniques used by the wind energy industry is provided by *Sumner et al.* [111].

The majority of flow modelling over complex terrain has used the RANS equations, with a two equation turbulence model. It is suggested that simpler turbulence models lack the sophistication to handle phenomena such as recirculation [111]. The RNG (Re-Normalisation Grid)  $k-\epsilon$  turbulence model has proven the most successful model for flow over real terrain [112, 113].

Large Eddy Simulation (LES) represents an alternative to the RANS equations. In LES low pass filtering is applied to the Navier-Stokes equations to remove the small scales of the solution, reducing the computational cost [114]. However, the computational burden is still greater than that of RANS solutions, primarily due to the grid requirements in the near-wall region (in this case the area next to the terrain) [115].

#### 4.3.5. WIND FLOW OVER TERRAIN

The terrain over which the wind blows can be broken down into two parts; the orography (the ground elevation) and terrain features (what is on the ground). Modelling wind flow over the orography is relatively straight forward; the orography can be used to create a surface geometry around which a mesh can be constructed. The terrain features can include trees, shrubs, and buildings, which affect wind patterns. Terrain roughness has a strong influence on wind speed in the zone near the ground.

Conventionally the terrain features are represented by a so called ‘sand grain’ roughness on the surface [116]. This roughness modifies the shape of the flow boundary layer depending on the roughness [117], which in turn alters the flow. This approach has been the subject of some criticism in ABL simulation, specifically as to whether it is possible to create a flow that

properly sustains itself throughout the domain using the standard models available in CFD packages [107, 118].

Since the terrain is modelled as a surface roughness rather than fully realized 3D objects, effects such as sheltering from vegetation are not represented. The flow of air through vegetation canopies can be modelled [119], but not on the scale required for this application. In wind energy resource assessment the flow over the canopy can be modelled, but not the flow within the vegetation [120]. Detailed simulations can be run over urban areas, but not on the large scales required for RTTR [121]. This means that while the simulations can accurately model changes in the shape of the boundary layer, they do not account for effects such as the wakes behind buildings or woodland, or the flow within these complex features.

#### 4.3.6. ALTERNATIVE METHODS

CFD is not the only method for estimating local scale wind flows. Previous, weather based, RTTR studies used inverse distance squared interpolation to estimate all weather parameters [44]. An alternative means of improving the estimation of wind speed would be to employ a more meaningful interpolation method such as Kriging [122]. However this would not have provided information about how the local terrain affects wind flows, which could be essential for identifying thermally vulnerable sections of network.

Another option was to try and establish the relationship between the wind flow and the local terrain using linear models; linear solvers such as WASP, [123] based on a wind atlas methodology reduce computational complexity, but lose detail when nonlinear phenomena are present. A method for using empirical correction factors and fractional speed-up ratios to account for roughness and terrain features is presented in [124]. This would not be appropriate when many features are present in a complex geometry, as is likely to be the case for real overhead line studies.

#### 4.3.7. FLOW SOLVERS

The decision was taken to use a RANS solver as one of the key variables required was the wind direction which was felt to be heavily influenced by the local terrain. The available options were:

- Nonlinear flow solvers such as WindSim [48] and RAMs [125] that are designed for modelling atmospheric flows, with WindSim being specifically designed for wind farm design [126].
- General purpose CFD packages, such as FLUENT 12.1 [127] that allow high levels of user customization.

Fluent had been used for wind simulations, and produced results comparable to dedicated wind modelling software [128, 129]. Consequently, it was considered an appropriate choice, and was used to perform the CFD simulations presented in this thesis.

### 4.4. METHODOLOGY

This section describes the methodology used to perform the CFD wind simulations to allow improved planning and operation of power systems with RTTR.

#### 4.4.1. INPUT DATA

To construct the CFD model, data is needed to represent the terrain and underlying orography. Orography data was available from the Ordnance Survey Digimap service. This data was in the form of a ‘point cloud’; grid spacing and starting coordinates are specified and the elevation at each point is provided. These data are used to create a 3D surface model of the orography.

Terrain data were provided by Astrium GEO-Information Services. The data was captured by LiDAR survey, and has a resolution of up to 0.5m [130]. The data categorises different terrain features by their roughness; these categories were then assigned a roughness height for use in the CFD simulation based on industry standard values [131], as shown in Table 4.1.

The height above ground for each terrain element was also available, but attempting to model this level of detail was beyond the state of the art for large scale wind simulation.

**Table 4.1: Terrain classes and the corresponding surface roughness values from the LiDAR data**

<i>Class</i>	<i>K<sub>s</sub> (m)</i>
Sea	0.0001
Inland Water	0.0001
Artificial Surfaces	0.015
Buildings	0.5
Bare Ground	0.0025
Herbaceous Vegetation	0.015
Shrubs	0.125
Tall Shrubs	0.25
Trees	0.5

In areas with large amounts of vegetation, it may be prudent to carry out simulations with two sets of roughness data: one observed in summer when there are leaves on plants and trees, and one in winter when much of the vegetation is bare.

#### 4.4.2. MESH CONSTRUCTION

The next stage in the CFD process was to create the computational mesh around the 3D surface model. The structure and quality of this mesh affect the duration and quality of the numerical solutions [132]. For this application, it was important to have a large number of cells close to the terrain; this is where the most complex interactions take place, and is where the power lines were to be located, hence the area of interest. The cells then grow in size as they expand upwards into the ABL. This reduces the computational requirements, but is not detrimental to the results since this is far from the area of interest, and there are few complex interactions at this altitude. It is also necessary to use a finer grid where the underlying orography is particularly complex. An example of this mesh structure is shown in Figure 4.2.

There are three categories of mesh available: structured, unstructured and hybrid. Structured mesh comprises of hexahedral elements, unstructured

mesh comprises of tetrahedral elements, and hybrid mesh contains both elements. Structured mesh provides better solution quality and less computational effort, but unstructured mesh can be created via automated mesh generation, which reduces the time required by the user, and can be applied to more complex geometries [132]. Structured mesh was used in this application, but wind simulations featuring fully modelled terrain features, such as building and vegetation, would likely have to use automatically generated, unstructured meshes, since the geometry would be too complicated to mesh manually.

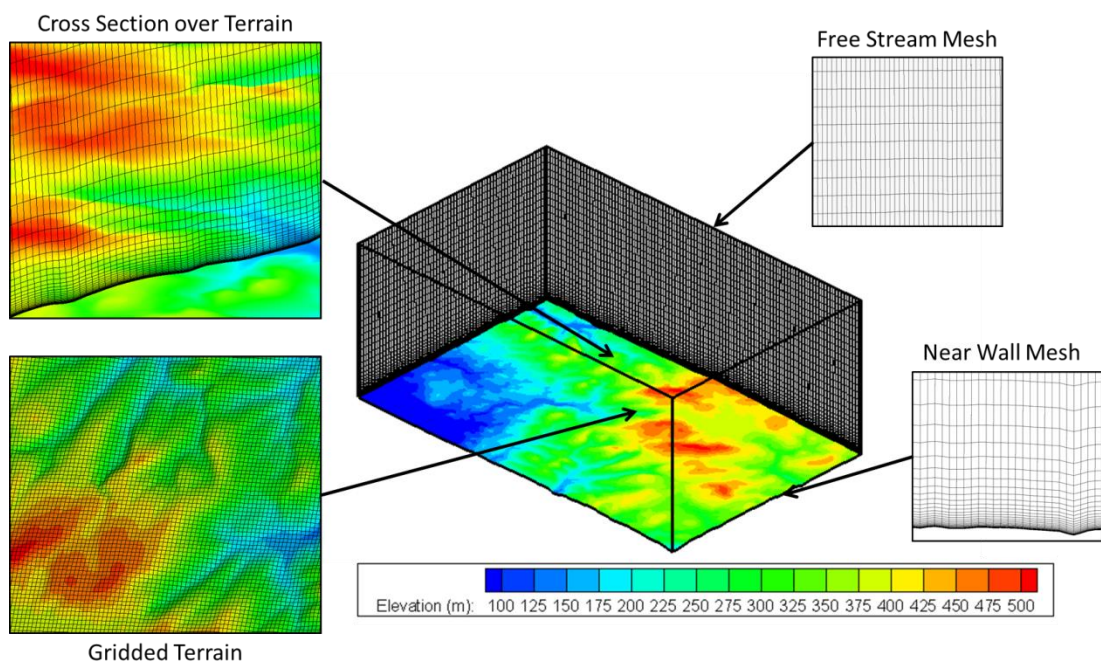


**Figure 4.2:** An illustration of mesh structure, with small cells close to the boundary and larger cells at higher altitudes. The mesh is also refined where the terrain is particularly complex. This illustration shows a structured hexahedral mesh.

#### 4.4.3. BOUNDARY AND INITIAL CONDITIONS

In order to run the calculations, boundary conditions (BCs) and initial conditions (ICs) must be properly set up to ensure speed and accuracy. There are four types of BC in the FLUENT calculation:

- Inlets, where the fluid flows into the domain. The speed and direction, as well as the turbulent properties can be specified across the domain. This is set to represent the incoming wind flow. The wind is assumed to be

stationary at the interface with the ground, with the velocity increasing as the distance from the ground increases, forming a boundary layer profile. This can be represented using a power or log law, an example of this from the Bolund Hill validation study (section 4.6) is shown in Figure 4.3. The boundary layer is dependent on the underlying terrain, but it will develop naturally as part of the simulation, assuming the areas of interest are not too close to the inlets.

- Outlets, where the fluid leaves the domain. Again the speed and direction can be set, though this is typically derived from a neighbouring cell.
- Walls. This BC is only used for the terrain and it incorporates a roughness profile to represent the physical terrain on the surface. It applies a law of the wall and non-slip condition.
- Symmetry. This is used to apply a frictionless wall, and is used for the top of the domain, as well as for any sides that are neither inlets nor outlets.

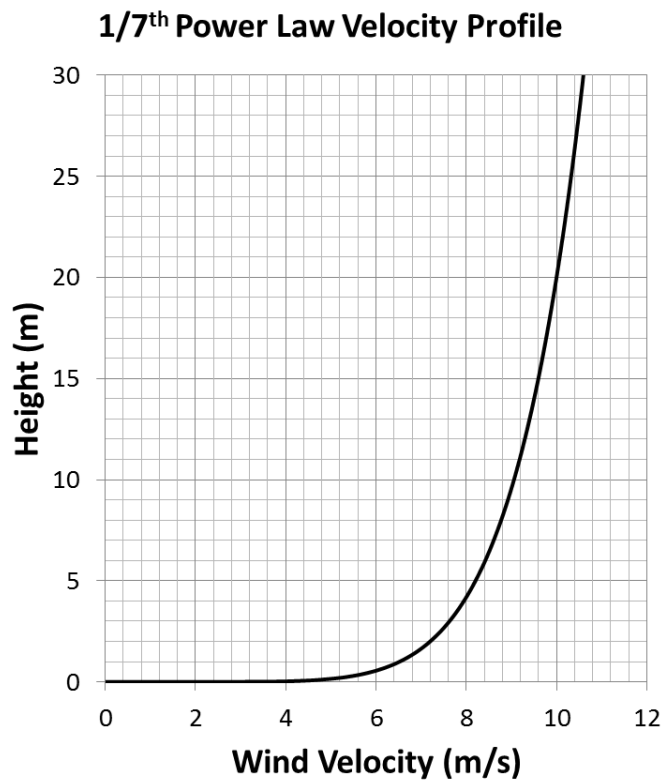


**Figure 4.3: A typical velocity inlet profile for a CFD wind study**

For these simulations The logarithmic inlet boundary profiles used are those suggested by [133] and revised in [134]. The Reynolds number based on a typical wind speed and domain width was  $6 \times 10^6$  so a k- $\epsilon$  RNG turbulence model was used, with a non-equilibrium wall function [133, 134]. Other turbulence models were tested but these did not change the results significantly.

The bottom wall of the computational domain where the terrain is located was treated as a rough wall. The data provided by Astrium Geo-Information Services was converted into an equivalent sand grain roughness. This is demonstrated in Figure 4.4.

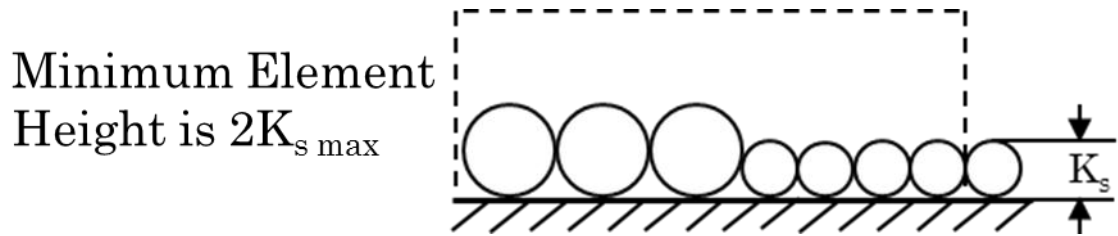


Figure 4.4: Sand grains on a smooth wall, and their effect on the first element height [117]

The presence of the roughness elements alters the universal law of the wall, which dictates the profile of the flow in the near wall region. Equation (37) shows the standard law of the wall [117]:

$$u^+ = \frac{1}{k} \ln y^+ + C^+ \quad (37)$$

In equation (37)  $u^+$  is the dimensionless velocity, defined as the velocity parallel to the wall,  $u$ , as a function of the distance from the wall,  $y$ , divided by the friction velocity  $u_\tau$ ;  $y^+$  is the cell coordinate, defined as the distance to the wall,  $y$ , made dimensionless with  $u_\tau$  and the kinematic viscosity,  $\nu$ ;  $k$  is the Von Kármán constant and  $C^+$  is a constant. Equation (38) shows the law of the wall modified for roughness, as it is applied by FLUENT [135]:

$$\frac{u^+ u^*}{\tau_\omega / \rho} = \frac{1}{k} \ln \left( E \frac{\rho u^* y^+}{\mu} \right) - \frac{1}{k} \ln \left( 1 + C_s \frac{\rho K_s u^*}{u} \right) \quad (38)$$

In equation (38)  $K_s$  is the physical roughness height,  $u^*$  is the friction velocity and  $\tau_w$  is the wall shear stress.

The initial conditions (ICs) represent a ‘first guess’ at the solution. Typically the ICs are derived from the BCs, but if the boundary conditions have only changed slightly from a previous calculation, the results from that calculation can be used as the ICs to reduce computational time.

#### 4.5. SIMULATION SCHEME FOR RTTR

The aim of the CFD simulations was to create a representative data set of the area in which RTTR was to be applied. Once a model had been created, a set of simulations had to be run to create this data set. For the studies presented in this thesis, the data set was created by altering the prevailing wind direction in  $10^\circ$  steps, resulting in a set of 36 simulations to represent a domain. Details of the meshes created and simulations performed are provided in Table 4.2.

**Table 4.2: Details of the CFD meshes created for the study and the number of simulations run**

<i>Mesh Name</i>	<i>Number of Cells</i>	<i>Number of Simulations</i>
Bolund Hill	3.5 Million	4
Planning Case Study	3.5 Million	36
State Estimation Case Study	2.8 Million	36

The calculations made the following assumptions:

- Incompressibility
- Uniform inlet wind direction
- Terrain features modelled as roughness rather than 3D objects
- Orography and roughness resolutions of 10m

#### 4.6. CFD VALIDATION USING BOLUND HILL

A validation exercise was conducted using the Bolund Experiment [136]. Bolund hill is a 12m high costal hill situated in Denmark [137]. In 2007/2008 ten wind masts were set up, with a total of 35 monitoring

stations on and around the hill for a period of three months to record the effect of the hill's complex topography on local wind flow. This data has since been used to validate computational wind simulation packages and CFD simulations [138] including Windsim [139], WASP and general purpose RANS based packages. The Bolund Hill orography and wind data were used to validate the CFD approach of using FLUENT to inform and improve RTTR.

Bolund Hill was selected for its steep gradients, which many solvers have difficulty modelling correctly. A similar study was conducted at Askervein Hill [140], which features a much simpler topography. Figure 4.5 shows contours of the hill's elevation along with the location of the weather masts used during the study. The weather masts took readings at heights of 1m, 2m, 5m and 9m above the ground.

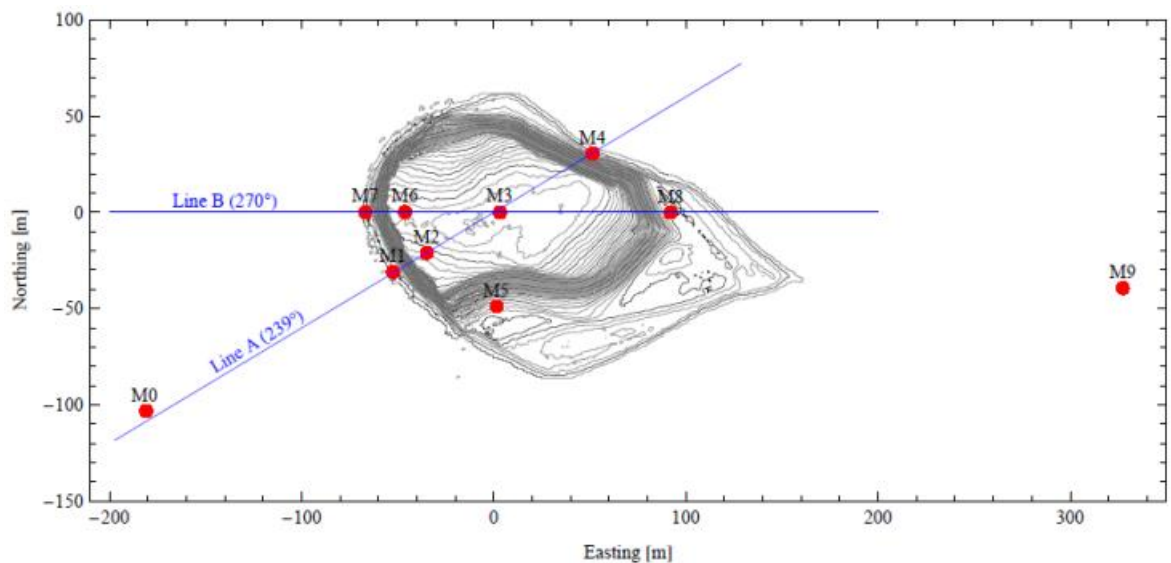


**Figure 4.5: Contours of Bolund hill showing the location of the ten weather masts. Masts M0 and M9 were outside the simulation domain [136]**

The method described in section 4.4 was applied to the Bolund Hill topography to ensure that the simulation methods used produced comparable results to other state of the art wind models.

#### 4.6.1. METHOD

The topography and surface roughness files for Bolund Hill are publicly available [136], so these were acquired from the study's website. The

topography was converted into a 3D model using Rhinoceros 4.0 and a hexahedral mesh was applied using ICEM CFD version 12.1. The cell size was 1mx1m at ground level, with the z-dimension 1m at the lowest level, and increasing further from the area of interest. The elements all had a quality of 0.5 or better. The mesh comprises 3.5 million cells. Figure 4.6 shows the layout of the simulation domain and a cross section of the mesh across the hill with contours of wind speed.

Calculations were run using a variety of settings. All results presented used a k-ε RNG turbulence model, and were converged at second order. The inlet flow profile to that depicted in Figure 4.3 was used; it followed a  $1/7^{\text{th}}$  power law profile, with the free stream height set at 213m, which is standard for wind flow over water [131].

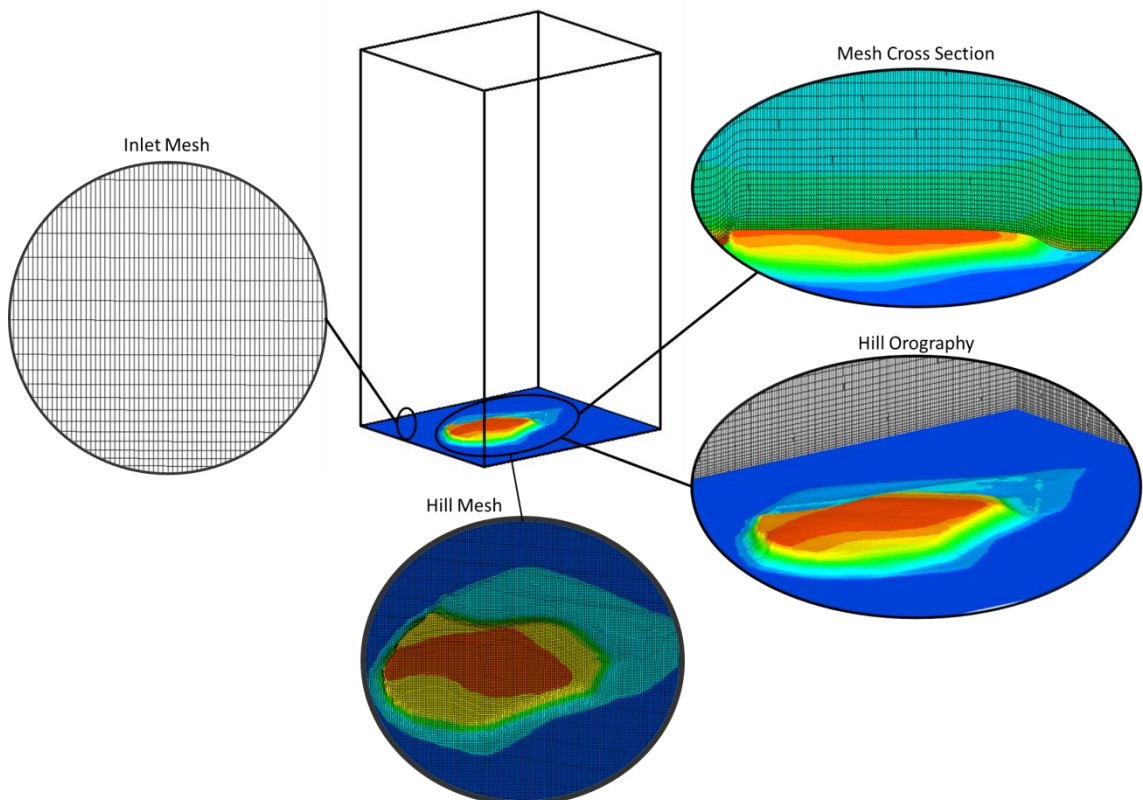


**Figure 4.6:** The layout of the computational domain, showing the inlet/outlet surfaces, mesh structure and topography

Because a square domain was used for the simulations, in the cases where the flow was not perpendicular to the boundary it was necessary to have two

inlets and two outlets. In the cases where the flow was perpendicular to the boundaries, the other two sides were modelled as symmetry planes. The top of the domain was modelled as a symmetry plane, at a height of 500m. The terrain was modelled as a wall. Calculations were performed with the terrain as a frictionless wall, with a uniform surface roughness, and with different surface roughness values for areas of land and areas of water.

#### 4.6.2. RESULTS

The Bolund Hill study required simulations to be performed at four different inlet conditions, 270°, 239°, 255° and 90° [138]. The study used the ‘speed up’ characteristic at 239° (see Figure 4.5) inlet condition to assess the velocity modelling of the simulations. All velocities shown were normalised by dividing by the free stream inlet condition, to allow a dimensionless comparison to the results measured by the experiment.

##### 4.6.2.1. SPEED UP CHARACTERISTIC

The ‘speed-up’ characteristic is designed to see how well the flow solver deals with the sharp changes in velocity due to the underlying terrain for the 239° inlet condition. By taking the measurements at a given height for measuring stations 1, 2, 3 and 4, it is possible to observe these changes. The 239° inlet condition was run 3 times, once modelling the terrain as a smooth surface, once with a constant roughness height of 0.001m, and once with the roughness profile supplied with the Bolund Hill topography data. The results are shown in Figure 4.7.

Figure 4.7 shows that for all cases, the model captured the acceleration caused by the initial ascent of the hill. However, the smooth case failed to model the deceleration along the top of the plateau, or that caused by the expansion after the hill. In all cases, the simulation using full surface roughness data was closest to the measured results.

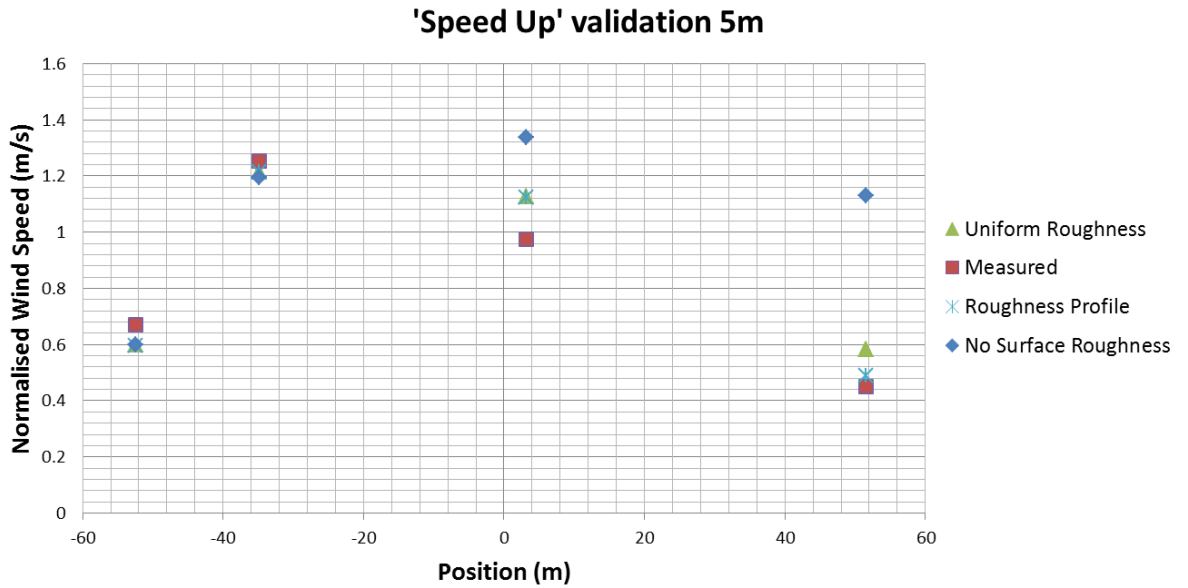


Figure 4.7: Speed-up characteristics compared to measured results for 239° inlet condition. The position is equivalent to the Easting in Figure 4.5.

Table 4.3: Average errors in the speed up case at 5m height

<i>Simulation Case</i>	<i>Average Error (%)</i>
No Surface Roughness	29.3%
Uniform Roughness	9.9%
Full Roughness Profile	7.5%

Table 4.3 shows the average error for the speed up characteristic at a height of 5m. Using the full roughness profile, the average error of 7.5% is comparable to the best simulations submitted to the Bolund Experiment [138], whose average errors varied from 4% to 10%

Table 4.4 shows the average absolute error between simulated and measured speed and direction for each of the four simulation cases using the full roughness profile.

Table 4.4: Average Wind Speed and Direction Errors at all heights

<i>Inlet Flow Direction (degrees)</i>	<i>90</i>	<i>239</i>	<i>255</i>	<i>270</i>
Wind Speed Error (%)	11.48%	19.08%	24.09%	16.41%
Wind Direction Error (degrees)	5.52	6.47	6.55	4.63

The wind direction predictions have an average error of less than 7°, while the wind speed predictions have average errors up to 25%. The simulation results are much worse when compared to the weather stations at 1m and

2m above ground. Since overhead conductors generally have a minimum ground clearance of at least 7m [141], these results are not relevant for this application. Furthermore, the Bolund Blind Comparison found that the majority of simulations had difficulty predicting wind conditions at low heights [138]. Table 4.5 shows the averages recalculated using only measurements taken 5m above ground and higher. The error is greater in the 255° inlet case, with high errors at masts 2, 5 and 6. These masts are all located next to sharp changes in the hill's orography, at an angle to the inlet condition; these are challenging phenomena for the CFD simulation to fully capture.

**Table 4.5: Average Wind Speed and direction errors for measurements taken at 5m or higher**

<i>Inlet Flow Direction (degrees)</i>	<i>90</i>	<i>239</i>	<i>255</i>	<i>270</i>
<b>Wind Speed Error (%)</b>	9.23%	11.04%	19.28%	9.25%
<b>Wind Direction Error (degrees)</b>	4.76	5.51	3.91	1.82

#### 4.6.3. DISCUSSION

Running the Bolund Hill validation case demonstrates that the CFD methods being used in this thesis are comparable to those being used within the wind energy industry. The simulation results are less accurate at low elevations, but this is acceptable for this application since overhead conductors are sufficiently far from the ground. It is clear from these results that applying appropriate surface roughness is important in realistically modelling the effect of terrain on wind flow, since it gave a considerable improvement in the 'speed-up' characteristic used as part of the Bolund experiment.

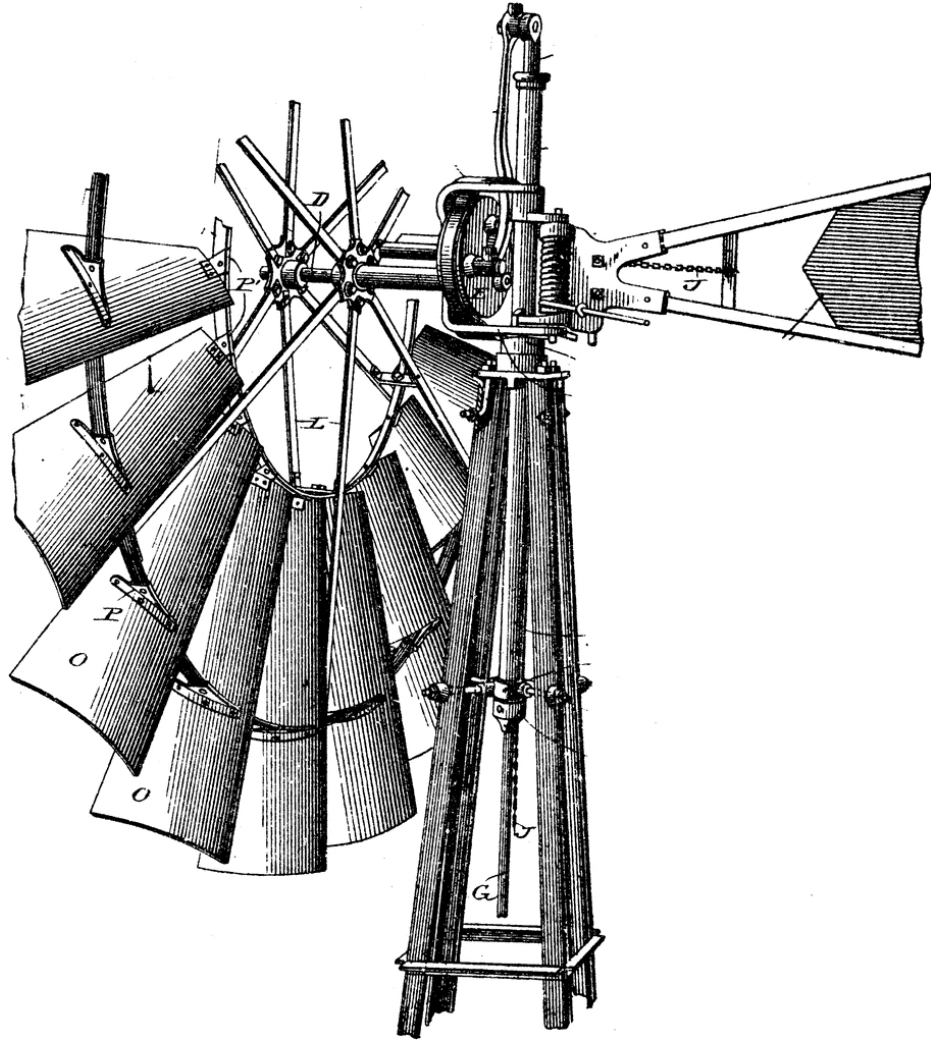
It is important to consider that the requirements for a Real-Time Thermal Rating wind model differ from that of the rest of the wind industry; while a wind farm will be concerned by average bulk wind speeds, wind direction and shorter term effects are important for the RTTR application. However, within the context of offline planning, being able to identify areas of high and low wind is valuable.

## 4.7. CONCLUSION

This chapter has described the CFD wind modelling approach applied to allow estimation of wind speed and direction for RTTR. This was done because wind speed and direction are the weather parameters with the greatest influence on conductor current carrying capacity. This, coupled with the high variability of the wind on small time and space scales, necessitated a means of estimating the relationship between wind flows and local terrain.

A RANS solver was used to calculate how wind flows are affected by local terrain and orography. An industry standard case study was used to validate the simulation approach. The validation approach showed that this approach was in line with other state of the art wind models, and could therefore be applied to RTTR problems with confidence.

## Chapter 5. Wind Simulations: Applications



## 5.1. INTRODUCTION

The simulations described in Chapter 4 can be utilised in both the planning and operation of electrical networks. This chapter describes new methods that have been devised to apply CFD wind simulation results to inform the planning of new sections of network, planning the implementation of RTTR on existing sections of network and in improving state estimation during operation. The chapter is broken down into network planning in section 5.2 and operational methods in section 5.3, with a case study provided for each application.

## 5.2. NETWORK PLANNING WITH A CFD WIND MODEL

Key challenges in RTTR planning are predicting the rating increases before deploying any RTTR hardware to the network, and identifying the determining spans, or thermal bottlenecks, within the network. These problems can be solved by using a computational wind model to analyse the prevailing wind speeds and directions within the area of interest. A similar approach is widely used in the wind energy industry for the siting of turbines and estimation of energy yields [120]. Since conductor ratings are highly dependent on both wind speed and direction, many of the same techniques can be used here. Further to this, the CFD results can also be applied to estimate the energy yield of distributed generators connected to networks making use of RTTR, and to assist in optimal sensor placement.

### 5.2.1. CREATING DATA REPRESENTATIVE OF LOCAL WIND REGIMES

The CFD results, calculated using the methods in Chapter 4, are used to generate a grid of normalised wind speeds, known as speedup values, across the area of interest. This is done by taking a surface of points at a set height above the ground, and dividing the velocity magnitude at each point by the mean velocity magnitude across the domain, as shown in equation (39). All of the examples presented here take the surface at 10m above ground level. This is because 10m is the height at which wind speed measurements are generally taken [142], and 10m provides a reasonable approximation to the

height of overhead conductors, which is variable depending on the tower, point in the span and which phase is being considered.

$$S_i = \frac{\widehat{W}s_i}{\frac{\sum_{j=1}^n \widehat{W}s_j}{n}} \quad (39)$$

In Equation (39), the value  $S_i$  is the Speedup value at point  $i$ ,  $\widehat{W}s$  is the simulated wind speed and  $n$  is the number of points. A database of these Speedup values must be computed for each set of inlet conditions input to the CFD model. Figure 5.1 shows a contour plot of Speedup values at 90° inlet condition (an easterly wind), from the planning case study in North Wales illustrating the high level of spatial variation. For example, if a conductor was running from the north to the south of the domain, with a weather station roughly every 10km (the spacing used in Scottish Power’s demonstration project [143]), it would pass through areas where the wind speed varies from 20% to 120% of the average value, which would not be accounted for by observations.

Local measured data were combined with the Speedup data to create a representative data set, created using the CFD models described in Chapter 4. For each data point in the hourly data set (provided by the UK Met Office), the appropriate Speedup data should be selected based on the measured wind direction,  $Wd$ . This is then multiplied by the measured wind speed,  $Ws$ , to give time series of estimated wind speed,  $\widetilde{W}s$ , for every point in the domain, as shown in equation (40):

$$\widetilde{W}s_i = S_{i,Wd} \cdot Ws \quad (40)$$

These time series can then be used to evaluate the benefits that could be provided through RTTR, identify where thermal bottlenecks are likely to be located and assist in the optimal placement of monitoring equipment. The methods devised to calculate these are described in sections 5.2.2-5.2.6.

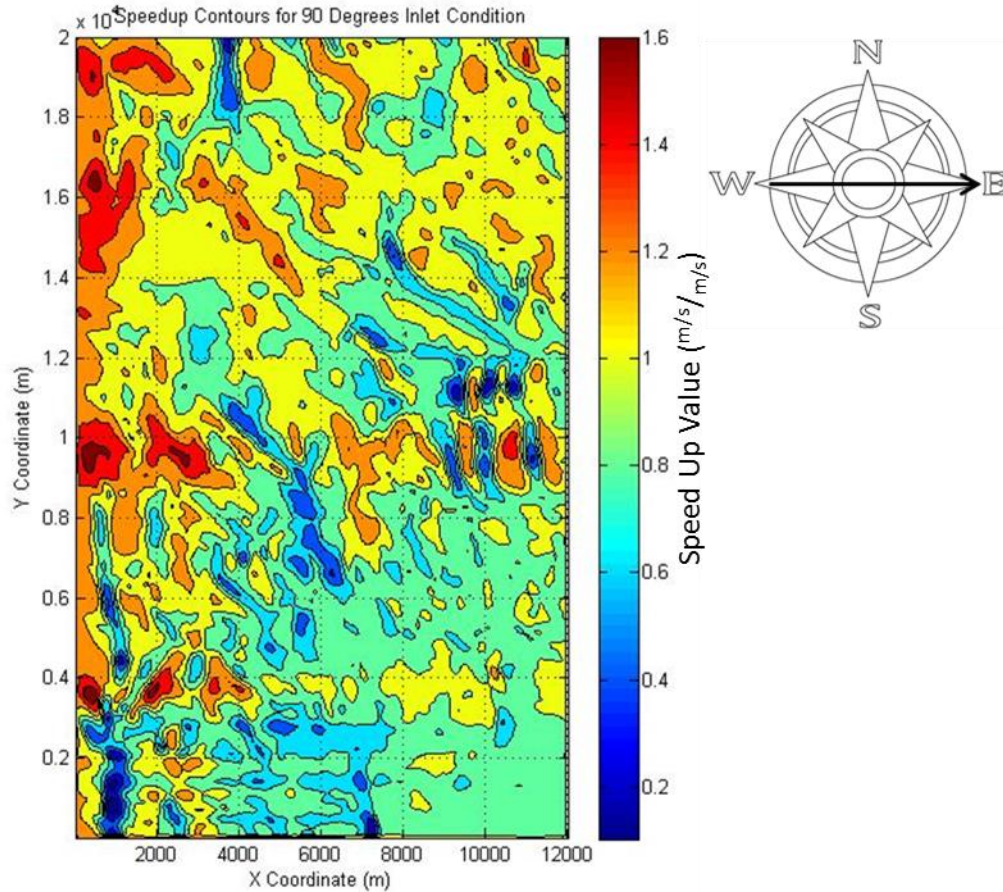


**Figure 5.1: Example of a contour plot of speed up characteristics**

### 5.2.2. AVERAGE RATING CALCULATION

Though knowing the average rating of a conductor does not give a complete understanding of its behaviour, it is a useful tool for knowing where critical spans are likely to occur. A flow chart illustrating the steps in this calculation is shown in Figure 5.2.

There are two different methods for calculating the average rating:

- Calculate the rating at each point in the time series, and use these results to calculate the average rating.
- Calculate the average weather values and use these to calculate the average rating.

The first method requires more computer time, but allows the variance of the rating to be calculated as well. The speed-up database was calculated using one year of wind data sampled at a rate of one hour.

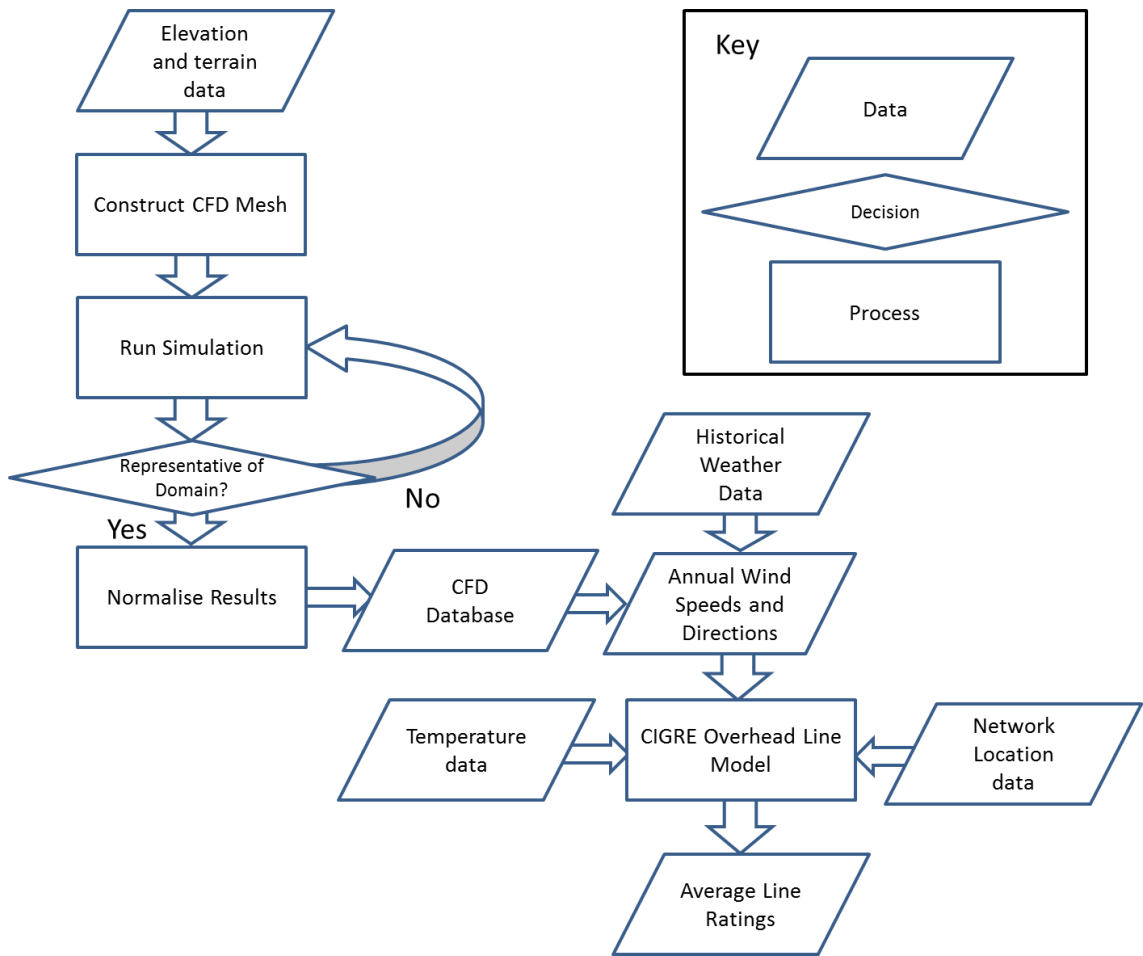


**Figure 5.2: A flow chart illustrating the methodology for calculating average line ratings and hence identifying thermal bottlenecks and selecting new conductor routes. In the work presented in this thesis, 36 simulations was deemed sufficient to represent the domain.**

The ambient temperature values from the historical weather data can be applied directly, since temperature has a relatively low variation over the space scales of an overhead line. If several sets of temperature data were available, then inverse distance squared interpolation, shown in equation (41), could be used to calculate the appropriate value:

$$T(x) = \frac{\sum_{i=1}^n \frac{T(x_i)}{\|x - x_i\|^2}}{\sum_{i=1}^n \frac{1}{\|x - x_i\|^2}} \tag{41}$$

Where  $T(x)$  represents the temperature at a point  $x$ , and  $x-x_i$  represents the distance between the points  $x$  and  $x_i$ .

Wind direction should be assumed to be  $0^\circ$  relative to the conductor at this stage (a worst case assumption), and solar radiation should be ignored, given that its impact is minor (a difference of around 30A, over a range of credible values for a Lynx conductor [12]), and it cannot be sufficiently represented by a single value or through interpolation in the majority of cases.

### 5.2.3. CRITICAL SPAN IDENTIFICATION

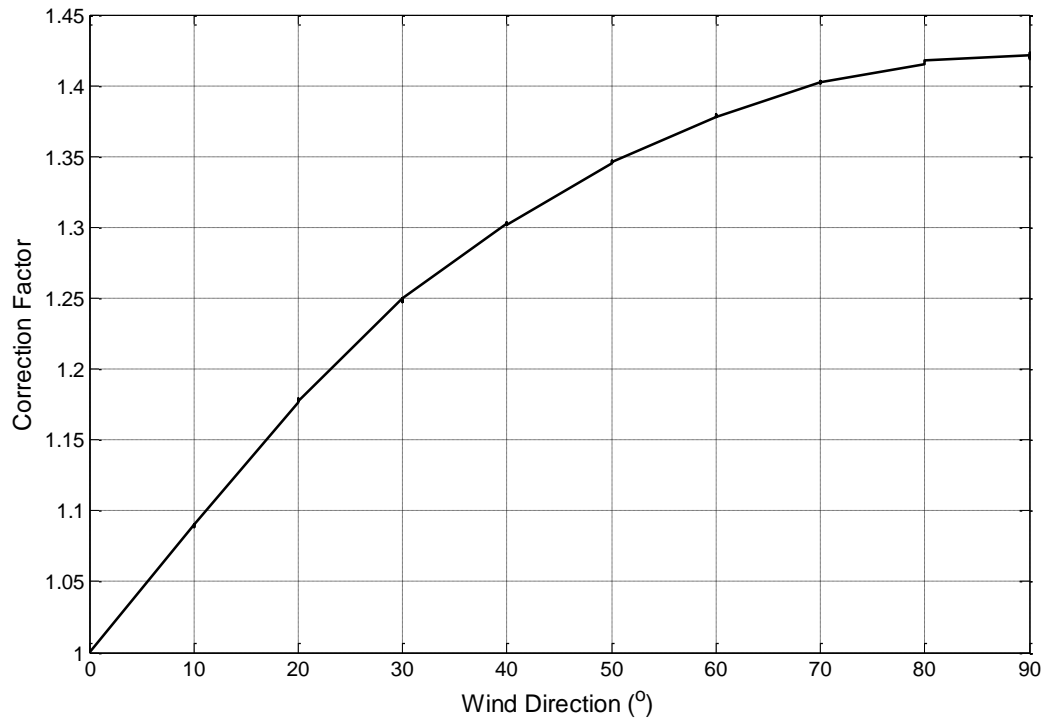


**Figure 5.3 : Wind direction correction factors for conductor rating**

In many cases, the rating of a circuit can only be as high as the rating of its lowest rated section. Consequently it is important to identify which span, or spans, this is likely to be. It may be necessary to add extra instrumentation here, or even to re-conductor just one span. Average annual rating values provide a good initial estimate of where a critical span is likely to be located. GIS models of the network can be superimposed over the estimated ratings, and spans that cross areas with low average ratings can be identified.

The wind direction relative to the line was assumed to be  $0^\circ$  for the average rating calculations. However, the prevailing wind direction at each point in the CFD domain can be calculated in the same way as the average wind

speed. This can be combined with the angle correction factor shown in Figure 5.3 to calculate the average annual rating of a conductor. An example of the angles between the mean wind direction and conductor orientation is shown in Figure 5.4. Equation (42) shows how to calculate this corrected mean rating,  $\bar{r}_{corrected}$ , from the mean rating  $\bar{r}$ , the correction factor  $CF$ , and the difference between the orientation of the conductor  $\theta_c$  and the mean wind direction  $Wd$ .

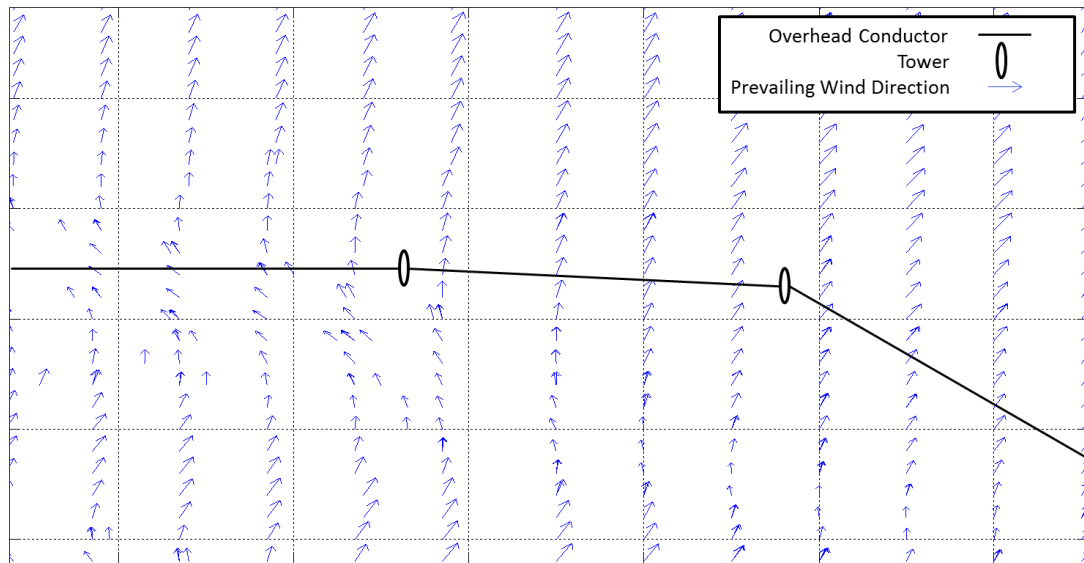


**Figure 5.4: Example of mean wind direction relative to conductor location**

$$\bar{r}_{corrected} = \bar{r} \cdot CF(\theta_c - Wd) \quad (42)$$

These average rating values can be used to identify where critical spans are likely to occur, or to identify areas that are likely to maximise benefits or minimise the risks from RTTR.

#### 5.2.4. NEW CONDUCTOR SITING

The siting of new overhead lines is a complex process. Various steps must be taken including environmental surveys and planning consultations [5, 6]. The conductor is often sited where it will have the least visual impact, such as in a valley or behind a tree line; this is directly at odds with obtaining the greatest benefit from RTTR. If RTTR was considered at the planning and design stage, it would be possible to factor the potential benefits into the planning process. This could lead to situations where fewer circuits need to be built, or lower rated conductors can be used. One example is that rather

than building a steel tower line through a valley, a wood pole line could be built along a ridge.

The method for siting new overhead lines is similar to the method for identifying critical spans. Rather than looking at the average rating at the location of the existing conductors, the average rating at the location of proposed route corridors can be examined.

Again, a wind direction correction can be applied. However, since the route corridors can be a few hundred metres wide, in some locations it may be possible for the conductor to be aligned to increase the average rating.

#### 5.2.5. WIND FARM ENERGY AND CONSTRAINT ASSESSMENT

While the average rating is a reasonable indicator of which conductors are likely to be critical spans, it does not give an indication of when the additional capacity is available. This is relevant if the circuit is being used to connect wind generation, because it is important to know how high the rating of the conductor will be when the wind farm is working at rated capacity. Lines with a low average rating could be sufficient to facilitate additional wind generation if their periods of high rating coincide with high wind speed at the wind farm site.

The rest of this section describes a method for calculating the constraints and energy yield for a wind farm connected to a network using RTTR. A flow chart illustrating the method is shown in Figure 5.5.

The CFD model can be used to give an indication of where high wind speeds occur in the area of interest concurrently with high wind speeds at the wind farm site. The following steps can be taken:

- Select a point in the domain to represent the wind farm location. This makes the assumption that the wind farm, which covers a large area, can be adequately represented by one point.
- Calculate time series of wind data for the time interval to be considered,  $T$ , at the location of the wind farm and the possible locations of the conductors.

- Wind turbine hub height is often around 100m, so the 10m wind speed must be to give the speed at turbine hub height, using standard wind height correction in equation (43) [44]:

$$\widetilde{W}_s = \widetilde{W}_{s_\alpha} \cdot \left(\frac{z_h}{z_\alpha}\right)^{k_{shear}} \quad (43)$$

$\widetilde{W}_s$  is the simulated wind speed at the height of the turbine hub,  $\widetilde{W}_{s_\alpha}$  is the simulated wind speed at conductor height,  $z_h$  is the turbine hub height and  $z_\alpha$  is conductor height (assumed to be 10m).  $K_{shear}$  is a ground roughness value. Appropriate values of  $K_{shear}$  for different ground types can be found in [144]. Alternatively, the speed up value could be taken from the simulation at turbine hub height. However, this method allows several turbines with varying hub heights to be compared, without having to extract additional data from the CFD results

- Use the wind speed at this location to calculate the wind farm power output. The wind turbine power curve used throughout this thesis is depicted in Figure 5.6. This is a simplified power curve, with a 3.5m/s cut in, 14m/s maximum power and 25m/s cut out. The ramp rate is assumed to be linear, to allow example calculations on generic turbines to be easily performed. Of course for a study of an actual wind farm the precise power curve of the wind turbine, or a wind farm power curve accounting for the spatial variability within the wind farm [145], could be substituted.
- Use the wind data at the conductor sites, along with temperature data if available, to calculate the conductor rating at the sites of the conductors.

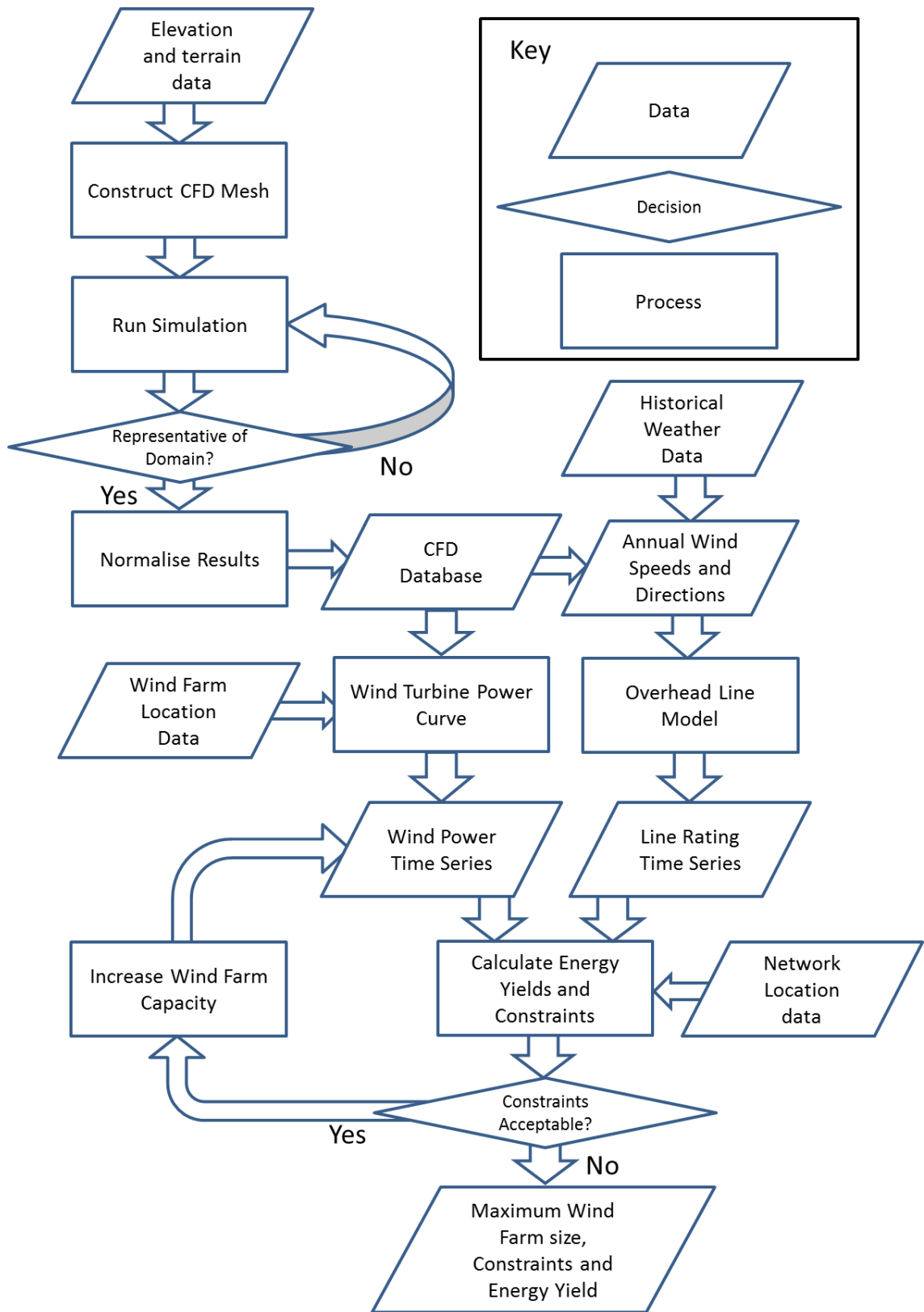


Figure 5.5: A flow chart describing the method for quantifying wind farm size, constraints and energy yields

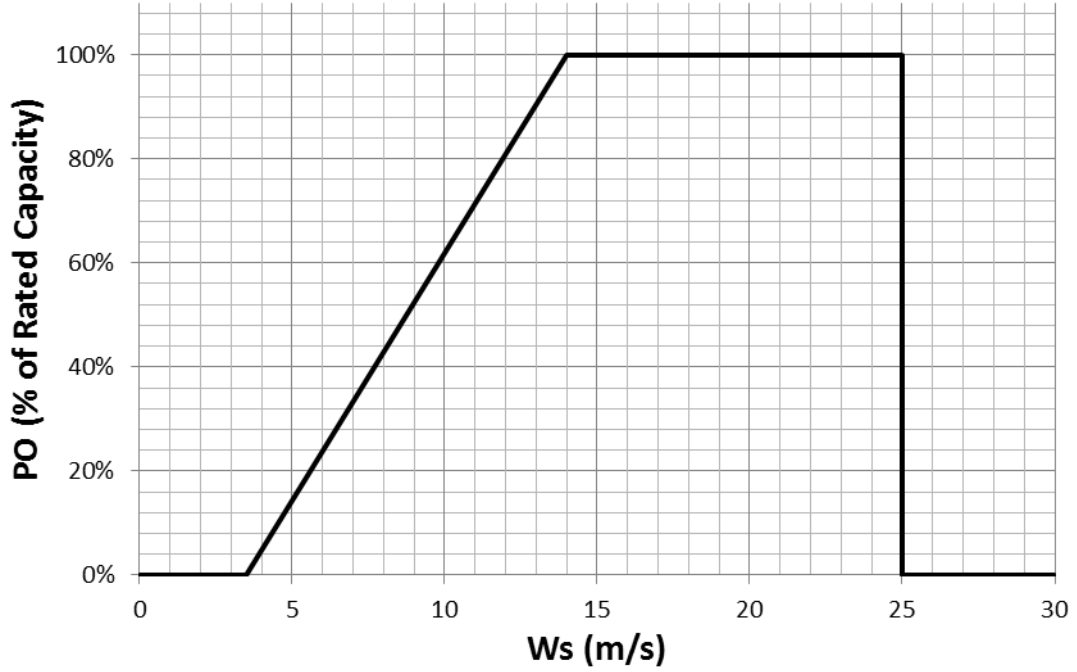


Figure 5.6: Simplified wind turbine power curve

- Scale the wind power output by the maximum output of the wind farm:

$$P = P_{Rated} \cdot PO \quad (44)$$

- Calculate the current in the line:

$$I_{WF} = \frac{P}{3V \cos \phi} \quad (45)$$

Where  $I_{WF}$  is the line current produced by the wind farm and  $\phi$  is the power factor angle. Assuming unity power factor:

$$I_{WF} = \frac{P}{3V} \quad (46)$$

- At each point in the time series, compare the power to the line rating and evaluate the constraint and energy yield:

$$C = 3V \cdot \sum_{t=0}^T \begin{cases} I_{WF} - r > 0, I_{WF} - r \\ I_{WF} - r < 0, 0 \end{cases} \quad (47)$$

$$E = \sum_{t=0}^T P - C \quad (48)$$

$$C_{prop} = \frac{C}{\sum_{t=0}^T P} \quad (49)$$

In equations (47)-(49)  $r$  represents the conductor rating in amps,  $C$  represents the wind farm constraint in terms of energy,  $E$  represents the total energy yield after constraints and  $C_{prop}$  is the constraint as a proportion of the available energy yield.

This method can be used to consider varying sizes of wind farms, ranging from those that would be permitted by the static ratings, to those with peak power outputs greater than the conductors would allow. This could allow network planners and designers to offer connection agreements to windfarms with greater capacity based on predicted levels of constraint.

#### 5.2.6. WHERE TO INSTRUMENT

In any RTTR deployment it is essential to have adequate instrumentation to be able to infer the ratings throughout the system with precision and accuracy. However, the instrumentation can be expensive, particularly purpose built devices. Consequently it is prudent to plan a deployment that minimizes the cost of instrumentation without compromising observability. The following rules should be applied:

- Meteorological observation stations should be sited in locations that are representative of large areas.
- Other instrumentation, such as sag/tension monitors should be deployed in areas that are not well represented by the weather stations or are likely to contain determining spans.

To determine which areas are appropriate sites for meteorological stations, and which parts of the network will require additional instrumentation, the correlation structure of the domain must be determined. The example shown below uses wind speed correlations, since this is the parameter that varies the most on the relevant space scales. However, it would be equally valid to use the correlation between predicted rating values. The correlation structure was calculated as follows:

- Create time series of wind speed at each point in the domain using CFD results and historical data.
- Calculate the correlation between each pair of time series using equation (50) [146]. Large domains may need the data reducing to make this computationally manageable.

$$\text{corr}(X, Y) = \frac{\text{cov}(X, Y)}{\sigma_x \sigma_y} = \frac{E[(X - \mu_x)(Y - \mu_y)]}{\sigma_x \sigma_y} \quad (50)$$

Equation (50) represents the product-moment correlation between two variables,  $X$  and  $Y$ , defined by the covariance divided by the product of the standard deviations.

- This will yield a matrix of correlations, where element  $i, j$  represents the correlation between locations  $i$  and  $j$ . Taking the mean of each column will give the average correlation between that element and the rest of the domain.
- These average correlations can then be plotted against their positions, showing which areas are well correlated, and which are comparatively independent. An example is shown in Figure 5.7.

The red areas in Figure 5.7 show locations that have a high correlation with the rest of the domain. Meteorological stations in the red areas would be able to give a strong representation of the majority of other locations. The yellow and blue areas represent sites with a lower correlation to the rest of the domain. These areas have wind conditions that are not generally representative of the domain; if conductors pass through these areas, additional instrumentation should be deployed to ensure that the system observability is high. This is especially true if these areas have been identified as containing critical spans.

The other point of interest in sensor placement is to establish appropriate spacing between meteorological stations. As the distance between two points increases, the correlation between the weather, and hence the rating of a conductor, at those points decreases. Figure 5.8 shows how this correlation decays over relatively short distances. The points on the graph indicate the

correlation of rating between two observation locations separated by a stated distance. It also shows that distance is not the only parameter that governs this correlation; if one of the points is in a location where the weather is heavily influenced by local effects, the correlation will be lower than the general trend would suggest. The maximum spacing between meteorological stations will give a minimum correlation in the system equivalent to half of the maximum spacing, since the most remote location will be equidistant between the two stations.

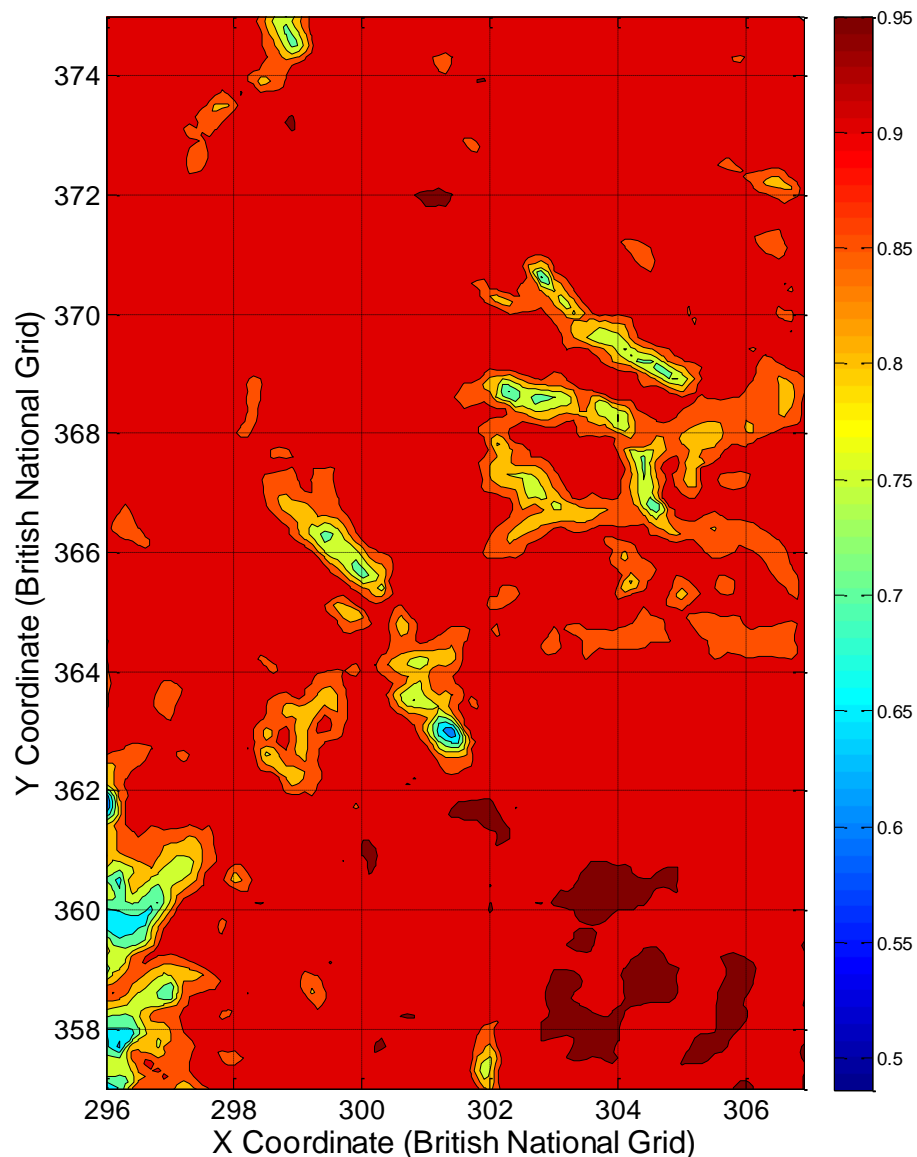


**Figure 5.7: Average point correlation with the other points in the domain.**

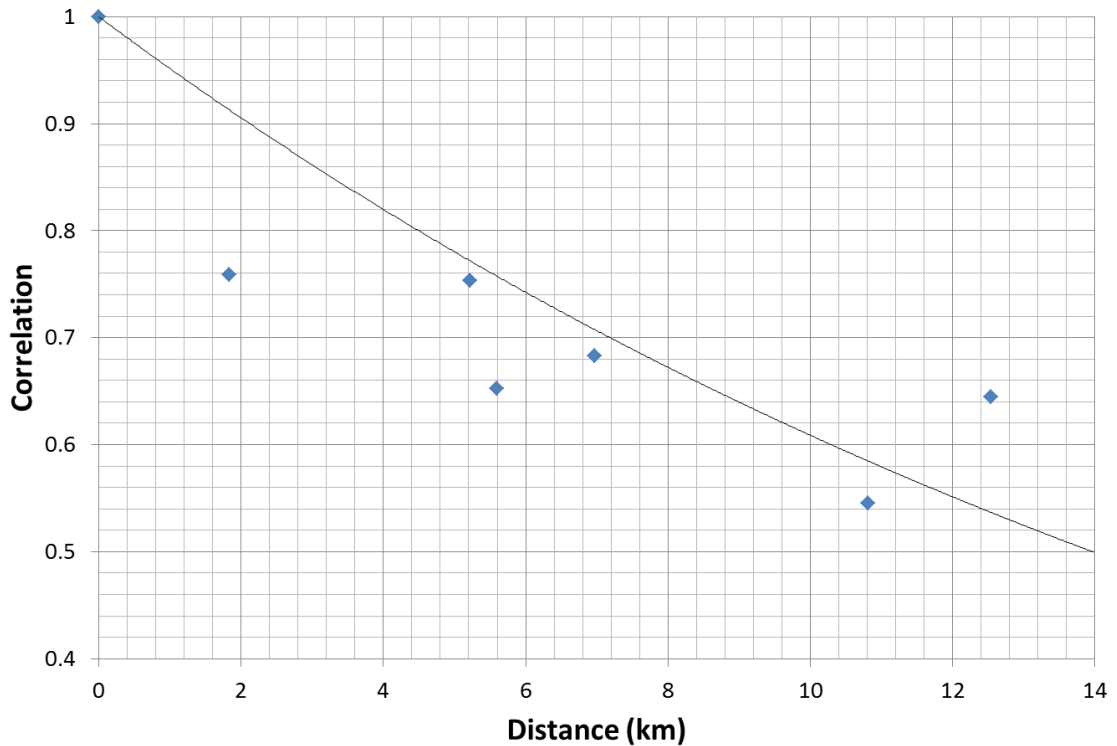


**Figure 5.8: Rating correlation against distance between two points**

In the majority of cases, the number of locations where sensors, particularly meteorological stations, can be placed may be limited; for example they may only be placed at substations, where they are guaranteed power and data connections as was the case in Scottish Power’s North Wales test case [143]. However the method presented is still valid for suggesting which of these locations would provide the best coverage, and which could provide redundant cover of well monitored areas. Limited options would also reduce the computational burden of calculating the correlation structure.

#### 5.2.7. CASE STUDY

##### 5.2.7.1. DESCRIPTION OF CASE STUDY

The case study was in north Wales, just south of the city of St Asaph. Several new onshore wind farms were attempting to connect to the 132kV network, which required the construction of a new overhead line. The potential routes for this line are shown in Figure 5.9, along with the location of the existing network and the wind farm site. The proposed overhead line

had a static summer rating of 89MVA. This study aims to quantify whether additional wind generation could be facilitated through RTTR [147].

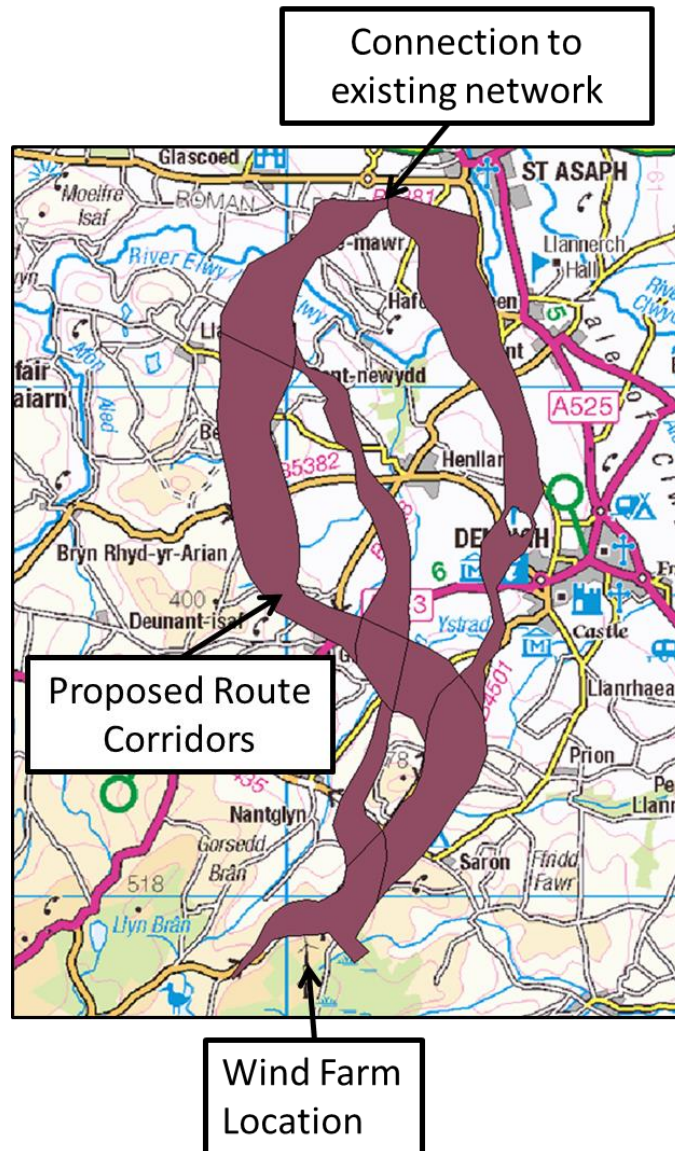


**Figure 5.9:** A map of the case study area showing the route corridors for potential overhead lines.

The route corridors were a result of an environmental study performed by the DNO. A planning consultation must then take place before the final route is determined.

#### 5.2.7.2. STUDIES UNDERTAKEN

A CFD mesh of the trial site, shown in Figure 4.2, was created. 36 simulations were performed, altering the inlet condition by 10° for each

simulation, to give representations of the wind regime for a variety of prevailing wind conditions. The goals of the case study were as follows:

- Identify which overhead line route would result in the greatest energy yield from the wind farm.
- Calculate the size of wind farm that could be accommodated.
- Calculate the energy yield and constraints for the wind farm.

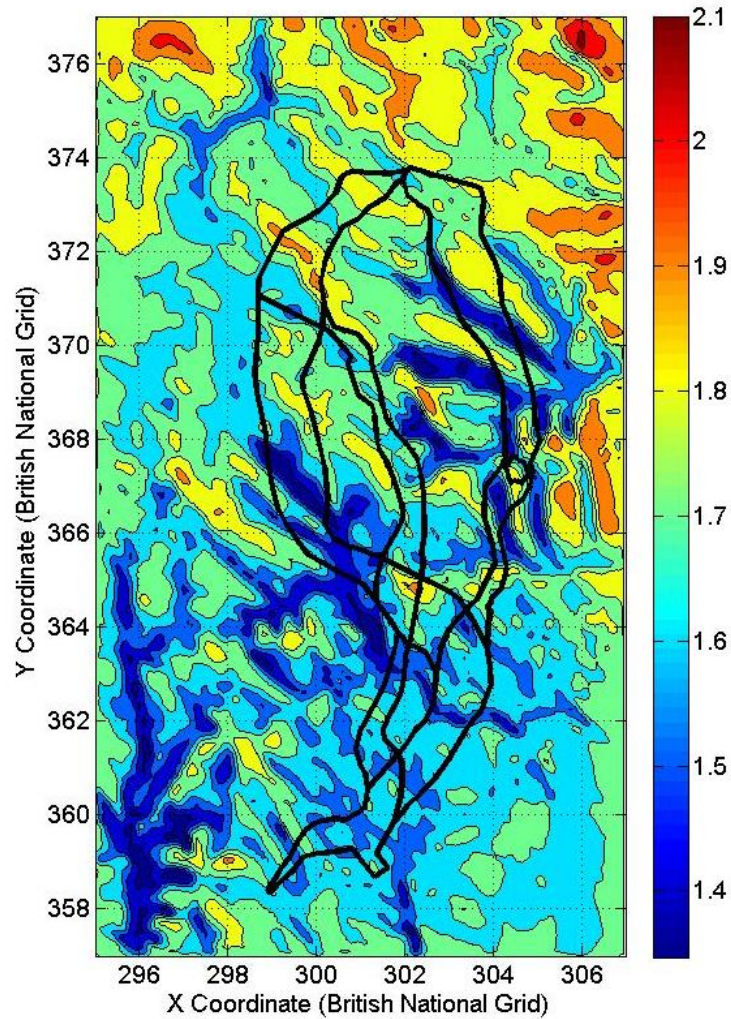


**Figure 5.10: Map of annual average conductor rating as a proportion of seasonal ratings. The locations of the approved route corridors are shown on the plot.**

The method described in section 5.2.2 was applied to calculate the average ratings throughout the domain, as shown in Figure 5.10. The ratings are shown as a proportion of the seasonal ratings to give an indication of the additional capacity available. These ratings suggest that the central (rather than East or West) route corridor would allow the wind farm with the

greatest generating capacity to be connected – although the connection may be limited by a critical span passing through one of the dark blue areas. It is possible that a higher rated conductor could be built for just this span, which would increase the capacity of the entire circuit. What this does not mean is that a line with an average rating of 60% above the seasonal rating could support a 60% larger wind farm. It was important to consider energy throughput rather than average capacity.

The goal of this planning study was to maximise the energy output from a wind farm connected to the 132kV network by a new overhead line. Consequently it was more important to consider the power output from the wind farm at the same time as the rating of the overhead lines.

### 5.2.7.3. ENERGY THROUGHPUT

The method described in section 5.2.5 was applied for wind farms with an 80, 100, 120 and 140MW capacity.

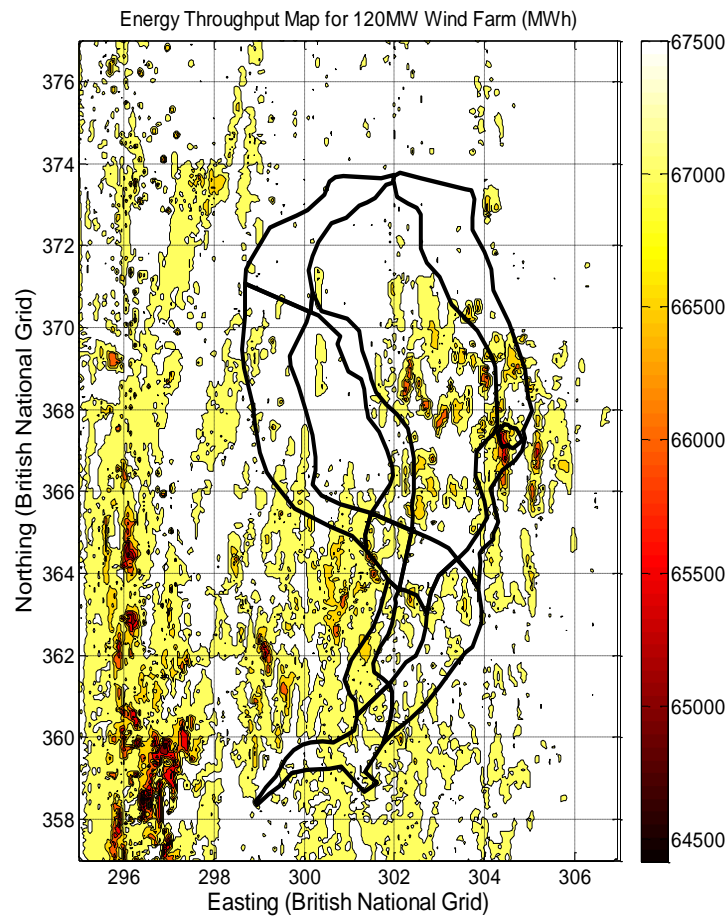


**Figure 5.11: Energy throughput map for a 120MW Wind Generator (MWh)**

Energy throughput data, showing the total energy supplied to the system in a year, for a 120MW wind farm are shown in Figure 5.11. There are low energy throughput areas similar to the low capacity regions in Figure 5.10. However, the north western corridor now seems to be the best route, in spite of the comparatively low average rating, because it has a high energy yield and correspondingly low constraints.

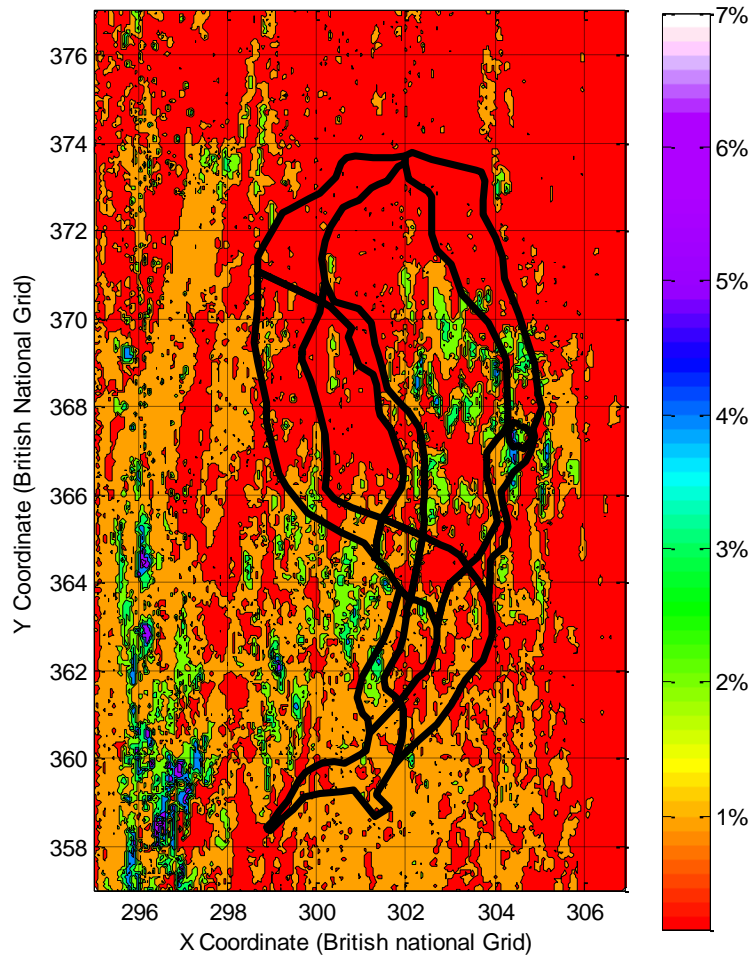


**Figure 5.12: A map of constraints to wind generation as a proportion of the annual energy yield of a 140MW wind farm**

A consequence of connecting a wind farm with a greater capacity than the rating suggests the generator can support is that the generator will sometimes have to be constrained. There have been a number of studies on constrained wind farm connections demonstrating that this is a realisable solution [63, 148]. Figure 5.12 shows the energy that would be constrained, as a proportion of the total energy the wind farm would produce for a

140MW wind farm, the greatest generation capacity considered in this study.

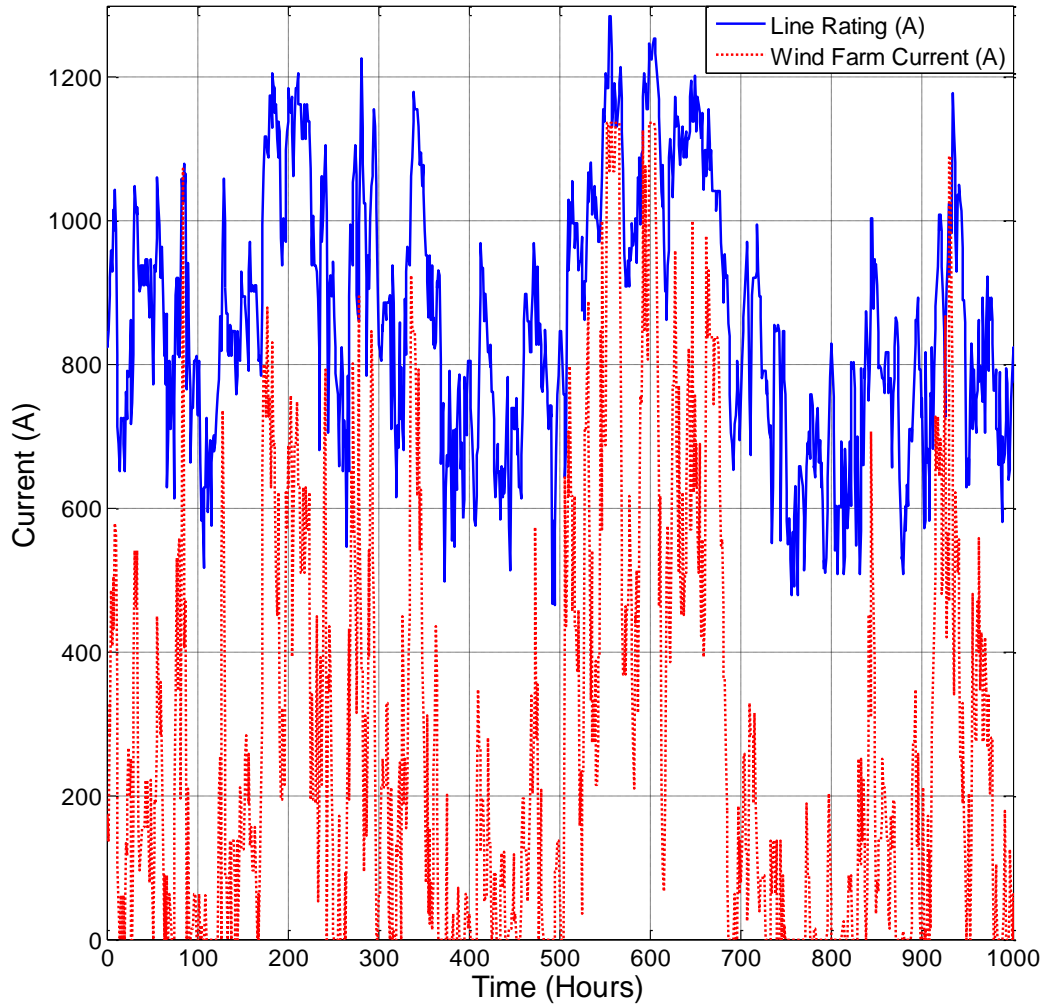


**Figure 5.13: Time series of conductor rating and line current due to the wind farm. The two follow similar trends, meaning constraints are rarely required**

These data suggest that from an energy yield perspective the best location for an overhead line connecting a wind farm in this area would be the northwest corridor, followed by the south east corridor. This suggests that 140MW of wind generation could be connected using an overhead line that would normally only support 89MW, with energy constraints of 1-2% of annual energy yield.

### 5.3. REAL-TIME STATE ESTIMATION

#### 5.3.1. MOTIVATION

Weather based RTTR offers wide coverage of network current carrying capacity while using relatively few instruments [44] compared with line monitoring devices. However, the existing techniques for applying weather based RTTR use simple interpolation methods to estimate the weather conditions, and hence the rating, throughout the system. This method does not account for the variability of wind on the relevant space scales [77, 96], resulting in errors in state estimation, given that wind speed and direction have a significant impact on conductor current carrying capacity,

Wind simulation can provide detailed information about how the terrain affects the local wind flow. However, the simulations are time consuming and consequently cannot be run during operation. This is because the thermal time constant of an overhead conductor requires the rating to be updated every 10 minutes to avoid exceeding the conductor's design temperature [49]. Consequently, a method was required to allow detailed simulation results to be applied in an operational timeframe.

#### 5.3.2. METHODOLOGY

The CFD simulations provided a relationship between the terrain and the wind flow. The next step was to use this relationship in the estimation of conductor ratings. As discussed in section 4.5, a database of simulation results was required to implement the operational state estimation. The state estimation took place at discrete time intervals, with the calculated rating being applied for the time step. This methodology assumes that a weather based RTTR system is being deployed, with several meteorological stations sited throughout an area of network.

Observed measurements are used to select the simulation data set that most closely matches the observations. To this end, at each interval, the most representative set of wind simulation data must be selected from the database. This was done by normalising the observed wind speeds by the

mean observed wind speed, comparing them to each set of simulation results and minimizing the error in  $X$  and  $Y$  direction vectors.

$$\widehat{W}_{S_N} = \frac{\widehat{W}_s}{\frac{\sum_{j=1}^m \widehat{W}_{S_j}}{m}} \quad (51)$$

$$S_{BF} = \min_{i=1,n} \sum_{j=1}^m [(u_{Nj} - Sx_{i,j})^2 + (v_{Nj} - Sy_{i,j})^2] \quad (52)$$

Where  $\widehat{W}_s$  represents the wind speed at a meteorological station, and  $\widehat{W}_{S_N}$  represents the normalised wind speed at that same station,  $u_{Nj}$  represents the normalised  $x$  axis observation at weather station  $j$  and  $Sx_{i,j}$  is the  $x$  axis speed-up value at weather station  $j$  in simulation  $I$ ,  $n$  and  $m$  represent the number of observations and simulation data sets respectively.  $S$  represents the speed-up characteristic selected from the CFD database. The measured and calculated values were decomposed into  $x$  and  $y$  direction vectors. In this thesis,  $z$  direction flows were not considered because the available weather data did not contain  $z$  direction values. This is a conservative assumption, since if the  $z$  direction values were included the overall wind velocity and hence cooling effect, would be increased.

$$\tilde{u}_i = Sx_j \left( \sum_{j=1}^m \frac{W_{S_j}}{m} \right), \quad \tilde{v}_i = Sy_j \left( \sum_{j=1}^m \frac{W_{S_j}}{m} \right) \quad (53)$$

In equation (53),  $\tilde{u}_i$  and  $\tilde{v}_i$  represent the estimated  $x$  and  $y$  direction wind speeds at point  $i$ , calculated as the speedup value at point  $i$  multiplied by the mean observed wind velocity.

The ambient temperature and incident solar radiation were estimated using inverse distance squared interpolation as in the RTTR methodology described by *Michiorri et al* [44]. The full methodology is shown in Figure 5.14.

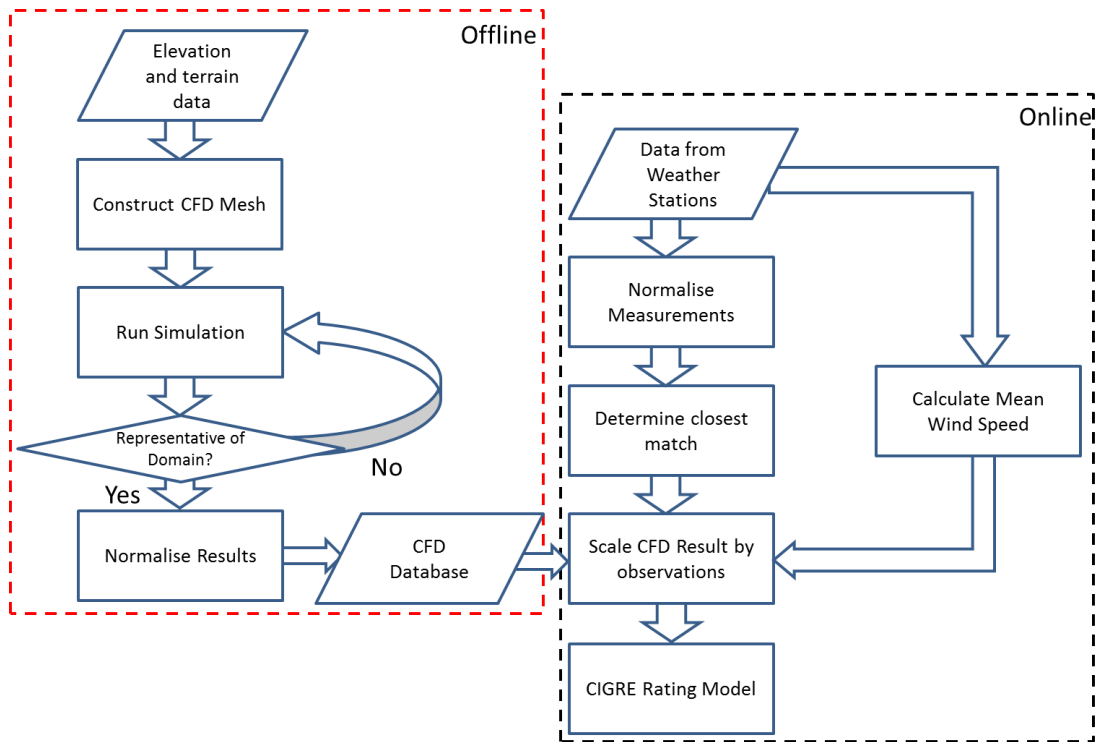


Figure 5.14: The complete methodology used to apply CFD results to state estimation, broken down into offline and online processes.

### 5.3.3. CASE STUDY

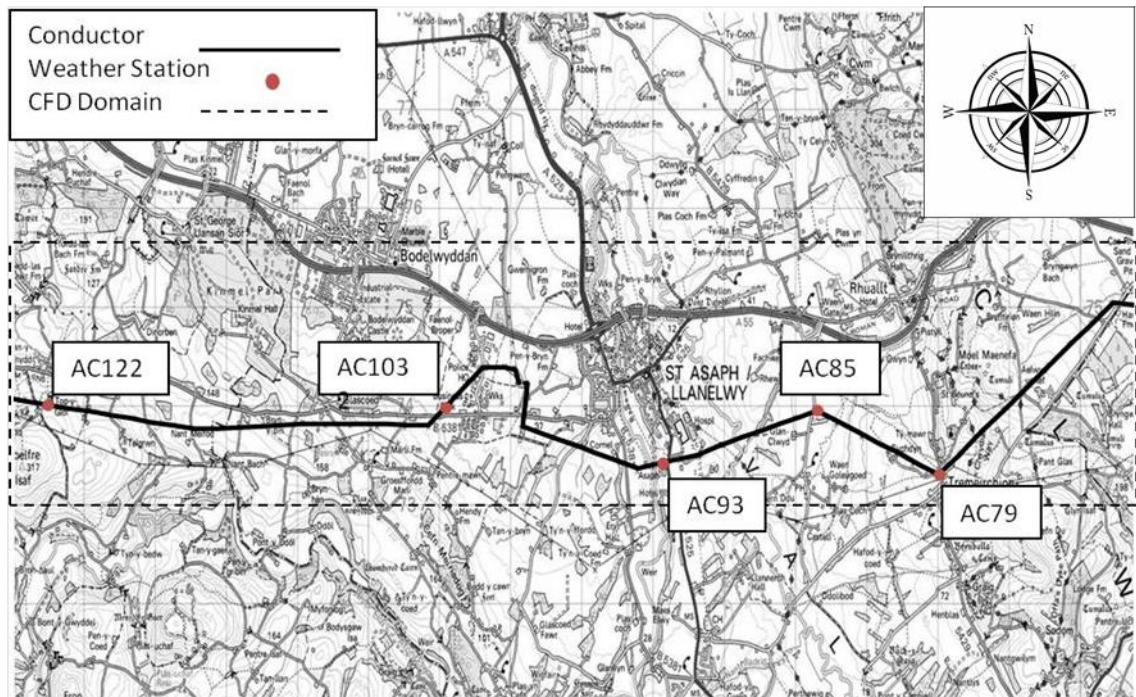
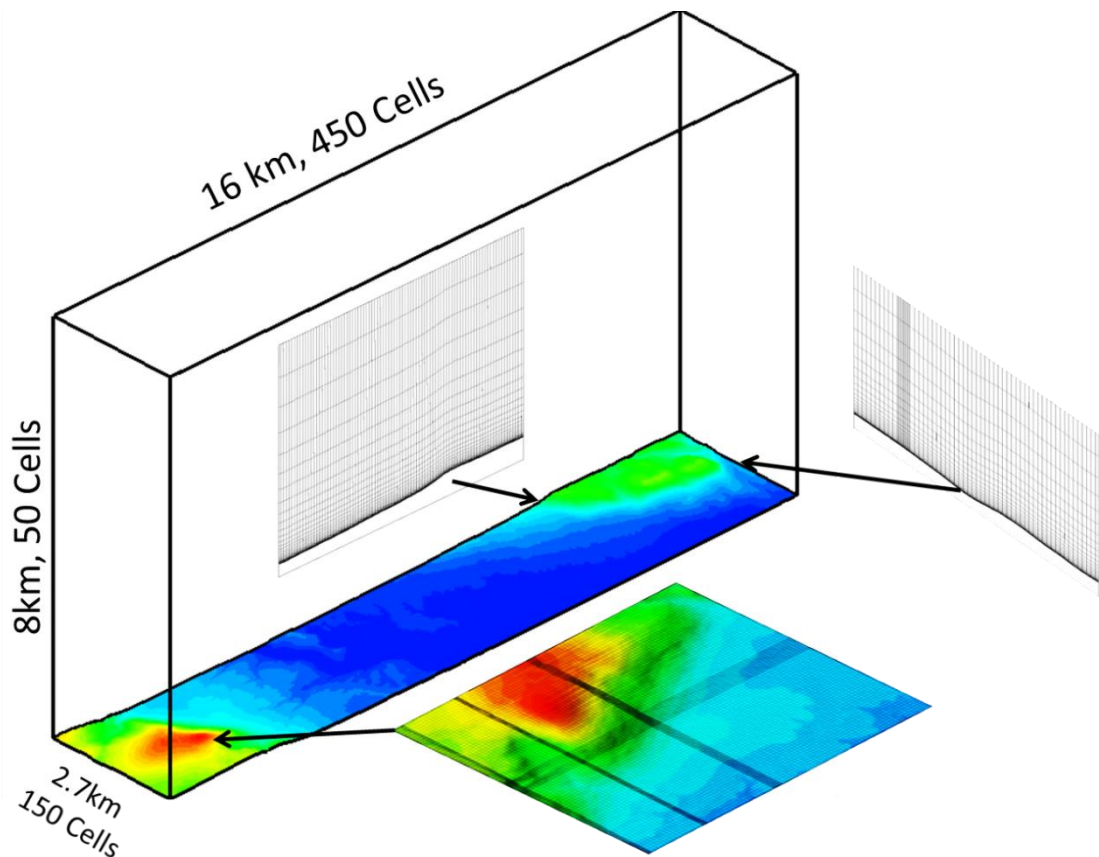


Figure 5.15: A map of the trial site area, showing local features and the location of the meteorological stations and conductors

The case study presented in this thesis is the same as that used by Michiorri *et al.* [44]. It was a section of 132kV distribution network located

in north Wales. The area of interest spanned 20km, with five meteorological stations deployed across the network. A map of the local area depicting the location of the meteorological stations and overhead conductors is shown in Figure 5.15.

The area included towns, wooded areas, hills and valleys. The elevation varied from sea level to 304m. The power conductors ran parallel to the north coast of Wales, approximately 6km inland. The conductors used in the study were generally under-utilized; however, proposed onshore and offshore wind farm developments meant that in the next few years the circuits were expected to be at capacity, making it an ideal test area for RTTR.



**Figure 5.16:** The CFD set up used for the state estimation case study. The surface is shaded with contours of elevation. The mesh structure on the edges and surface are shown.

Figure 5.16 shows the CFD set-up for the state estimation case study. The mesh structure both on the terrain, and as the mesh expands upwards, can be seen. The number of cells in each direction is shown.

### 5.3.3.1. CFD RESULTS

The CFD results were compared to the average normalized wind speeds from weather measurement stations using a sample of observations from similar prevailing wind conditions. Figure 5.17 shows some of the flow behaviours captured by the CFD simulation. As the flow passes over the hills, the curvature causes the flow to accelerate, resulting in a reduction in pressure. The surface plot shows contours of pressure, while the cross sectional views show wind speed, with stream lines of the flow.

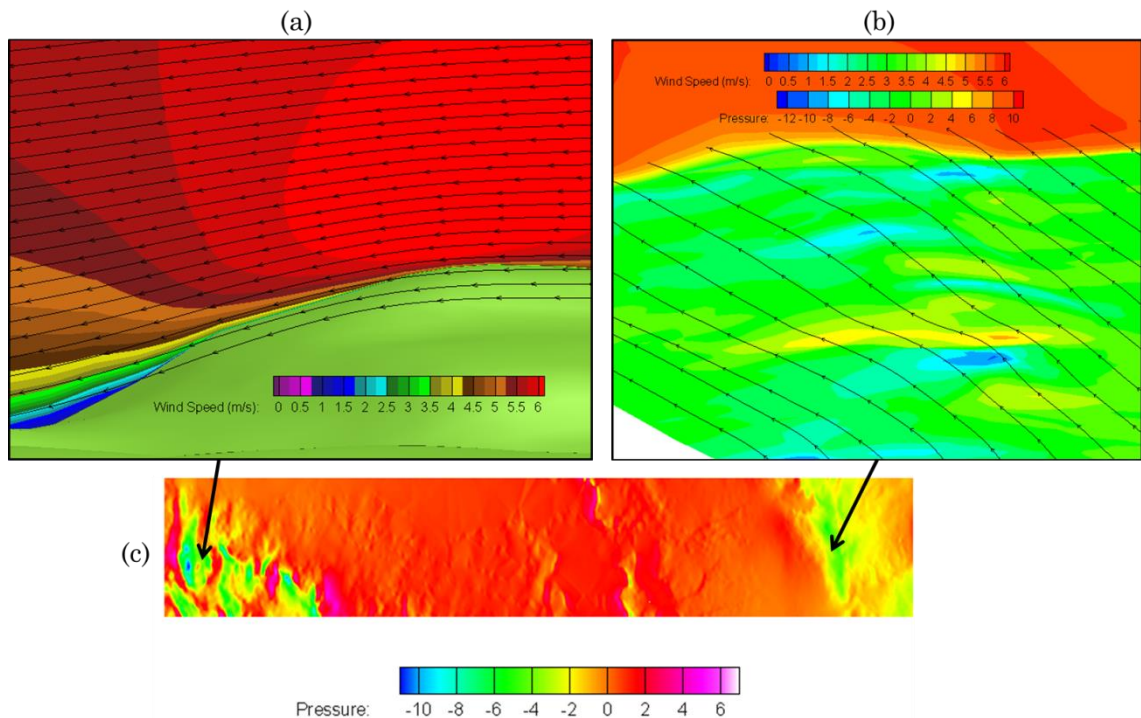


**Figure 5.17: Wind flow results for 290° inlet condition:**

**(a) – The change in velocity as the flow passes over a hill.**

**(b) – The structure of the boundary layer, with wind speed increasing as a function of height. Streamlines across the terrain are shown, and the terrain is shaded with contours of pressure.**

**(c) – The pressure changes across the domain; as the domain a section of valley, the complex pressure effects take place in the sloped regions at either end of the valley.**

Wind estimation validations were performed, by using the data from four of the weather stations to calculate the wind speed at the fifth. There are

therefore five validations conducted on the data. In Figure 5.17 a sample set of results is shown to illustrate the changes in speed and direction introduced into the flow by the terrain.

Figure 5.18 shows a comparison of the simulation results and those measured using the weather stations. Table 5.1 and

Table 5.2 show a comparison of the estimation process, combining the CFD simulations and the weather observations, and those measured using the weather stations. In general, the errors between the observed and calculated wind speeds were low as shown in Table 5.1. The main exceptions were weather station AC93 and AC122. AC93 station is located just to the south of a town, and for wind flows where the town comes between the inlet and the weather station the CFD wind speeds are much higher than the observations. This town was represented in the model by an area with high surface roughness.

What this did not account for was the increased height above ground level of any structures. In the actual environment this created a shadowing effect when the wind was blowing over the urban area, leading to the low wind speeds observed at AC93, which are not accounted for in the CFD model. This effect can be seen in the wind speed characteristic for 180° in Figure 5.18.

AC122 is remote from the other observation points. This suggests that RTTR deployments require meteorological stations to be spaced no more than 5km apart, which corresponds to a correlation of 0.8 in Figure 5.8.

**Table 5.1: Average errors in wind speed and direction estimation using the CFD Method**

	<i>AC93</i>	<i>AC85</i>	<i>AC79</i>	<i>AC103</i>	<i>AC122</i>
<b>Average CFD Error (m/s)</b>	2.01	1.00	0.98	1.04	2.62
<b>Average CFD Error (°)</b>	48.1	35.1	43.5	50.6	42.1

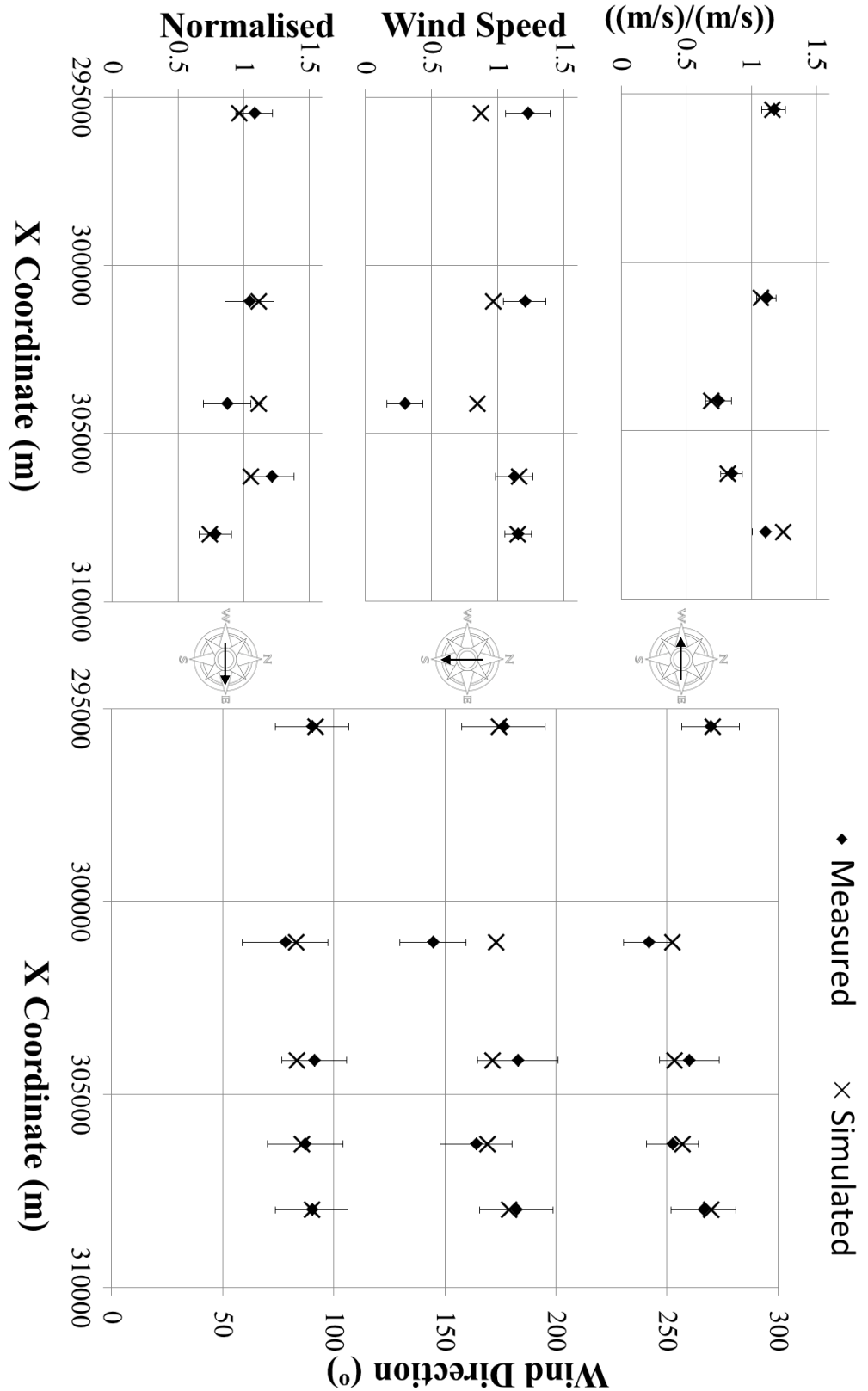


Figure 5.18: A Comparison of measured and simulated wind speeds and directions for 270° inlet condition (top), 180° inlet condition (middle) and 90° inlet condition (bottom). Measured results are calculated using 50 sets of observations of the appropriate prevailing wind direction, and error bars show one standard deviation of these values.

The wind model used a uniform inlet condition; this assumes that the wind flow into the domain is uniform, when in reality this will be a function of the weather across the region in which the domain is situated. Future work could try to address this by implementing different inlet conditions, and selecting which one to use based on regional weather, or by simulating a much larger area at a lower resolution and using this to inform boundary conditions for the high resolution domain.

### 5.3.3.2. REAL-TIME THERMAL RATING RESULTS

The aim of this work was to determine whether the CFD wind simulation results could be used in online state estimation. A validation was performed by estimating the rating at each meteorological station using observations from the other 4. Figure 5.19 shows the calculated rating using the new CFD method, compared with the actual ratings (assuming the rating is the same as it would be at the measurement station). The results shown here used data with a sampling rate of 5 minutes.

The estimated rating follows the trends in the measured rating, but is unable to accurately calculate high frequency changes. This could be because these are a result of local effects that could not be accounted for using remote measurement, even with a model to account for terrain effects.

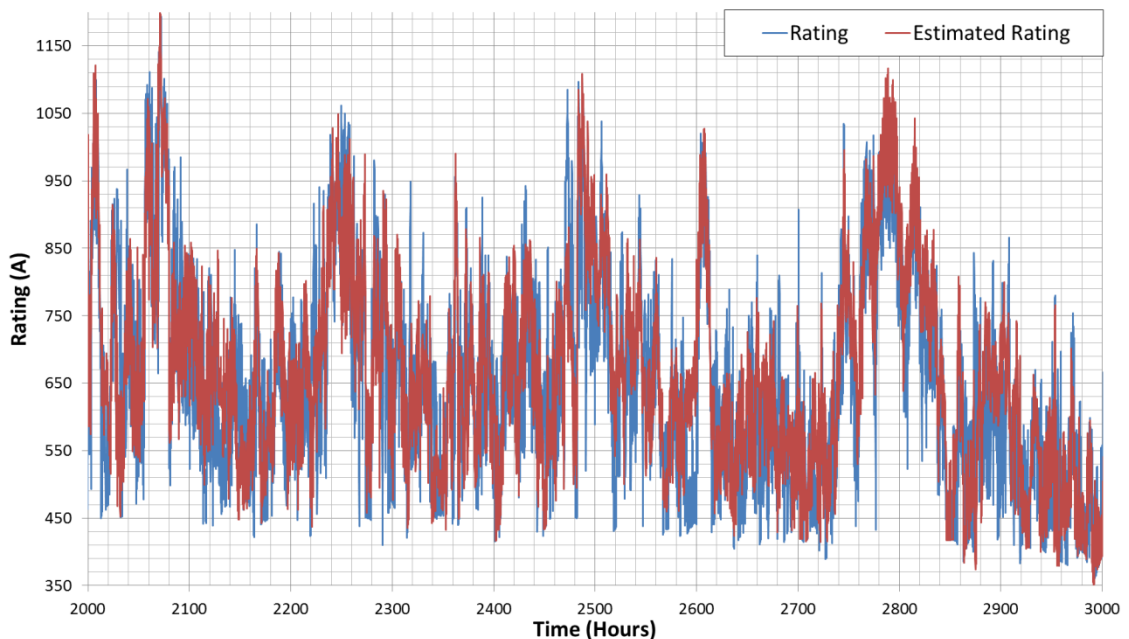


Figure 5.19: Comparison of CFD rating estimation and measured values

**Table 5.2: The absolute average error in rating prediction using the CFD method and using inverse distance interpolation**

	<i>AC93</i>	<i>AC85</i>	<i>AC79</i>	<i>AC103</i>	<i>AC122</i>
CFD Ratings Error (A)	161.5	93.9	86.4	102.7	176.2
CFD Ratings Error (%)	28.3	13.6	12.5	14.2	21.1
Inverse Distance Ratings Error (A)	145.5	118.6	97.7	88.3	180.6
Inverse Distance Ratings Error (%)	25.5	17.2	14.1	12.21	21.6

Table 5.2 shows the absolute average error using the CFD method. There are larger errors at AC122, the most remote weather station, and AC93, which is directly in the shadow of the city of St Asaph. This illustrates some of the limitations of using these methods; the applicability of weather observations is dependent on the distance between the observation and the area of interest, and assumptions in the CFD model can lead to poor estimation in some locations. The sensor placement guidelines in section 5.2.6 could alleviate these issues to some extent.

One of the key benefits provided by CFD modelling of the area around the conductors was that it provided additional information about the wind flow at unobserved locations. Figure 5.20 shows the effect of this; the top contour plot shows the elevation across the domain, the middle contour shows ratings across the geographical area simulated using the CFD method, while the bottom plot shows the ratings as estimated using inverse distance interpolation. The CFD provides a level of extra information about where low and high wind speed areas are within the domain. However, the method used to apply the CFD results to the problem has room for improvement; since it only uses the current observation it does not make full use of the known information. The effect of the low wind speed station AC93 is more pronounced in the bottom contour plot, leading to a reduction in rating over a large area, based on a localized effect.

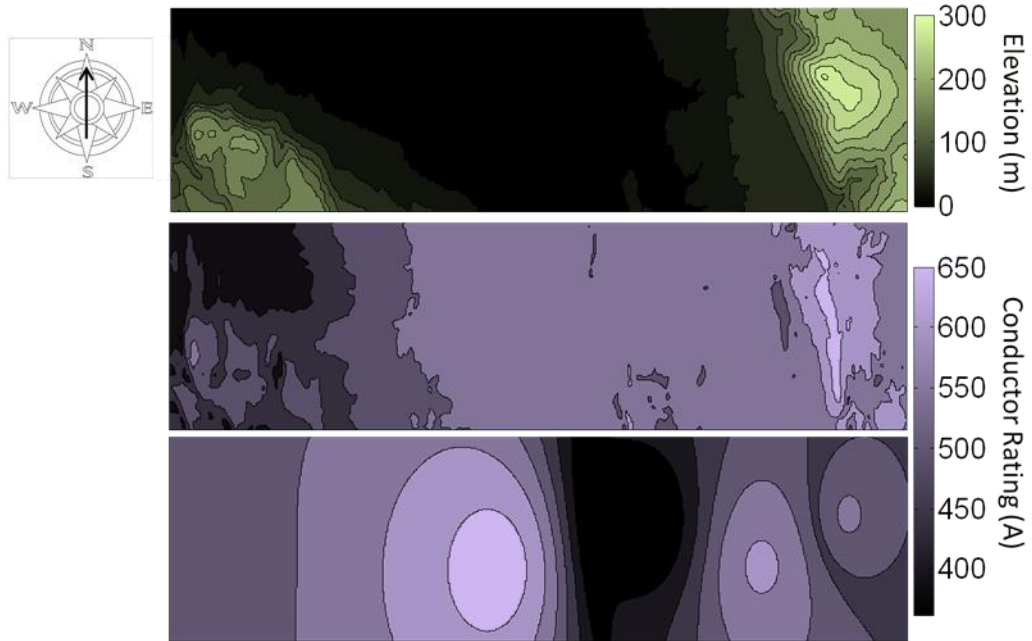


**Figure 5.20: Terrain geometry compared to line rating using CFD interpolation (middle) and inverse distance interpolation (bottom)**

#### 5.4. CONCLUSIONS

This chapter has described how wind simulations were used to provide information about wind flows local to RTTR schemes, both in network planning and operation. Planning methods were proposed, using concepts commonly applied in the wind energy industry, to identify thermal bottlenecks in the network, allow RTTR informed planning of new network assets, inform sensor placement and allow network operators to see the potential benefits of RTTR prior to deployment. Further to this, a time series analysis method was described to calculate the constraints and energy yield of new wind farms connecting to the network.

A case study using a real wind farm connection in north Wales was considered, and the capability to connect a 140MW wind farm to a line that could only support 89MVA with a low level of constraint was demonstrated. If the overhead line was built through only high wind areas, the level of constraint could be as low as 1-2% of total energy yield.

These methods allow network planners and designers to estimate how much additional capacity will be provided through RTTR before deploying any

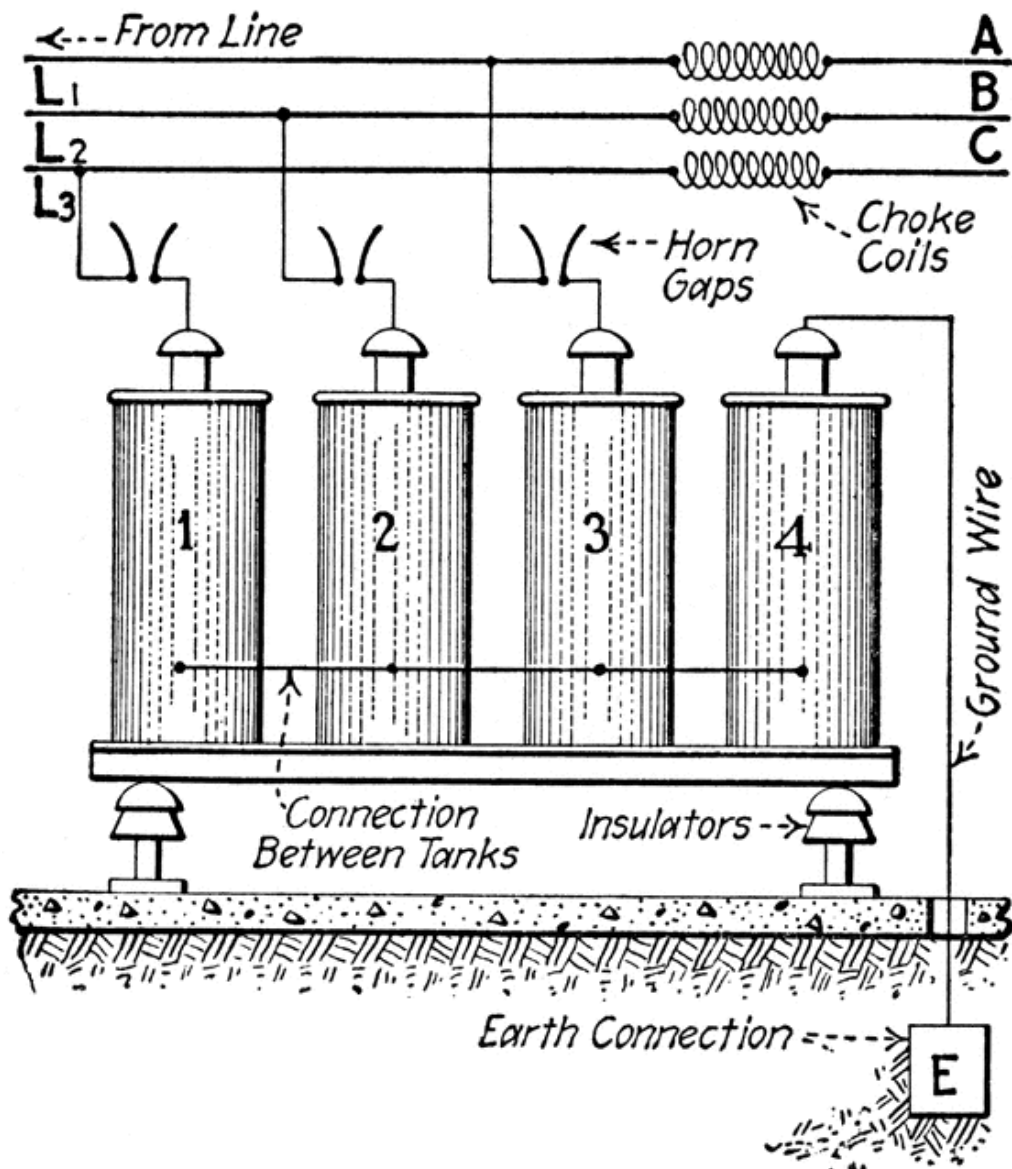
equipment to the network. Furthermore, the methods can be used in the planning of new assets, allowing these to be appropriately selected and located to maximise the benefit of RTTR. The ability of RTTR to facilitate additional wind generation has been extensively researched, but this work investigates it from a unique perspective. The use of wind simulations to estimate generation output and line rating concurrently allow the estimation of energy yields while accounting for thermal bottlenecks. Finally, the ability to predict which areas of network can be well represented by wide area meteorological monitoring, and which require additional instrumentation will allow RTTR deployments to balance cost effectiveness and accurate measurement.

A methodology for estimating wind speeds and directions in a weather based RTTR system was also developed. Existing interpolation based methods [44] took no account of the relationship between terrain topography and wind flows. The method provided reasonable estimation, though the errors were higher than is desirable for operation. The method as it stands could be applied with sufficient uncertainty quantification and improvements to the simulation and state estimation methods could reduce this error.

This new method allows that relationship between terrain and conductor rating to be accounted for. By coupling pre-calculated wind speed and direction values with real time observations, the method allows conductor ratings to be calculated quickly, which is essential to avoid conductors exceeding their design temperature.

These methods have been demonstrated using real world case studies, demonstrating that the methods suggested are not just theory; they can provide real benefits to network operators.

## Chapter 6. Impact on Network Reliability



## 6.1. INTRODUCTION

While Chapter 3 described a method for evaluating how much additional load could be accommodated at a specific supply point, this chapter considers the same problem from a system-wide perspective. The variable conductor ratings present in a network utilising RTTR will affect the reliability of that network. Outages coinciding with times of high rating or low demand are unlikely to result in a loss of load, but if a contingency coincides with low ratings (on a warm, still day for instance), then the network operator may be required to take corrective action even though the conductors are operating within their seasonal rating.

## 6.2. BACKGROUND

Power system reliability has always been important to network operators. Since the advent of computing power, more complex solutions, both analytical and Monte Carlo (MC) based, have become available. There are two problems to be solved within power system reliability; generation adequacy, whether there is sufficient generation to meet demand and transmission adequacy, whether there is sufficient transmission capacity to connect generation to load [149]. Transmission systems are concerned with both problems, while distribution networks are only concerned with transmission adequacy. That being said, generation at lower voltages can be used to assist in transmission adequacy [91]. Since RTTR provides a benefit to transmission adequacy, only that was considered in this work.

Network reliability can be quantified in different ways. Loss of Load Expectation (LOLE) is the amount of time over a given period for which the load is not adequately supplied [149]. Loss of Energy Expectation (LOEE) goes further by assessing the deficit between the load and the supply.

### 6.2.1. PROBABILISTIC RELIABILITY ASSESSMENT

Power systems are large and complex, and as such the number of possible states the system can occupy during operation can be extremely large. This large state space makes analytical state space enumeration, where the

probability and consequence of each state is evaluated, difficult and time consuming. MC simulations offer a way to explore this state space by simulating a large number of random input states to assess system behaviour.

MC simulations can take various forms. For this application one option is state sampling MC [150, 151], where each input variable is assigned a probability distribution. Samples from these distributions are then used to perform a large number of calculations to explore the state space. This method is simple, but does not account for any time dependencies within the model. The sequential MC simulation [152, 153] keeps this time dependency intact, but at the cost of greater computational resources and complexity. A method for pseudo sequential MC simulation was proposed [154] where states are sampled randomly from a time series, but on occasions where the system was not adequate the duration of this inadequacy was examined by looking at the appropriate section of the time series.

A key difficulty in evaluating the impact of RTTR on system security is the correlation structure between the ratings of the lines in the network. Networks cover a wide geographical area, so while overhead lines which are directly connected will have highly correlated ratings, while lines which are more remote will have weakly correlated ratings. This implies that stronger correlation will be present in distribution networks than transmission networks, since in distribution networks a large number of conductors cover a smaller geographical area. The correlation between conductors in transmission networks will generally be lower than those in distribution networks, because the transmission network spans a larger geographical area. In all cases, the terrain local to the conductors will have an impact on these correlations. The effect of wind speed correlation on the reliability provided by wind generation was investigated by [155] and a methodology for incorporating these correlations into the MC simulation was developed. The method used a genetic algorithm to ensure the sampled variables corresponded to a previously selected correlation between wind sites. The methodology used an Auto-Regressive Moving Average (ARMA) model of

wind speed [156]. This allowed a synthetic data set much larger than the real data set available to be used in a sequential MC simulation. The paper concludes that multiple independent wind farms provide a higher contribution to network security than a single wind farm, or multiple wind farms in the same wind regime. A similar approach was taken by [157] to allow wind data to be incorporated into power systems studies in the UK. The study used vector auto regression to account for the geographic correlations.

This concept is important for assessing the impact of RTTR, though the effect of the correlations may be different. The correlation between the ratings of lines must be accounted for in any model of network security incorporating RTTR.

A MC approach to evaluating steady state security is presented in [158], considering power flows and defining security in terms of power and voltage limit violations and stability, rather than by more conventional LOLE indices. This kind of approach could ultimately be incorporated into a reliability assessment involving RTTR, but is currently beyond the scope of this work.

#### 6.2.2. NOVEL RELIABILITY ASSESSMENT METHODS

Although MC simulations are an effective means of estimating power system reliability, alternate methods have been proposed which attempt to provide the same level of detail at a reduced computational cost.

In an attempt to deal with the complexity of incorporating wind generation into a reliability analysis it is possible to group areas of network into individual reliability models [159]. Each element has a single failure rate and repair rate to represent all amalgamated components. This works well for the intended application, since it vastly reduces the state space. However, this approach does not work well with RTTR, since each conductor has a variable rating and cannot easily be amalgamated into a sub network.

Many solutions attempt to search the state space more effectively. State space enumeration becomes difficult once a network is sufficiently large, but many of the states are extremely low probability. In [160], a composite state-space enumeration/MC approach is suggested. State Space enumeration is used to assess the high probability states while MC is used to evaluate the low probability states. If the correct threshold is used to determine to what extent state space enumeration is performed the improvement in computational time is significant.

Particle swarm optimization is suggested as a means to quickly and intelligently search the state space [161, 162]. Again, considerable improvements can be made in computational time compared to MC methods.

Unfortunately these approaches are not well suited to the RTTR application. The variable conductor ratings mean that each conductor has many states representing different rating levels. This vastly increases the number of low probability states, making state enumeration far more intensive. The number of states could be reduced by breaking the rating of the line into a small number of discrete states, but this would lead to a loss of detail in the results. The complex correlations between the conductor ratings in the network are also difficult to assess using a state space method, but can be accounted for using a sequential MC simulation. This correlation structure would also make the state probabilities difficult to calculate analytically.

After investigating the available methods for assessing power system reliability, sequential Monte Carlo simulation seems most appropriate for the RTTR application. MC is an effective means of exploring a large number of low probability states [160], and sequential ARMA models with pre-specified correlations can allow the correlations between line ratings to be accounted for. The downside of MC is that long calculations are required. Because this work deals with network reliability from a planning perspective, time consuming calculations are acceptable.

### 6.2.3. STUDIES INVOLVING SMART GRIDS

Implementing smart grid projects will have an impact on network security [163]. It is possible that by pushing the existing infrastructure harder than before, Smart Grids may reduce system reliability. Reliability may also be damaged by reduced infrastructure investment, which is a problem that could be exacerbated by network operators investing in smart grids rather than building new conductors.

The consensus is that smart grids will rely heavily on IT and communications infrastructure [154, 163], and that the reliability of these components will heavily influence the reliability of the smart grid. It is clear that in assessing the impact of RTTR on power network reliability, the reliability of the RTTR technology must be taken into account.

Conductor ratings are calculated such that there is redundancy in the system for the majority of normal operation [10]. However studies have tried to increase the network efficiency by looking at standalone conductors [164]. This study takes a risk based approach to conductor ratings, assigning the factors which govern the rating probability distributions in order to come up with a risk based rating. Some of these probability distributions are not appropriately selected, for example wind speed was modelled using a normal distribution when a Weibull or Rayleigh distribution is generally considered more appropriate [165]. Additionally, conductor ratings are already calculated using a risk based approach [10].

## 6.3. METHODOLOGY

### 6.3.1. OVERHEAD LINE RELIABILITY MODEL

The reliability of the overhead lines in this study was represented as a two state Markov process; an up state (available) and a down state (unavailable) [166]. The probability of being in the down state is given by equation (54):

$$P_{line} = \frac{MTTR}{MTTF + MTTR} = f \frac{MTTR}{8760} \quad (54)$$

Where MTTR is mean time to repair, MTTF is mean time to fail (in hours) and  $f$  is the failure rate (failures per year). Transmission system reliability data were available [167].

### 6.3.2. RELIABILITY TEST NETWORKS

In order to develop a methodology for assessing the reliability of an RTTR enabled network, a test case must be used. Probabilistic reliability analysis is more commonly performed on transmission networks (though perhaps not as frequently as would be prudent), due to the high complexity and comparatively low impact of individual distribution network faults on loss of load.

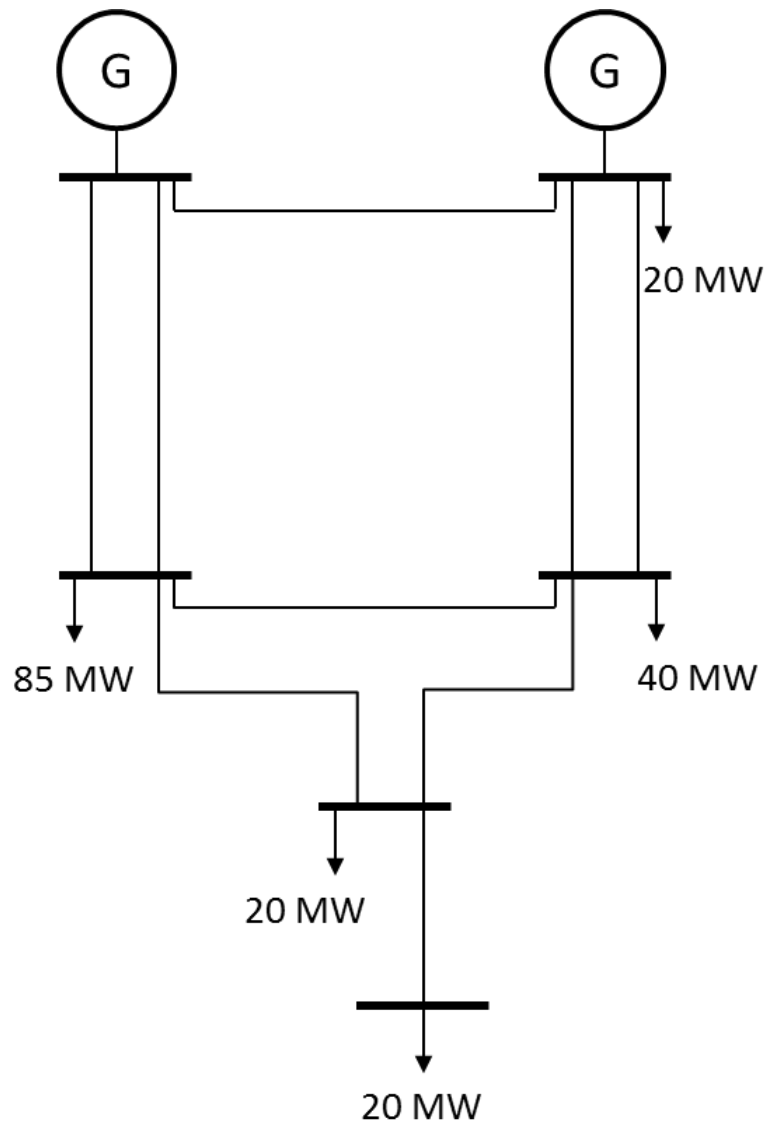


Figure 6.1: Diagram of the test network

Various test networks are available. Figure 6.1 shows the RBTS [168] is a 6 bus, 9 transmission line system. This small network was used because it allowed results to be easily analysed. The changes in power flows due to outages are obvious, so it is easy to see where RTTR is providing a benefit. The IEEE 14-bus, 24-bus and 39-bus networks were used to test the scalability of the method.

### 6.3.3. STATE SAMPLING SIMULATIONS

State sampling Monte Carlo simulations are simple to perform. The different parameters in the model are represented by probability distributions. In each calculation, every parameter is represented by a random sample from these probability distributions. The model is then run a large number of times to effectively explore the state space. Reliabilities can be represented as a simple probability derived from the MTTF and MTTR, since the state sampling method does not use any kind of time series.

The line ratings were approximated by a normal distribution with  $\mu=1.7$  and  $\sigma=0.35$  as a proportion of static rating. The load data were sampled from a simple load distribution curve.

Since this study is concerned with the impact of RTTR on transmission adequacy the generation was considered to be perfectly reliable. The impact of RTTR on composite system reliability could be considered in a future study.

State sampling studies gave reasonable results, but the impact of outage durations, the time domain behaviour of the line rating and loading and the correlation structure between the line ratings were all of interest, and could only be properly represented by a sequential simulation.

### 6.3.4. SEQUENTIAL MONTE CARLO

Sequential MC was used to give a more complete and realistic representation of the system. Synthetic time series were used rather than PDFs, and a Markov model was used to represent the reliabilities.

To perform sequential MC studies, the existing sampling method for generating rating data was replaced with synthetic time series calculated using real data. An Auto Regressive Moving Average (ARMA) model was used to represent the ratings. Third order auto regressive and first order moving average models were used. The model was generated using the square root of the ratings data, since this provided a closer approximation to a normal distribution than the ratings themselves. The distribution used is dependent on the specific historical data, and an appropriately selected model will lead to more representative results.

The auto regressive model was fitted using Matlab, and was of the form:

$$r_{(t)} = 1 + 1.47143R_{(t-1)} - 0.425698R_{(t-2)} - 0.0500508R_{(t-3)} - 0.825862\alpha_{(t-1)} \quad (55)$$

Where  $\alpha$  is a random sample from a normal distribution with  $\mu=0$  and  $\sigma=1.216$ . The model is based on data from a RTTR trial site with a sampling rate of 5 minutes [44]. The thermal time constant of the overhead line is such that the rating must be updated every 5 minutes to ensure the conductor operates within the thermal limit [93]. One year of historical data was available, so the ARMA model was used to allow simulations of time periods greater than one year.

The PDFs used were evaluated in terms of the average root mean square error (ARMS) [169]:

$$ARMS = \frac{\sqrt{\sum_{i=1}^N (F_{Mod,i} - F_{Ref,i})^2}}{N} \quad (56)$$

Where  $F_{Mod,i}$  and  $F_{Ref,i}$  are the  $i^{th}$  values on the CDF curves of the fitting model and the reference respectively.  $N$  is the number of selected points which are chosen from the range of the CDFs within a certain interval. The historical data were used as the reference. The ARMS values for the models used in the analysis are shown in Table 6.1.

<i>Parameter</i>	<i>ARMS Error</i>
Rating	3.57%
Load	2.70%
Square Root of Rating	2.03%
Square Root of Load	0.70%

**Table 6.1: Average Root Mean Square errors of the load and rating distributions**

### 6.3.5. CORRELATED RATING TIME SERIES

In a network, conductors at geographically close locations will have ratings which are correlated to one another in some way. Figure 6.2 shows correlations calculated using weather data from the UK. The weather data was used to calculate conductor ratings via the CIGRÉ overhead line model [17]. Two sets of weather stations were used; one set of tightly grouped stations, with a maximum spacing of 15km, and four stations spread across the UK with a maximum spacing of over 600km. The correlations were calculated using the Pearson product-moment correlation [146]:

$$\text{corr}(X, Y) = \frac{\text{cov}(X, Y)}{\sigma_x \sigma_y} = \frac{E[(X - \mu_x)(Y - \mu_y)]}{\sigma_x \sigma_y} \quad (57)$$

Where *cov* is the covariance, *E* is the expectation;  $\mu$  is the mean and  $\sigma$  is the standard deviation.

The results demonstrate that although the high correlation between the ratings of nearby conductors decays quickly with distance, there is still some correlation between conductors hundreds of kilometres apart. Conductor ratings are governed by weather conditions, and conductors hundreds of kilometres apart will still be affected by the same large scale weather phenomena.

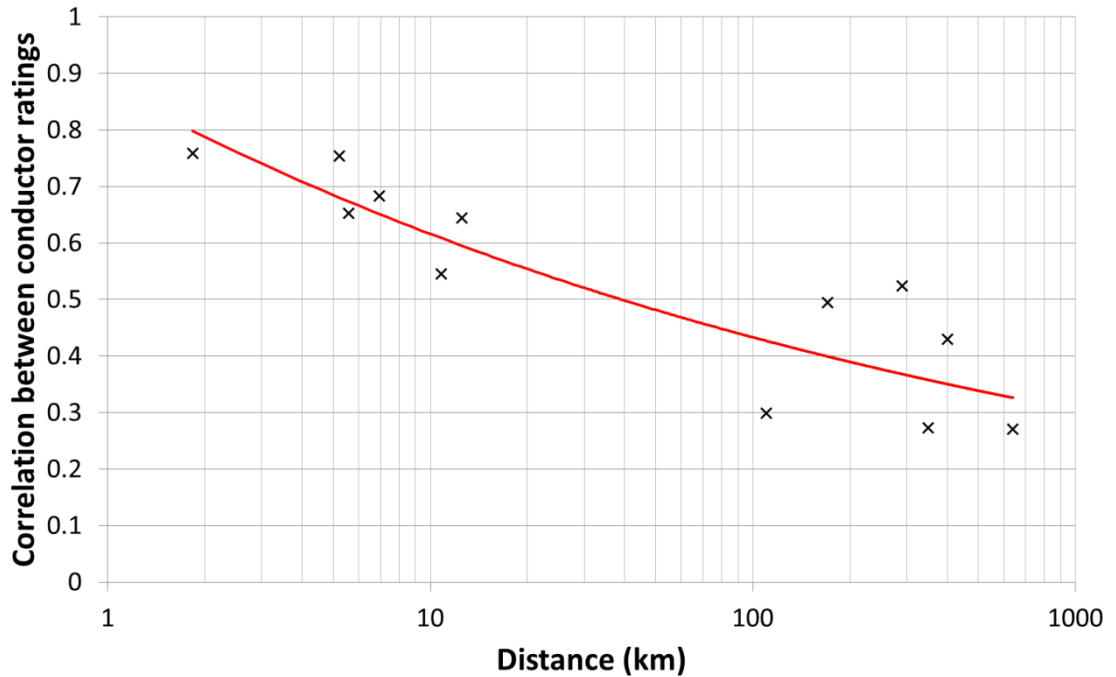


**Figure 6.2: Plot of correlation between conductor ratings against distance between conductors**

These correlations must be represented in the model. The ARMA model used to represent the ratings uses a random number string as part of the moving average model. If these strings are specified with set correlations to one another, then the resulting ratings data will have a similar correlation [155].

Specified random number series can be generated using Cholesky decomposition [170]. This approach requires a positive definite matrix to be specified, where element (a,b) represents the desired correlation between conductors a and b (resulting in 1s on the leading diagonal, since this represents the correlation of a rating with itself). Cholesky decomposition is performed, to give the matrix U. A matrix of uncorrelated random numbers, R, can then be multiplied by U to give Rc, a matrix of correlated random numbers. This is shown in equation (59).

$$C = \begin{bmatrix} 1 & 0.75 & 0.60 & 0.75 & 0.60 & 0.75 & 0.45 \\ 0.75 & 1 & 0.75 & 0.75 & 0.75 & 0.6 & 0.60 \\ 0.60 & 0.75 & 1 & 0.75 & 0.65 & 0.75 & 0.60 \\ 0.75 & 0.75 & 0.75 & 1 & 0.75 & 0.75 & 0.60 \\ 0.60 & 0.75 & 0.75 & 0.75 & 1 & 0.75 & 0.75 \\ 0.75 & 0.60 & 0.75 & 0.75 & 0.75 & 1 & 0.75 \\ 0.45 & 0.60 & 0.60 & 0.60 & 0.75 & 0.75 & 1 \end{bmatrix} \quad (58)$$

$$R_C = RU \quad (59)$$

An example of this for the RBTS ratings is shown in equation (58) above. Conductors 1 and 6 and conductors 2 and 7 were assumed to have the same rating, so only seven sets of correlated ratings were generated. Figure 6.3 shows an example of this data. The correlations were checked against the desired values before the simulations were carried out. Alternatively the correlated random number series could be created through eigenvalue decomposition or using genetic algorithms [155].

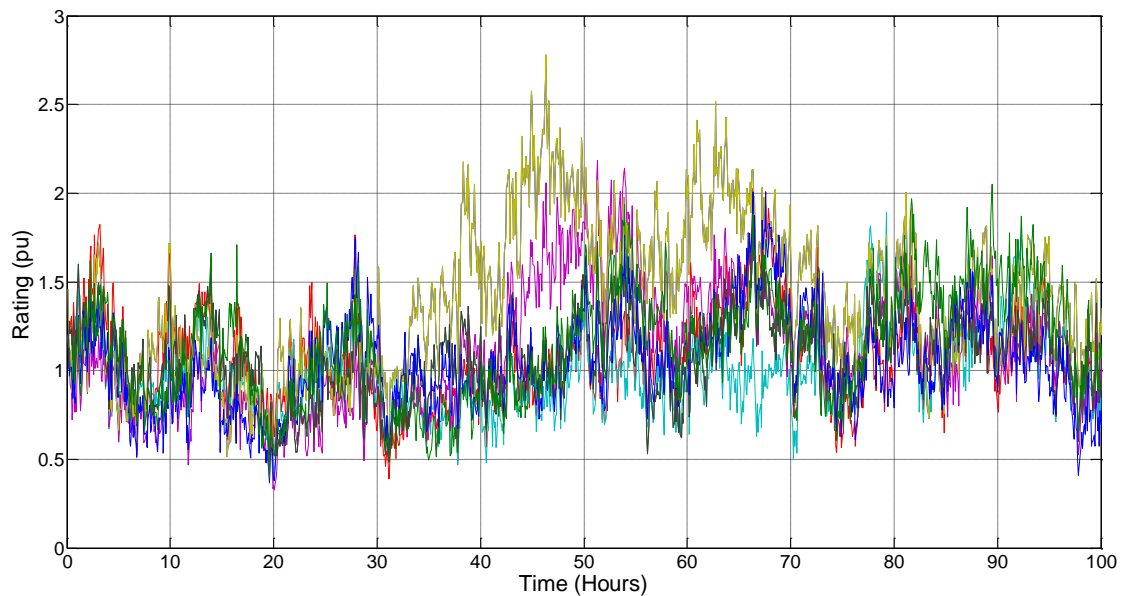


**Figure 6.3: 7 sets of rating data with pre specified correlations. Each time series shows the rating of a circuit in the network. The ratings follow the same general trends, but with a level of variation corresponding to the chosen correlations.**

Load data were created using the same method; the correlation between all loads was set to 0.8 and the model parameters were selected using historical load data. Again, the ARMA model used a normal distribution based on the

square root of the load data, since this gave the best approximation to the data.

The conductor reliability model was calculated ahead of time, with time series of data with each conductor in either the 0 (down) or 1 (up) state. A model was also included for the reliability of the RTTR system. When the RTTR system is in the 0 state, the conductor reverts to its static seasonal rating. This is a worst case assumption, since in operation some form of graceful degradation could be applied [171]. The MTTF and MTTR values for the conductors were taken from [168]. The RTTR system was assigned an MTTF of 3 months and an MTTR of 10 hours, though in reality these values would vary depending on which RTTR technology was implemented.

### 6.3.6. UNCERTAINTY QUANTIFICATION

In a real system, the operator will not have perfect information about the rating of the conductors. If weather based RTTR [44] is used, there are uncertainties in the measurement of weather parameters, the line rating model and using weather station data to estimate conductor ratings at an unobserved location. If a tension or sag monitoring solution [38] is used then there is uncertainty in the measurement of sag or tension, error in the model used to infer a rating from this data and further uncertainty because it is unlikely that every conductor span will be instrumented. If this methodology is to provide an accurate assessment of the benefits of RTTR then these uncertainties must be accounted for. Equation (60) shows an uncertainty model for RTTR, where  $e_{mod}$  is the uncertainty associated with the CIGRÉ ratings equations,  $e_{meas}$  is the uncertainty in weather or conductor rating measurements  $e_{PDF}$  represents the difference between the assumed probability distribution and the true data and  $e_{interpo}$  is the uncertainty arising from calculating the rating of a conductor based on measurements that are some distance away.

$$e = f(e_{mod}, e_{meas}, e_{interpo}, e_{PDF}) \quad (60)$$

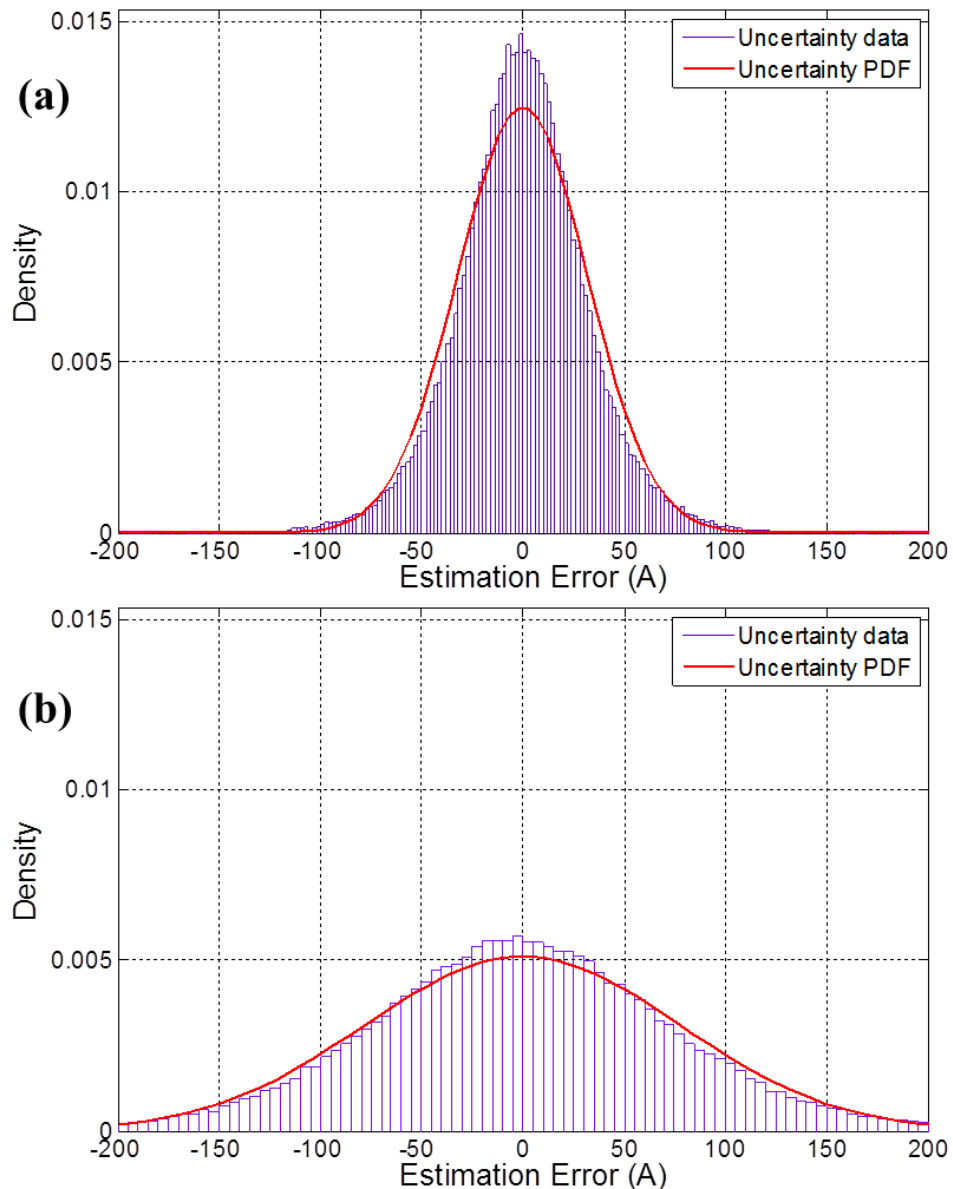


**Figure 6.4: Probability distribution of error in rating estimation**

This function was evaluated using a Monte Carlo model, using typical uncertainty values from RTTR proof of concept studies [44, 172] and the uncertainty in the CIGRÉ rating model [173]. The rating equations, along with randomly generated input errors, were used to calculate the distribution of errors as shown in Figure 6.4. The largest source of error is the interpolation error, which stems from the physical spacing of measurement equipment and the variability of weather conditions on relevant space scales. This could be alleviated by heavily instrumenting the network or by pre-identifying critical spans and instrumenting those areas. Figure 6.4(a) shows the error distribution with a 0% interpolation error (the

error at the location of the measurement), while Figure 6.4(b) shows the error distribution with an interpolation error of 10% (equivalent to a distance of 1km from the measurement location).

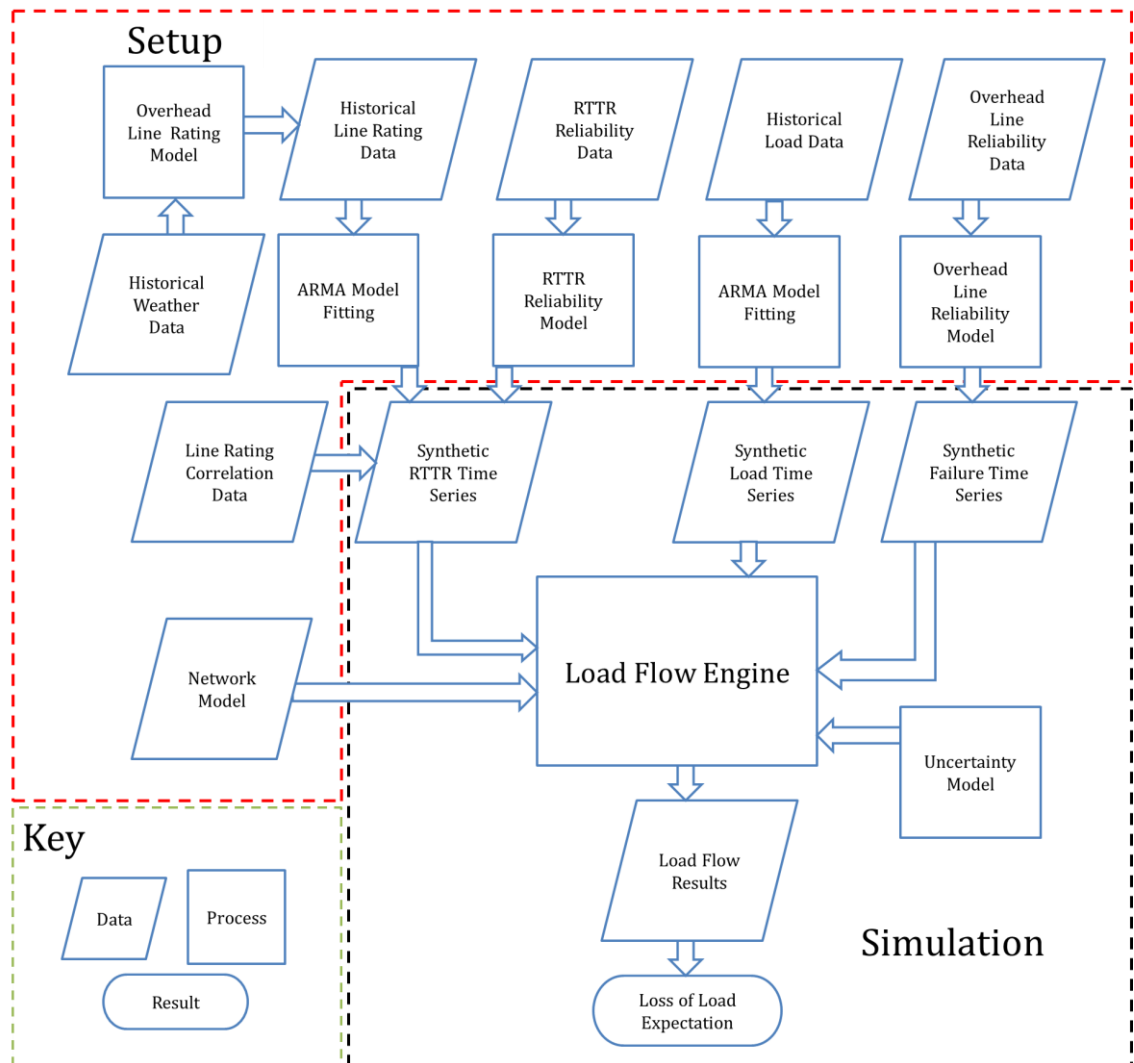


**Figure 6.5: A Flow chart showing the complete methodology, broken into setup and simulation steps**

The sequential simulation was run with different levels of rating uncertainty to see how this would affect the system reliability.

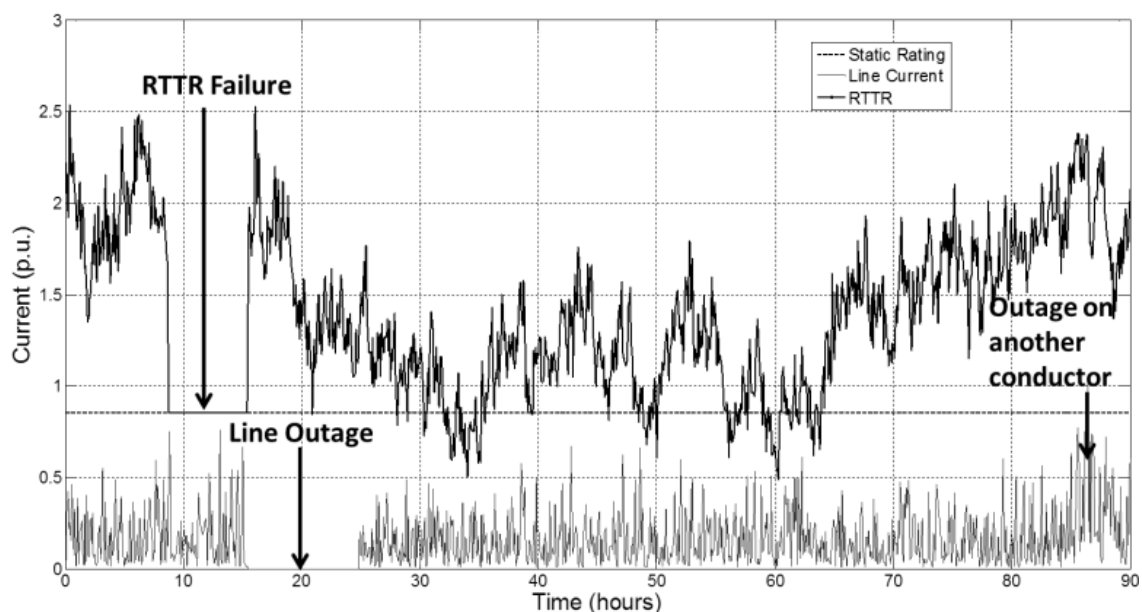
The complete methodology is shown in a flow chart in Figure 6.5. The method is broken up into set up and simulation steps. The power flows were solved using the Power Systems Analysis Toolbox (PSAT) in Matlab [174].

## 6.4. RESULTS

### 6.4.1. SYSTEM BEHAVIOUR

The main goal of this chapter is to produce a methodology to assess the impact of RTTR on transmission reliability. In order to do this it is important to first establish confidence that the methodology delivers a good representation of system behaviour with and without RTTR.

Figure 6.6 shows 90 hours of data from one line from a simulation of the test network. The figure shows a failure of the RTTR system, where the rating reverts to the static value and a failure of the overhead line where the line flow drops to zero. This capacity is made up by the other lines in the network, which could cause them to exceed their static ratings. An outage on another conductor is also shown, leading to a rise in the current flowing through the observed line.



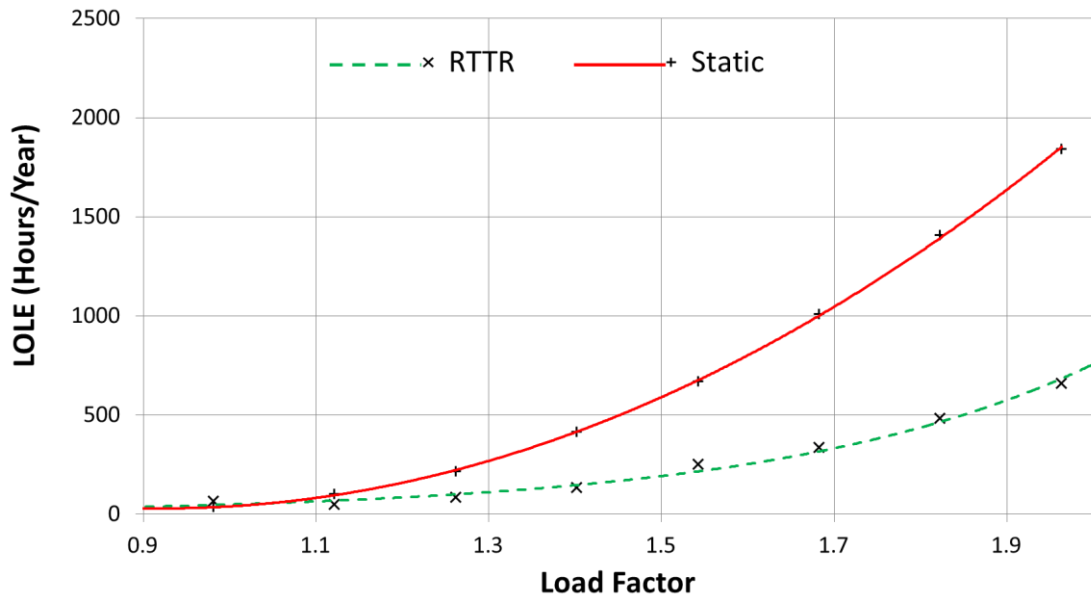
**Figure 6.6:** A plot of RTTR, static rating and line flow in amps, with an RTTR failure a line outage, the line flow exceeding the static rating and the RTTR dropping below the static rating all shown

Figure 6.6 also illustrates the behaviour of the line flow and the rating in a system using RTTR. On some occasions the RTTR drops below the static rating; having knowledge of this could help network operators make decisions during an outage to prevent damage to a conductor or a potential cascading failure. On other occasions the line flow goes above the static

limit, but still stays well below the RTTR. This demonstrates the benefit of RTTR not just to reliability, but to network capacity.

#### 6.4.2. RELIABILITY INDICES

The network was assessed in terms of its LOLE for a variety of loading conditions using sequential MC simulations.



**Figure 6.7: LOLE in hours per year for RTTR and static ratings at different network loading conditions**

Figure 6.7 shows the LOLE of the RBTS for different loading conditions. The load was increased uniformly taking the mean loading from 0.285pu up to 0.855pu. For low loading conditions the static rating appears to give a lower LOLE. This is an artefact from the calculation method used for overhead lines, and is effectively giving network operators a false sense of security. Conventionally lines are rated such that there is a low, but non-zero, probability of the actual rating being below the nominal rating.

At higher loading conditions the two data series diverge, with the RTTR providing a substantially lower LOLE. This is because often the high current flows required in the event of an outage can be supported by the enhanced capacity provided by RTTR, while using the static rating would require load to be shed or other corrective action to be taken.

### 6.4.3. EFFECT OF CORRELATION

More geographically dispersed networks will have a lower correlation between conductor ratings. Figure 6.8 shows the reliability of the network for different levels of correlation between conductor ratings, varying from complete independence to complete dependence.

The impact of correlation on reliability is small when compared with the overall improvement of using RTTR. The case with completely independent ratings yielded the lowest reliability. This is because there is greater variance between the ratings of lines within the network, leading to a higher likelihood of one line having a low rating and resulting in a loss of load. The effect of correlation increases with loading, because at higher loads reliability is more dependent on RTTR.

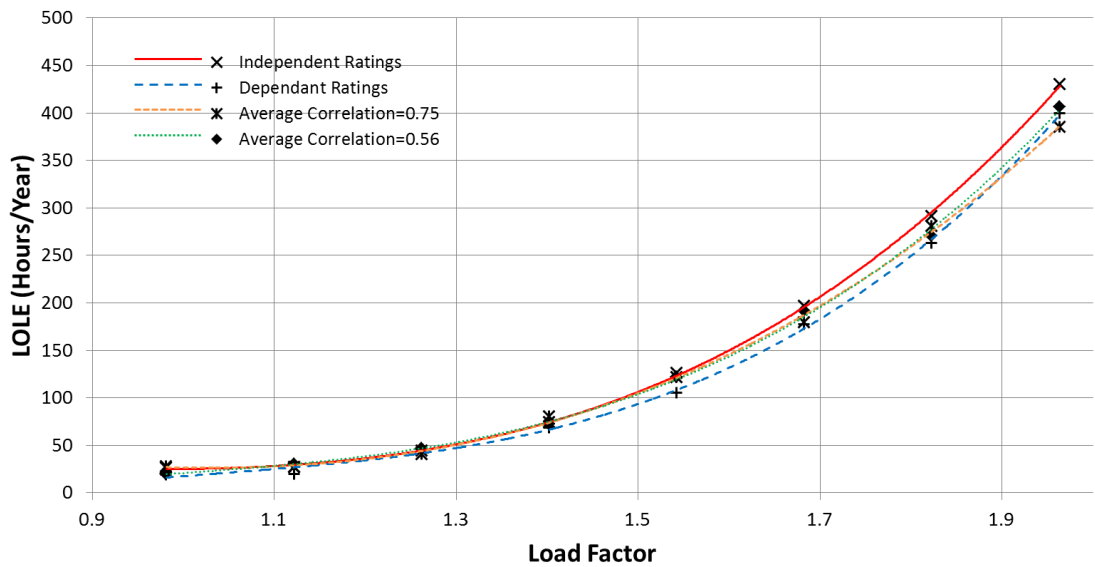


**Figure 6.8: The impact of correlation between ratings on network reliability. The results demonstrate that although the high correlation between the ratings of nearby conductors decays quickly with distance, there is still some correlation between conductors hundreds of kilometres apart.**

### 6.4.4. IMPACT OF UNCERTAINTY

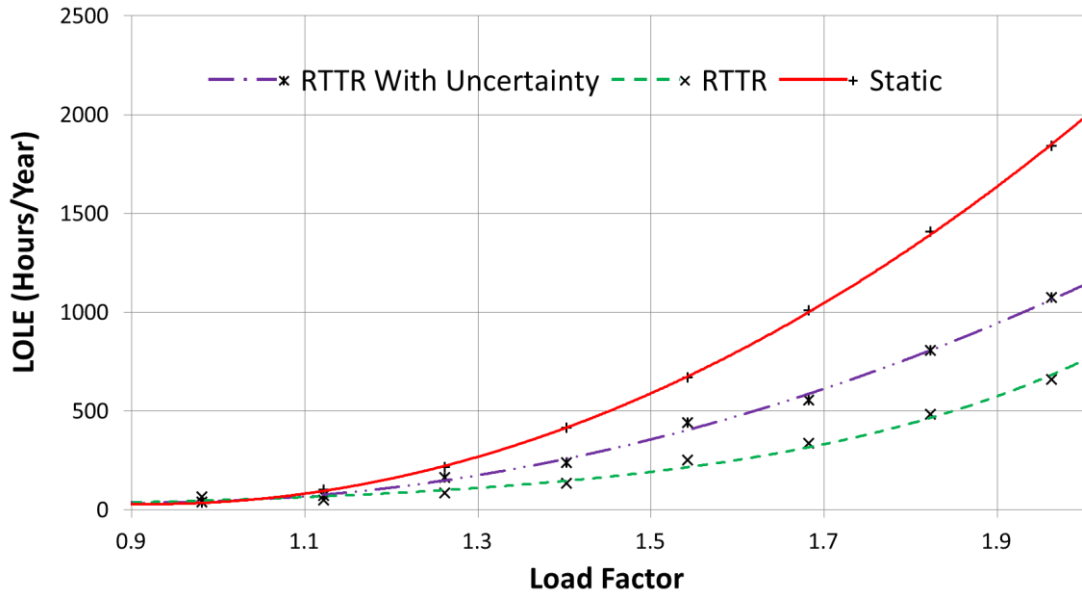
Rather than using a confidence interval, for each step in the time series the LOLE was evaluated probabilistically.

$$LOL_{k,j} = P(R_{k,j} < i_{k,j}) \quad (61)$$

And from the concept of expectation:

$$LOLE = 1 - \frac{\sum_{k=1}^m \prod_{j=1}^n (1 - LOL_{k,j})}{m} \quad (62)$$

Where  $m$  is the number of iterations,  $n$  is the number of circuits,  $R$  is the line rating,  $i$  is the line current,  $j$  is the line number and  $k$  is the time step.



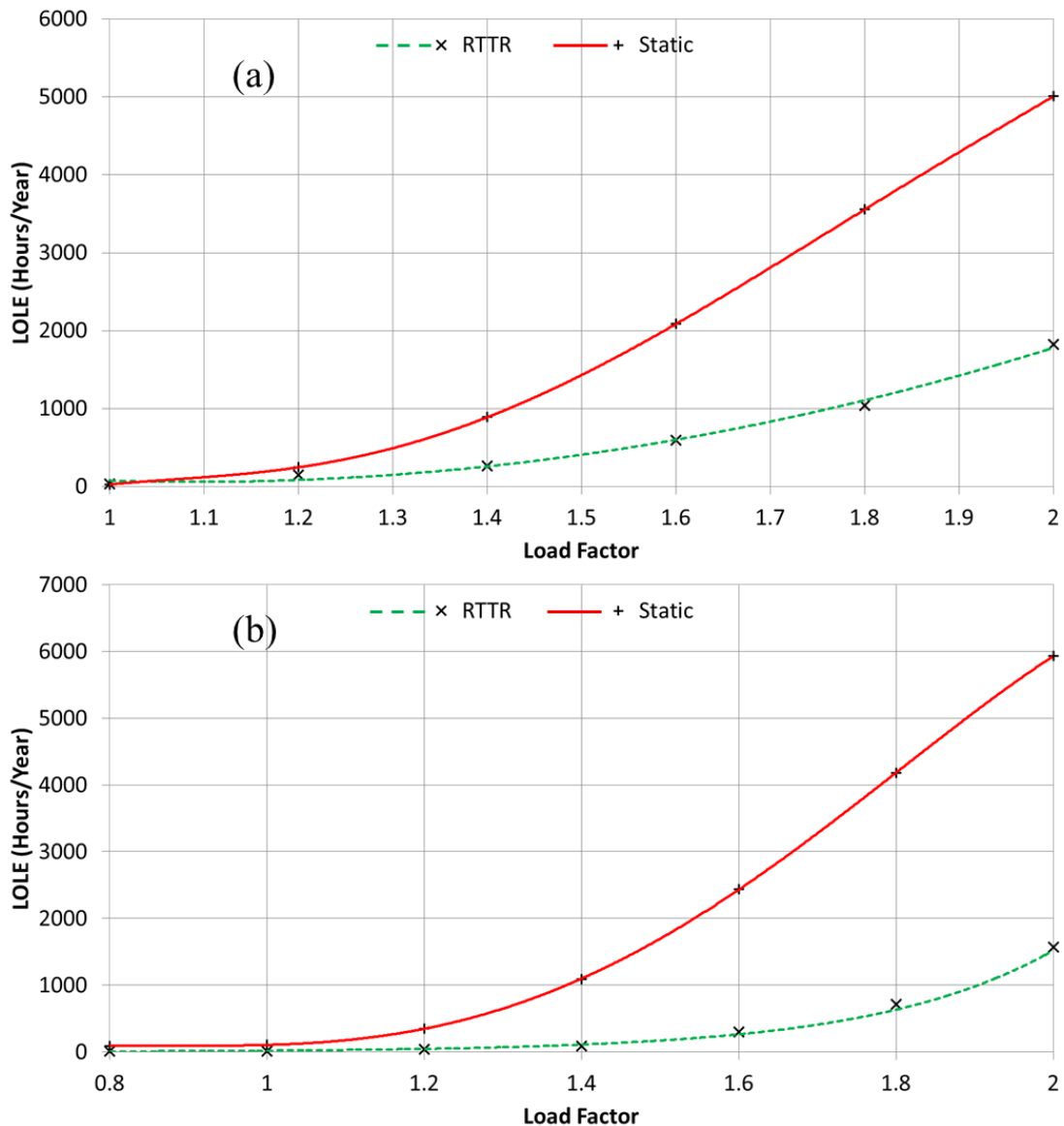
**Figure 6.9: LOLE in hours per year for RTTR with and without uncertainty. While the uncertainty reduces the improvement in LOLE there is still a significant benefit.**

Figure 6.9 shows the impact of accounting for uncertainty on the perceived benefit. The uncertainty shown had a standard deviation of 28.5A, which corresponds to the error at the location of a sensor. As the distance from the sensor increased, the uncertainty increased considerably and consequently the LOLE was greater.

With the uncertainty in the RTTR represented in the simulation there is still a benefit to reliability as loading increases. If a more accurate sensor or conductor thermal model were available, the LOLE would further decrease, approaching the benefit of the ideal RTTR system.

## 6.4.5. SCALABILITY

The results presented so far used the 6 bus RBTS. Since real power systems are larger, it is important to ensure the method functions on larger networks and scales reasonably in terms of computational time. RTTR calculations were performed for the IEEE 14, 24 and 39-bus test networks to test the system at multiple voltage levels and to see how well the simulation scaled with network size.



**Figure 6.10: LOLE in hours per year for the (a) 14 and (b) 24 bus network with and without RTTR**

Table 6.2 shows that the simulation time scales well with network size. These simulations were performed on a desktop PC with an Intel i5 processor and 8 GB of RAM. A more powerful computer could reduce the

computational times. Figure 6.10 shows the results of these simulations in terms of LOLE for the 14 and 24 bus network. The general trends are similar to that of the RBTS, with RTTR providing lower LOLE at higher load levels. However, the specific results depend on the network topology and loading conditions.

Initial RTTR deployments are likely to only cover small sections of network, allowing this kind of analysis to be easily performed. As computational power continues to increase, it will be possible to simulate larger systems in line with RTTR, and other Smart Grid deployments.

<i>No. of Buses</i>	<i>Simulation Time (100,000 Iterations)</i>
6	53 minutes
14	58 minutes
24	72 minutes
39	80 minutes

**Table 6.2: The impact of network size on simulation time**

## 6.5. DISCUSSION

### 6.5.1. HOLISTIC SMART GRID APPROACH

The results show that RTTR can give a substantial reduction in LOLE for heavily loaded networks. However the resulting LOLE at particularly high loads is still higher than network operators would accept. Consequently it is clear that RTTR cannot allow a doubling of network capacity in isolation. However as part of a holistic smart grid deployment RTTR could allow substantial increases in network capacity at a lower cost than conventional reinforcement.

For example if RTTR was employed alongside energy storage and demand side response (DSR) it should be possible to maintain the same high levels of reliability the network enjoys today. When the RTTR is high, energy could be transferred into storage facilities, and when the rating is low the additional capacity could be made up through storage. If this was not

sufficient, DSR could be used to ensure no customers are disconnected. Distributed generation could also be used to compensate during periods of low rating.

### 6.5.2. FINANCIAL BENEFITS

One of the incentives for network operators to connect distributed generation is that it can defer investment in new conductors [83]. RTTR can offer a similar financial benefit. A scheme implemented by Scottish Power Energy Networks in the UK [143] suggests that implementing RTTR could cost less than 10% of the cost of otherwise required network reinforcement. RTTR is currently still a new technology; if it is widely adopted then economies of scale will drive this price down further.

There is an argument that by using variable technologies and accepting a level of risk, networks can deliver better value for money to consumers and system operators [90]. Network capacity is currently deterministic (albeit based on some probabilistic analysis), and is provided through asset based redundancy; this may be expensive and inefficient in many cases. If network capacity was subject to a cost-benefit analysis, technologies such as RTTR would compare favourably to the existing approach. This chapter has demonstrated the benefit that RTTR can provide to network reliability. However changes in policy and standards may be required before the full benefits can be unlocked.

### 6.5.3. NETWORK MANAGEMENT AND RTTR DEPLOYMENT

The work presented in this chapter has not accounted for the benefits of active network management informed by the RTTR. In reality it would be possible for network operators to embed RTTR into their Network Management System (NMS) [171] and use active control to minimize the probability of exceeding the RTTR.

When an outage occurs network operators take steps to reconfigure the remaining network such that customers remain connected. RTTR will both alleviate the need to reconfigure the network, and provide a powerful tool to reconfigure it effectively should it become necessary. The benefits of

combining network reconfiguration and RTTR has been demonstrated by [175].

When deploying smart grids, the technology developers must be mindful of providing the correct information for system operators to make informed decisions. Too much information can cause decisions to become too complicated. In this case, the ideal information would be the rating of the determining span of each circuit, and information about the uncertainty of that value.

RTTR may not be an appropriate solution for all networks as many conductors will soon be in need of replacement. However, there are areas of network that are fit for purpose, but may need reinforcing before they would be replaced. These are the areas where RTTR, along with other smart grid technologies, could be successfully implemented. Further to this, there is no reason that RTTR could not be deployed on new networks; indeed networks could even be designed with RTTR in mind, possibly leading to a reduction in the number of conductors required, as discussed in Chapter 5 and [34].

## 6.6. CONCLUSION

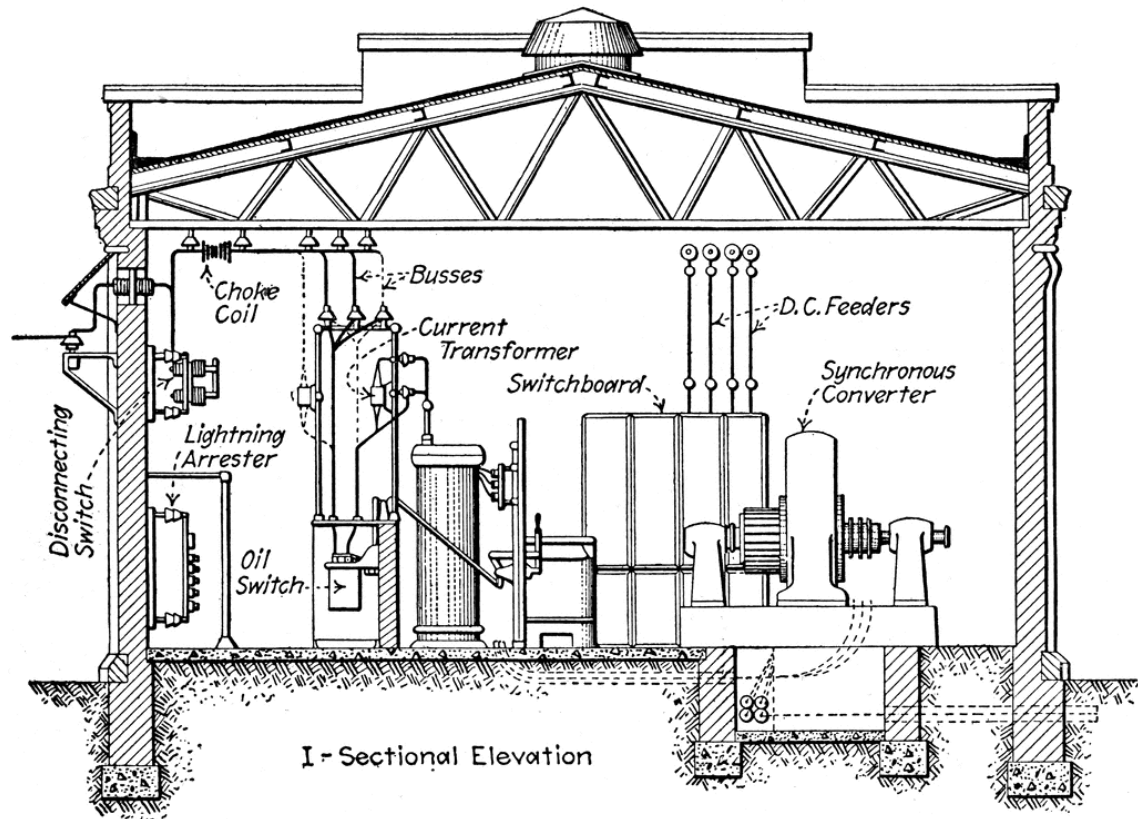
The primary contribution of this chapter is a novel method for assessing the contribution of RTTR to power system reliability. Though current transmission and distribution systems are very reliable, if more load is connected the reliability rapidly degrades and corrective action must be taken. Conventionally new lines would be used to alleviate the risks and provide further reliability. However this work shows how deploying RTTR could offset much of the risk without the need for any new infrastructure.

RTTR alone cannot deliver the high reliability the power systems currently operate under. However if it is deployed as part of a holistic smart grid strategy, network reliability could be maintained with a minimum of new conductors, instead relying on RTTR, DSR and energy storage to keep customers connected.

The analysis takes account of the reliability and uncertainty inherent in the use of RTTR. The uncertainty analysis suggests that for RTTR the greatest uncertainty arises from calculating the rating of components far from observation points. To offer the greatest benefit critical spans must be identified and instrumented, the whole network must be heavily instrumented or some means of predicting how ratings vary with distance must be devised and implemented.

Though this chapter has demonstrated that RTTR can make a significant contribution to network reliability, it does not fit in to the existing paradigm of network design. Network design and planning standards must move away from asset based redundancy and accept the capacity provided by technologies such as RTTR. With proper planning and analysis, this will yield more cost-effective networks without compromising reliability.

## Chapter 7. Discussion



## 7.1. INTRODUCTION

The preceding chapters have described the research that has been carried out over the course of the author's PhD. In each chapter, specific pieces of work were described, and their findings discussed. This chapter discusses the broader implications of the work, and how it could affect the electricity industry. Additionally, while the research fills gaps in the state of knowledge, and builds on some existing work, there is still more research that could be undertaken in this area. This chapter describes several of these proposed research avenues, discussing what the additional value of the work could be.

## 7.2. DISCUSSION

The methods described in the preceding chapters solve individual problems, or remove barriers to the implementation of RTTR. However, up until this point they have been looked at in isolation, when often they could be applied together. This section discusses how the combination of these methods is useful to network operators, and how they combine to form a significant contribution to the power systems domain.

Chapter 3 describes a method for assessing the likelihood of overhead lines being insufficient to supply customer demand. This is useful to network operators in and of itself, but this work also adds a level of transparency that is absent from the existing ratings approaches in the UK and elsewhere. Having a robust understanding of the likelihood of exceedance, and exceedance of varying size and duration, combined with knowledge about the reliability of assets, can allow better informed decisions to be taken than by using a single line ratings standard.

This transparency is a valuable asset in attempting to make a case for using RTTR instead of conventional line ratings. RTTR is seen by operators as introducing risk whereas, in the opinion of operators, with static ratings, there is no risk. This is not correct: with static ratings there is already a risk that loading will exceed the actual (as opposed to the nominal) rating. This

work helps to demonstrate that risk is already present; RTTR simply allows it to be identified, and for corrective action to be taken. Taking advantage of the additional capacity released through RTTR may increase the potential risk, but providing additional information to inform control decisions reduces the actual risk – depending on the level of risk the network operator deems acceptable. Given the high value that network operators put on safety and reliability, the work in this thesis should help to build confidence in the adoption of RTTR. If a network operator understands that by deploying RTTR their network can become safer and more reliable, they are more likely to see this in a favourable light. Conversely, suggesting that RTTR allows additional demand and generation to be connected adds to the perception that RTTR will result in additional risk.

The CFD wind data provides useful information for network planners and operators. The ability to know how much additional capacity is likely to be available, along with how variable it is likely to be, further contributes to the ability to make well informed decisions, and allow the likely benefits to be understood before implementation. Furthermore, by identifying where thermal bottlenecks are likely to occur planners have additional information about where problems could occur, and where instrumentation is likely to be required. The location of critical spans could also feed into reliability calculations, allowing the determining span rating values to be used to give a realistic estimate of network reliability.

The wind estimation methods have been applied to real case studies, and have been validated through an industry standard case study. This should help to build confidence in the approaches suggested.

Prior to this research, no method had been demonstrated to assess how the variable conductor ratings resulting from RTTR affected network reliability. The method that has been developed suggests that RTTR yields a significant increase in network reliability for heavily loaded systems. However, this will vary based on the local weather conditions, and based on the specific network topology. Additionally, the method allows the

correlation between line ratings, which are a result of the overhead lines being affected by the same large scale weather phenomena, to be accounted for. Again, these correlations could be informed by the CFD wind results, allowing realistic correlation data, as well as rating data, to be applied.

### 7.3. BROADER IMPLICATIONS

#### 7.3.1. RTTR IN THE CONTEXT OF CLIMATE CHANGE

Electricity infrastructure has a long operational lifetime, typically more than 30 years. It is important therefore to understand how assets will perform over this durations. UK climate projections [176] indicate that mean temperatures are likely to rise by 2-3°C by 2050. It is suggested that this could lead to reductions in conductor ratings, particularly during the summer [177].

Wind speed has a greater impact on conductor rating than ambient temperature. UKCP09 wind projections suggest that average summer wind speeds are likely to decrease, while average winter wind speeds may increase, but are as likely to decrease or remain the same [178]. However, this projection comes with a ‘health warning’ due to the high levels of uncertainty. A study based on regional climate models of northern Europe, with boundary conditions informed by a global climate model, indicates that in the North Sea region wind energy density, which is dependent on wind speed, is likely to increase both on average and in winter, but decrease in summer [179]. The study also found that wind energy density is already highly variable, with changes of up to 19% annually, a result that is verified by other wind resource studies looking at large scale climate phenomena [180]. It is suggested that climate change could further increase this variability [179, 181].

The severities of these implications on the long-term feasibility of RTTR are dependent on other factors. It may be that these changes result in RTTR being deployed to alleviate the increased risk of infringing static ratings as a consequence of a warmer climate [177]. Should the UK remain a winter peaking system, it is likely that RTTR will be an effective solution even in

the more severe climate change scenarios. However, should an increase in temperature cause the UK to shift to a summer peak as a result of increased space cooling, RTTR may not be sufficient, and large scale infrastructure replacement and reinforcement may be necessary. This is exacerbated by strong evidence that in summer peaking power systems, demand is highly correlated with ambient temperature [182-184] as a result of space cooling.

There is strong evidence linking climate change to extreme weather events [185], and that extreme weather has an adverse effect on power system reliability [186]. Consequently, RTTR could provide benefits to system reliability given an increase in contingency situations. Some extreme weather events, such as storms, are likely to coincide with high overhead line ratings, meaning RTTR could support the system until the weather allowed repairs to be carried out. However other extremes, such as heat waves, could reduce the effectiveness of RTTR in providing additional capacity while damaging network assets, particularly at distribution level [187]. Conversely, RTTR could prove invaluable during a heat wave, by allowing network operators to identify which areas of network are at risk.

### 7.3.2. POLICY RECOMMENDATIONS

One of the key barriers to the wide scale implementation of RTTR is its absence from the existing policy and regulation. While other non-firm technologies are considered for ensuring security of supply, RTTR is conspicuous in its absence. Further to this, the existing security of supply standards for Distribution networks rely on deterministic rules and attempt to assign fixed values to variable quantities. As a result of the work carried out in this thesis, the author makes the following recommendations:

- RTTR should be included in the next iteration of network security of supply standards, not only government and industry standards, but internal policies used by individual network operators. In the UK this means RTTR should be accounted for in the upcoming fundamental review of the P2 standard.

- The contribution of RTTR to security should be considered in a manner that also quantifies the associated risks, requiring studies using local weather data when proposing new RTTR schemes for deferring network reinforcement or satisfying security of supply. This would also necessitate analysing how demand, rating and variable generation vary relative to one another.
- The industry as a whole, and RTTR specifically, would be best served by moving to an explicitly probabilistic or risk based security standard. A satisfactory level of network reliability should be evaluated by modelling loads, ratings, generators and reliabilities probabilistically rather than using deterministic characteristics such as n-k. The goal should be to calculate an acceptably low probability of loss of load, which could be determined by the network operator or the regulator.
- Rather than implementing individual policies for distinct smart grid technologies, a single policy which considers the combined impact of multiple smart grid innovations and the interactions between them should be used. For example analysing the sizes of predicted excursions above RTTR could be used to inform DSR and energy storage schemes. The combination of these assets gives a benefit to network security which cannot be properly quantified by evaluating them individually.

These policies would not only allow proper exploitation of the benefits of RTTR, but would allow policy makers and network operators to properly understand and utilise the benefits of integrated smart grid projects. Furthermore the level of network risk would be properly quantified, leading to a more efficient electricity system.

### 7.3.3. RECOMMENDED RTTR DEPLOYMENT

As described in section 2.3, there are many technical solutions available for implementation of RTTR. However tempting it may be to use a single ‘best technology’, in the opinion of the author this is not prudent. Instead different technologies should be applied based on their individual merits and the requirements of specific scenarios.

Weather based RTTR offers broad information at relatively low cost, and can be easily installed [44]. However weather, wind in particular, varies on small time and space scales, leading to doubts over the accuracy of this method [77]. Work in this thesis has demonstrated that meteorological stations can provide a good representation of a broad area, but can fail to accurately estimate the rating of conductors in specific locations with complex local terrain. This could particularly present a problem if these complex locations are likely to represent critical spans within the network.

Line monitoring solutions can provide accurate information about specific locations, though they require some information about local weather conditions to infer ampacity estimation. However, for the information they provide to be useful, they must be placed on the critical spans. This involves either instrumenting the entire network, which is likely to be prohibitively expensive, or pre-identifying critical spans. In existing networks, thermal cameras could be used to identify ‘hotspots’, but only for the weather and loading conditions at the time of observation. For new networks, even this is not an option. The methods described in section 5.2 allow this identification to take place, based on simulations of the local weather conditions.

When considering a new deployment of an RTTR project, the reliability of the components within the monitoring system should be considered, as should the consequence of their failure. For example, the failure of a meteorological station could conceivably be covered through other stations, provided they were deployed to provide a level of redundancy. Conversely, the failure of a line monitoring device is likely to result in a lack of information, especially if the line monitoring device is being used in isolation. If it was deployed in tandem with weather monitoring, it should be possible to continue estimating the ratings throughout the network, albeit with an increased level of uncertainty, until repairs can be carried out.

All of this leads to the conclusion that RTTR is best served by a suite of technologies, each deployed according to their strengths, and to offset each

other's weaknesses. The general rules described in section 5.2.6 are reiterated here:

- Meteorological observation stations should be sited in locations that are representative of large areas.
- Other instrumentation, such as sag/tension monitors should be deployed in areas that are not well represented by the weather stations or are likely to contain determining spans.

And further recommendations are made:

- Monitoring equipment should be deployed to offer sufficient redundancy in the case of equipment failures.
- In the cases where sufficient redundancy is not possible, graceful degradation algorithms should be implemented [171]
- The reliability of the system should be factored into any calculations of the risks and benefits of the RTTR system. The reliability may depend on local environmental conditions, and other external factors such as communications reliability, theft or vandalism.
- Uncertainties should be quantified, ideally through a measurement based validation exercise, but reasonable estimates can be provided if this is not feasible.

If these recommendations are followed, the result should be a reliable, cost effective RTTR system.

#### 7.3.4. HOLISTIC SMART GRID DEPLOYMENT

While RTTR can offer substantial benefits to network operators, the benefits are variable and cannot be controlled. Consequently it cannot solve most problems in isolation. Rather, RTTR is likely to provide the most substantial benefits when it is deployed alongside other smart grid technologies. Energy Storage can be deployed for demand peak shaving [188], but is unlikely to be economically viable based on only that application. If both were deployed together, the storage could provide peak shaving in the event of low ratings and high demand coinciding, and the RTTR could allow the storage device to

engage in arbitrage more effectively. Both could be informed by weather forecasts, giving an indication of both ratings and demand.

Demand Side Response could also be used in conjunction with these other technologies, potentially alleviating the need for asset replacement or reinforcement, while providing savings to customers. Each of these technologies provides a greater benefit when deployed alongside the others, and smart grids should be designed, planned and operated with this in mind.

#### 7.3.5. REINFORCEMENT WITH RTTR

Much of the research in this thesis has focussed on the idea that RTTR is an alternative to conventional network reinforcement. However this will not always be the case; in some situations new infrastructure will still be necessary. In these cases it is likely that RTTR can provide additional capacity for the new conductors, or reduce the number of new conductors that need to be built.

#### 7.3.6. FEASIBLE TRANSITION AND IMPLEMENTATION

Many of the recommendations made by this thesis are a long way from the current state of the electricity industry. Consequently it is important to note that while they could provide significant benefits, they cannot all be adopted at once. A gradual transition is required, to ensure network operators are not overwhelmed, and to build confidence in the new methods. An example of a gradual RTTR implementation, using wind simulation:

- Identify an area of network that may benefit from RTTR in future
- Deploy instrumentation
- Calculate wind flow patterns, and validate using deployed instrumentation
- Implement thermal state estimation, analyse capacity based on historical data
- Provide state estimation data to control room

These steps allow the network operators to see the benefits of RTTR, and to have confidence in the thermal state estimation. Consequently, when the system is fully online the operators will feel comfortable using the RTTR values. The historical data can also be used to quantify the uncertainties in the thermal state estimation, and to identify sections of network that may require additional instrumentation.

It is also important to consider how the data will be provided to the control room. If too much information is provided, then the control engineers could be overwhelmed and, the additional information will hinder, rather than help. The author recommends that the RTTR system be implemented such that the control room is given as little information as possible, but that this information is all that is required to make fully informed decisions. Generally this will simply be the rating of each circuit, and perhaps the location of each critical span. Further to this, the implementation should be carried out such that all the complex analysis is performed offline, and that once implemented the system operator can return to business as usual, but with variable conductor ratings rather than static ones.

#### 7.4. FURTHER RESEARCH

This section identifies further research that could be carried out to build on the foundations that have been laid by this thesis. These include extensions to what has been done, ways to combine the methods developed and new research that could benefit future RTTR projects. Because this thesis represents the first significant research into network planning with RTTR, and the first application of wind models to a power systems problem, there are significant areas for further investigation.

##### 7.4.1. IMPROVED CFD SIMULATIONS

Assumptions have been made in the existing simulation method, which do not necessarily represent the best possible solution. Further work could seek to identify the optimal CFD set up for wind flow estimation. The boundary condition in the existing solution assumes a uniform wind flow across the inlet to the domain. In reality, it is unlikely that this is the case. Instead, it

could be preferable to construct non-uniform BCs, based on the observed wind speeds and directions within the domain, with some interpolation applied between them. The difference between the two boundary conditions is shown in Figure 7.1. Alternatively, the inlet condition could be determined by running a simulation on a much larger domain and using the results from this at the location of the inlet to the original domain to determine the new inlet condition.

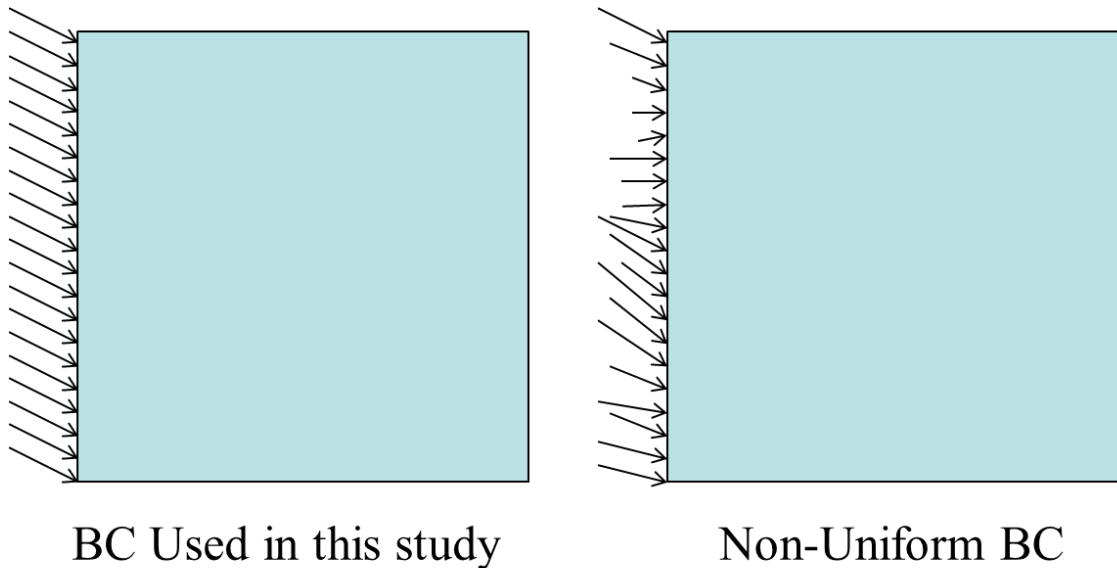


**Figure 7.1: The difference between a uniform and non-uniform inlet boundary condition**

In the existing CFD set up, the surface roughness data provided by Astrium is represented in the simulation as roughness elements at ground level. The function of these elements is to distort the shape of the boundary layer in the same way as the physical object the roughness element represents. However, since the roughness elements are at the same height as the ground, the roughness elements do not provide the same wake effect as the physical objects. This is apparent in the simulations, where AC93 is situated next to an urban area, and as a result the CFD over estimates the wind speeds at that location. Using fully realised objects, rather than a simple surface roughness model, could account for these wake effects, albeit at the cost of more computational time and resources. This method could account for the effect of trees and other vegetation near to the line much more

accurately than the existing method. The difference between the two roughness models is shown in Figure 7.2.

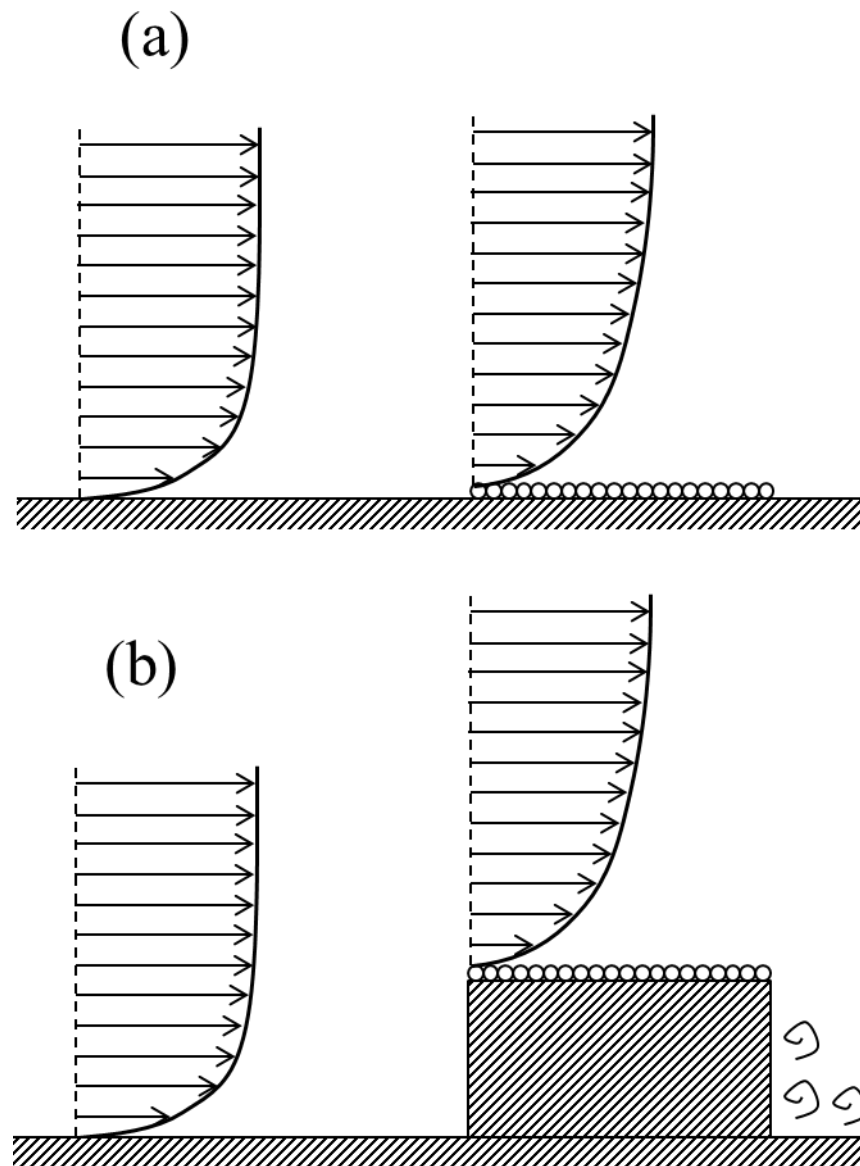


**Figure 7.2:** (a) shows the effect of roughness elements on a boundary layer, while (b) illustrates that in reality the boundary layer is also shifted physically upwards, and a wake is created behind the roughness object. This could be woodland, vegetation or a building.

Furthermore, the CFD meshes described in this thesis used manual mesh generation. This was time consuming, even for the relatively simple geometry representing just the orography. Automated mesh generation would not only reduce the time spent on this process, it would also allow more complex geometries to be simulated.

Research into wind simulations using automated mesh generation is now underway at Durham University as a result of the work carried out in this thesis.

#### 7.4.2. SIZE OF CFD RESULTS DATABASES

The research carried out so far relies on a database of 36 CFD simulations, created by varying the inlet condition by  $10^\circ$  for each simulation. The accuracy of the method could be improved by expanding the size of this database, both through increasing the resolution (for example simulations every  $5^\circ$ ) and through creating more representative inlet boundary conditions as suggested in section 7.4.1.

#### 7.4.3. IMPROVED THERMAL STATE ESTIMATION

When applying the CFD simulation results for online state estimation, a simple method was applied, resulting in reasonable results. However, there are more sophisticated techniques that could be applied, potentially resulting in more accurate state estimation. An interpolation method could be adapted to use the information provided by the CFD model, along with some weighting based on the location of the meteorological stations [122].

Another option would be to combine the CFD results with some sort of regressive model, allowing the state estimation to take advantage of not only the real-time observations, but the historical observations as well. Making use of all available data may improve prediction accuracy, provided the model was appropriately selected and sufficiently validated.

Alternatively, an ensemble Kalman Filter could be developed, combining a linearized version of the CFD model with historical data and observations [189]. This would allow the wind regimes to be calculated in real time, albeit based on a simplified, statistical model. At the time of writing, a proposal was being prepared at Durham University to carry out further research in this area as a direct result of the work presented in this thesis.

#### 7.4.4. UNCERTAINTY QUANTIFICATION

Chapter 5 discussed how CFD wind simulations can be employed to inform network planning and operation with RTTR. However, in order for this to be a realistic option, the wind model would have to have properly quantified uncertainties, such that the predicted energy yield and constraint projections could be considered robust. The errors associated with the following assumptions must be quantified:

- The error in the wind model
- The measurement error in the historical wind data
- The error associated with representing the wind farm using data from a single point.
- The error in the wind farm power curve model.

Clearly, the lower these uncertainties, the more informative the planning methods presented become.

#### 7.4.5. RELIABILITY WITH ACTIVE CONTROL

The method described in Chapter 6 allowed the reliability of a network with variable ratings to be calculated. However, the method was based around a simple load flow, and the reliability could therefore be improved if the network could be controlled based on rating of the components. Various control strategies could be applied; minimisation of risk and economic dispatch with a maximum acceptable LOL probability are clear starting points.

Active control is likely to lead to an improvement in reliability, which would be offset by an increase in operational cost. Network operators should be able to select a control strategy that gives them an acceptable compromise between the two. Furthermore, for active control to be a realistic prospect, forecasting methods would need to be properly developed, such that control decisions can be made ahead of time.

#### 7.4.6. SMART GRID RELIABILITY

The existing reliability assessment method allows the impact of variable conductor ratings on network reliability to be quantified. However, as described in section 7.3.4, RTTR is unlikely to be the only non-firm intervention on the network. Consequently, a key extension to this work would be to update the reliability method to allow RTTR, Energy Storage, Distributed Generation and Demand Side Response to be considered in combination.

Wind generation could be modelled using an ARMA model, with the correlation between the generator output and the conductor ratings being accounted for. Energy storage could either be represented by a probabilistic state of charge, or by implementing a realistic control system within the simulations. DSR could be represented by a control system, to represent action being taken, and a probabilistic response.

The goal of this work would be to understand how combinations of these technologies affect system reliability, and to investigate which proportions and control systems result in the most reliable system. Some economic analysis could also be factored in.

#### 7.4.7. WIND INFORMED RELIABILITY

The methods described in section 5.2.2 allow time series of conductor rating to be generated at different points in a network. These results could then be input into a reliability model, allowing the relationship between the conductor ratings to be explored more thoroughly than by the Cholesky Factorisation method described in section 6.3.5. The proposed methodology for implementing this is as follows:

- Create ARMA models based on local wind and temperature data.
- Run the ARMA model to create time series of the desired length of simulation.
- Combine the ARMA wind data with the CFD speedup characteristics to give time series of wind speed at each point in the network.

- Calculate conductor ratings for each of these values, using the ARMA temperature model.
- At each time step, select the lowest rating for each circuit and run the power flow.

This method not only combines two aspects of the work carried out by the author, it also allows network reliability assessment to be carried out with information about the thermal bottlenecks within the system, and with information about the correlations between the overhead line ratings. The limiting factor on performing these calculations would be the size of CFD domain that can reasonably and accurately be simulated. Consequently while this would be appropriate for areas of distribution network, it is unlikely to be possible for networks with larger geographical footprints, such as transmission networks. This method could also be extended to allow the impact of wind generation on the local network to be accounted for, rather than just on the circuit immediately connecting it to the network.

#### 7.4.8. DEMAND AND RATINGS

The approaches discussed in this thesis have assumed that demand and line ratings are independent. RTTR is at its most useful when there is a high probability of high current carrying capacity coinciding with high power flows; this is why the wind energy application is so widely researched. It would be prudent, then, to investigate the correlation between RTTR and demand, not only in the current system, but in predicted future scenarios. It seems likely, for example, that should electric heating become more prevalent, there would be a more pronounced correlation between demand and high conductor current carrying capacity.

If relationships were established between the two, it would allow a more accurate prediction of how likely high demand and low ratings are to coincide. This will allow better informed decisions to be taken, regardless of whether they suggest RTTR will be more or less effective than the existing predictions.

#### 7.4.9. ECONOMIC BENEFITS

The work described in this thesis has focussed on the technical aspects of planning networks for RTTR. However, if RTTR is going to be a successful part of future electrical networks, it has to justify itself financially. This section describes how the economic benefits of RTTR could be quantified at the planning stage.

In a report describing a trial of an RTTR system, Scottish Power Energy networks compared the cost of their RTTR system with the cost of otherwise required network reinforcements. The report found that using RTTR to enhance the existing circuit was around 10% of the cost of an additional circuit, or around 15% of the cost of refurbishing the existing circuit [143].

However, this study made the assumption that RTTR would simply allow an uplift of 30%. While it is true that, the majority of the time, RTTR would result in additional current carrying capacity, this will not always be the case. Consequently, any realistic representation of the business case for RTTR should account for the expected value of lost load (VoLL), however small. The Value of Lost Load Expectation (VoLLE) can be calculated using equation (63):

$$VoLLE = VoLL \cdot LOEE \quad (63)$$

The LOEE can be calculated using the Monte Carlo reliability method described in Chapter 6 or by using the methods described in Chapter 3, along with information about the expected downtime of the components in the system being considered. The VoLLE should also be considered for the alternatives to RTTR, allowing an informed decision to be taken. A complete economic assessment should also account for the impact of additional losses as a result of higher utilisation. Considering these aspects will allow network operators to see the business case for RTTR, and should help to build confidence in the technology.

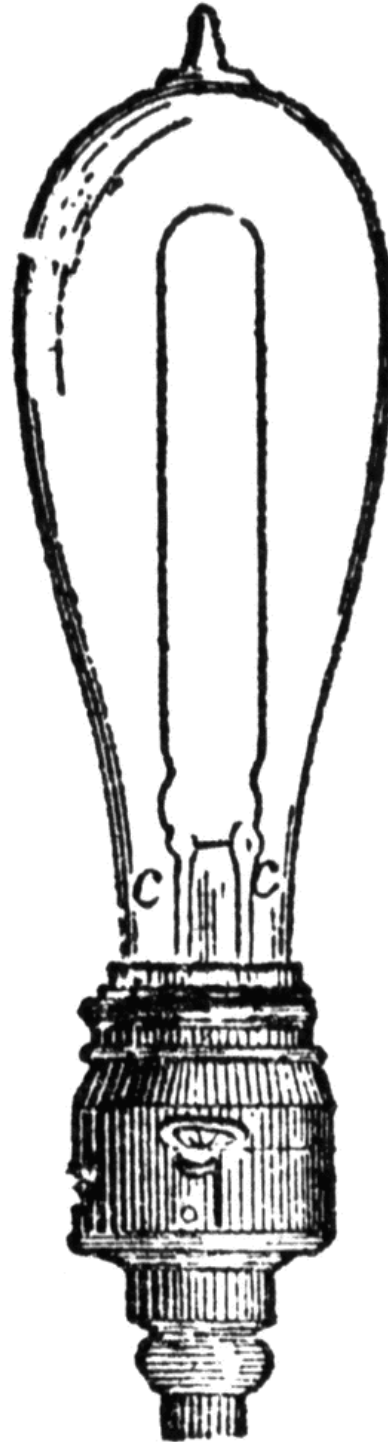
## 7.5. SUMMARY

This chapter has described how the work carried out by the author fits into the broader context of power network planning and operation. The combined impact of the methods described in Chapters 3-6 was discussed. Following this, the broader implications of the work were considered, including how RTTR can function in the context of climate change and how it can be best represented in industry standards and policies.

Recommendations were made as to how RTTR can be deployed. A combination of weather and line monitoring can provide wide coverage, as well as precise information about specific locations. This, combined with adequate monitoring redundancy and graceful degradation, is most likely to yield an accurate, dependable and cost effective solution. Additionally, the author noted that RTTR could be most effective when deployed alongside other smart grid technologies, or indeed alongside conventional network reinforcement. Some consideration was given to the difficulty of transitioning from a business as usual approach to the use of high levels of additional monitoring and online control. A basic transition plan was outlined, and it was noted that the purpose of the technology should be to aid in decision making, rather than overwhelming network operators with information.

Finally, further research opportunities were discussed. These included improvements to the CFD and thermal state estimation methods (which work has already begun on as a result of the research in this thesis), as well as extensions to the reliability and security of supply methods. Finally, research on the economic benefits of RTTR was considered an essential next step, in order to build confidence and demonstrate the value of RTTR to network operators.

## Chapter 8. Conclusions



## 8.1. OVERVIEW

This thesis has described methods to facilitate the integration of RTTR into electrical networks. The primary aim of these methods was to allow the benefits and risks of RTTR to be quantified at the network planning and design stage. Not only does this make it possible for planners and designers to take informed decisions about RTTR before deploying any equipment on the network, it also provides a framework for RTTR to be integrated into the policies and standards that govern network design and operation.

This section reiterates the key findings of each piece of work that has been carried out, and describes how the research objectives, set out in Section 1.6, have been fulfilled.

## 8.2. KEY FINDINGS

The key findings and contributions of this research are:

- The additional capacity provided by RTTR could provide many potential benefits to electrical networks, but it cannot be sensibly or effectively represented by a fixed rating value.
- RTTR can allow additional load to be connected to distribution networks, and can do so with a quantified level of risk to security of supply
- Wind simulations can be used to inform RTTR projects; wind data can allow identification of thermal bottlenecks, estimation of wind energy yields and identification of where instrumentation would be most effective. Methods have been developed to allow the quantification of these benefits.
- Wind simulations can also be used to inform thermal state estimation, allowing the effect of terrain on wind flow patterns to be accounted for during rating estimation.
- RTTR can improve reliability of networks, particularly in the case of heavily loaded networks. A method has been developed to allow this reliability to be quantified.

- Networks whose overhead lines have weakly correlated ratings can experience greater reliability improvements through RTTR.

### 8.3. FULFILMENT OF RESEARCH OBJECTIVES

1. Devise a method for assessing the impact of RTTR on distribution network security of supply, allowing both the benefits and risks to be quantified, to allow network operators to make informed decisions about network capacity.

The additional capacity that can be released through RTTR is variable, and dependant on many factors. Local weather and terrain, the specific layout of the local network, the required purpose of the additional capacity and the level of risk that a network operator is prepared to accept all influence how much additional energy can be transmitted via RTTR. What is clear is that attempting to assign fixed values to the additional capacity is misleading; while it may be true that a conductor's energy throughput can increase by 50% through RTTR, this does not mean its rating can be increased by 50%.

The level of additional load that can be securely accommodated through RTTR is not a fixed number; connecting any load to an electrical network will result in some probability of being unable to supply that load. The methods in this thesis allow the likelihood of disconnecting load to be calculated for different levels of demand. This probability is dependent on the weather conditions local to the conductors, the load patterns and the reliability of the network components. The goal should be to strike a balance between a low level of risk and a high level of asset utilisation.

It is important to observe that RTTR does not actually alter a conductor's current carrying capacity; it simply allows it to be measured or estimated in real time. Consequently, even if through connecting additional load there is an increase in the likelihood of the rating of a conductor being exceeded, the risk to safety and reliability is actually reduced because the network operator knows if the rating is being exceeded and can therefore take action

to mitigate the problems. This applies not only to the additional risk introduced through additional demand, but for the existing risk as well.

RTTR cannot be controlled; this means it is not guaranteed to provide a benefit when it is most needed. However, if RTTR was deployed alongside other, controllable network assets, it would work symbiotically, enhancing their usefulness during periods of high rating, while they made up capacity in periods of low rating. One potential example is RTTR allowing storage to perform arbitrage or frequency response more effectively, while storage provides additional capacity during low rating periods.

2. Develop methods to allow wind simulations, which are widely used in the wind energy industry, to be applied to quantify the benefits of RTTR at the planning stage, and provide additional information to weather based RTTR systems during operation.

Wind simulations can be used to help quantify the benefits of RTTR in specific locations. Methods have been devised that use a combination of local terrain and orography data and historical weather data to identify likely overhead line rating patterns. These can be used to identify thermal bottlenecks, identify which new conductor routes make best use of RTTR, inform sensor placement and quantify the energy yield of wind generation.

Through the use of CFD data, it was possible to identify where thermal bottlenecks were likely to occur within the network. By calculating the mean of the rating at each point in the system, it was possible to identify which conductors had a low average rating, and consequently were likely to result in thermal bottlenecks. By also calculating the variance of the rating at each point, it would be possible to identify the ratings at set probability levels. This could be important, because a low mean and low variance may be less likely to result in a thermal bottleneck than a high mean and a high variance.

The results of the case study in Chapter 5 indicated that RTTR could allow around 50% additional wind generating capacity to connect to the network.

However, this level of generation would occasionally have to be curtailed due to thermal rating constraints, leading to a predicted loss of energy yield of 1-2%.

The specific siting of new conductors depends on their application; in general they should be sited in areas that result in either a high average rating, or a low probability of a low rating. However, some specific situations, such as the connection of DG, may require the line to have a high current carrying capacity only in certain circumstances, such as when a generator is operating at capacity. In these cases, the conductor location should be selected based on a strong correlation between high capacity and high utilization.

Wind simulation results were used in online state estimation to provide information about the effect of terrain on local wind flow without the computational burden of performing the simulations in real-time. The results were reasonable, though not accurate enough for implementation at this stage. Improvements to both the simulation and estimation methods were suggested.

3. Design a means of quantification of the reliability of a network utilising RTTR, and provide indicative results using standard test networks.

The methods described in Chapter 6 allow the reliability of a network utilising RTTR to be quantified. The use of RTTR in current system designs appears to reduce system reliability, because the network is designed such that in the event of peak demand coinciding with an outage the static rating of conductors in the network will not be exceeded. Consequently, the additional capacity made available through RTTR is not relevant. However, the conductor ratings sometimes fall below the static rating. If this coincides with a contingency and peak demand, this may result in a loss of load.

In reality though, RTTR does not make the network less reliable, rather it leads to safer operation by removing the risk of conductors exceeding their design temperature and either tripping circuits or endangering lives due to

line sag. In fact, the 2003 blackout in the USA was initiated by ‘tree flashovers’ as a result of excessive line sag [190]. Had the system been operating with RTTR, network operators could have identified that the lines in question had exceeded their thermal limits and taken action.

If additional load is connected to the system, then the additional capacity unlocked through RTTR begins to support the network in the majority of contingency cases, leading to an improvement in reliability compared with conventional line rating approaches. The improvement is dependent on the local network design, and environmental conditions. The reliability provided through the use of RTTR is still unlikely to be high enough, and would need to be coupled with other interventions to result in a network as reliable as those operating today.

If the overhead lines in a network have highly correlated thermal ratings (i.e. they are governed by the same weather patterns) then the network will be marginally more reliable than the same network with weakly correlated thermal ratings (although this will also be affected by diversity and distribution of the demand on the network). This was attributed to the higher internal variance in a system with weaker correlations, leading to an increase in the probability that one circuit could have a low rating. In either case, the impact of the correlation of the system reliability was found to be minor.

#### 8.4. CONCLUSION

The primary contribution of the author has been to allow quantification of the benefits of RTTR in power networks. Very little work had previously been carried out on planning networks for the adoption of RTTR, or the quantification of its potential benefits and risks. This work has explored this from several perspectives, investigating the impact of RTTR on network reliability, enabling demand growth and connecting distributed generation. Furthermore, initial results have demonstrated that it is not prudent to attempt to assign fixed values to variable assets such as RTTR; the use of probability and understanding how different quantities vary relative to one

another are essential to maximising the benefit, and minimising the potential risks of RTTR. This work represents the first step into this research area, and areas for further research have been identified.

The author's other main contribution is the application of CFD wind models, which are used extensively in the wind energy industry, to RTTR. Conductor current carrying capacity is strongly influenced by wind speed and direction, consequently understanding local wind flow patterns is useful in both the planning and operation of power networks using RTTR. Methods have been developed to identify areas of high rating during network planning, and to estimate the current carrying capacity of overhead conductors during network operation. Extensions to this work have been identified, and research is already underway on several of these as a direct result of the work in this thesis.

---

## References

- [1] P. Fox-Penner, *Smart power*, Island Press, 2010.
- [2] DECC, *2050 Pathways*, Available: <https://www.gov.uk/2050-pathways-analysis>, Accessed: 18/07/2013
- [3] DECC, "Digest of UK energy statistics," 2012, Available: <https://www.gov.uk/government/collections/digest-of-uk-energy-statistics-dukes>
- [4] J. Oswald, M. Raine, and H. Ashraf-Ball, "Will British weather provide reliable electricity?," *Energy Policy*, vol. 36, pp. 3212-3225, 8, 2008.
- [5] P. Nefzger, U. Kaintzyk, and J. F. Nolasco, *Overhead power lines: planning, design, construction*, Springer, 2003.
- [6] H. Ritchie, M. Hardy, M. G. Lloyd, and S. McGreal, "Big Pylons: Mixed signals for transmission. Spatial planning for energy distribution," *Energy Policy*, vol. 63, pp. 311-320, 2013.
- [7] H. Gharavi and R. Ghafurian, *Smart grid: The electric energy system of the future*, IEEE, 2011.
- [8] M. C. Falvo, L. Martirano, D. Sbordone, and E. Bocci, "Technologies for smart grids: A brief review," in *12th Int. Conf. on Environment and Electrical Engineering*, 2013, pp. 369-375.
- [9] C. W. Gellings, *The smart grid: enabling energy efficiency and demand response*: The Fairmont Press, 2009.
- [10] C. F. Price and R. R. Gibbon, "Statistical approach to thermal rating of overhead lines for power transmission and distribution," *IEE Proc. C: Generation, Transmission and Distribution*, vol. 130, pp. 245-256, 1983.
- [11] *Current Rating Guide for High Voltage Overhead Lines Operating in the UK Distribution System*, ENA Engineering Recommendation P27, 1986.
- [12] A. Michiorri, P. C. Taylor, S. C. E. Jupe, and C. J. Berry, "Investigation into the influence of environmental conditions on power system ratings," *Proc. IMechE Part A: J. Power and Energy*, Vol. 223, pp. 743-757, 2009.
- [13] CIGRÉ WG B2/C1.19, "Increasing Capacity of Overhead Transmission Lines - Needs and Solutions -," *CIGRE Technical Brochure 425*, 2010.

- 
- [14] P. M. Brown and J. P. White, "Determination of the maximum cyclic rating of high-voltage power transformers," *Power Engineering J.*, vol. 12, pp. 17-20, 1998.
- [15] P. Caramia, G. Carpinelli, A. L. Vitola, and P. Verde, "Cyclic and emergency rating factors of distribution cables in presence of nonlinear loads," in *10th Int. Conf. on Harmonics and Quality of Power*, 2002, Vo. 2, pp. 716-723.
- [16] V. T. Morgan, "The thermal rating of overhead-line conductors Part I. The steady-state thermal model," *Electric Power Systems Research*, vol. 5, pp. 119-139, 1982.
- [17] CIGRÉ WG 22.12, "The thermal behaviour of overhead line conductors," *Electra*, vol. 114(3), pp. 107-25, 1992.
- [18] "Standard for calculating the current-temperature relationship of bare overhead line conductors," IEEE Standard 738, 2006.
- [19] "Overhead Electrical Conductors - Calculation Methods for Stranded Bare Conductors," IEC Standard TR 1597, 1985.
- [20] S. Abbott, S. Abdelkader, L. Bryans, and D. Flynn, "Experimental validation and comparison of IEEE and CIGRÉ dynamic line models," in *45th Int. Universities Power Engineering Conf.*, 2011, pp. 1-5.
- [21] M. Isozaki and N. Iwama, "Verification of forced convective cooling from conductors in breeze wind by wind tunnel testing," in *Asia Pacific IEEE/PES Transmission and Distribution Conf. and Exhibition*, 2002, pp. 1890-1894, vol.3.
- [22] CIGRÉ WG B2.12, "Guide for selection of weather parameters for bare overhead conductor ratings," *CIGRE Technical Brochure 299*, 2006.
- [23] CIGRÉ WG B2.36, "Guide for Application of Direct Real-Time Monitoring Systems," *CIGRE Technical Brochure 498*, 2012.
- [24] C. O. Boyse and N. G. Simpson, "The problem of conductor sagging on overhead transmission lines," *J. of the Institution of Electrical Engineers - Part II: Power Engineering*, vol. 91, pp. 219-238, 1944.
- [25] V. T. Morgan, "Effect of elevated temperature operation on the tensile strength of overhead conductors," *IEEE Trans. Power Del.*, vol. 11, pp. 345-352, 1996.
- [26] L. M. Olmsted, "Safe Ratings for Overhead Line Conductors," *Trans of the American Institute of Electrical Engineers*, vol. 62, pp. 845-853, 1943.

- 
- [27] M. W. Davis, "A New Thermal Rating Approach: The Real Time Thermal Rating System for Strategic Overhead Conductor Transmission Lines Part IV Daily Comparisons of Real-Time and Conventional Thermal Rating and Establishment of Typical Annual Weather Models," *IEEE Trans. Power Apparatus and Systems*, vol. PAS-99, pp. 2184-2192, 1980.
- [28] B. S. Howington and G. J. Ramon, "Dynamic Thermal Line Rating Summary and Status of the State-of-the-Art Technology," *IEEE Trans. Power Del.*, vol. 2, pp. 851-858, 1987.
- [29] D. A. Douglass, "Weather-dependent versus static thermal line ratings [power overhead lines]," *IEEE Trans. Power Del.*, vol. 3, pp. 742-753, 1988.
- [30] P. M. Callahan and D. A. Douglass, "An experimental evaluation of a thermal line uprating by conductor temperature and weather monitoring," *IEEE Trans. Power Delivery*, vol. 3, pp. 1960-1967, 1988.
- [31] W. Z. Black and W. R. Byrd, "Real-Time Ampacity Model for Overhead Lines," *IEEE Power Engineering Review*, vol. PER-3, pp. 56-56, 1983.
- [32] S. C. E. Jupe, M. Bartlett and K. Jackson, "Dynamic thermal ratings: the state of the art," *21st Int. Conf. on Electricity Distribution*, Frankfurt, 2011.
- [33] C. Mensah-Bonsu, U. F. Krekeler, G. T. Heydt, Y. Hoverson, J. Schilleci, and B. L. Agrawal, "Application of the Global Positioning System to the measurement of overhead power transmission conductor sag," *IEEE Trans. Power Del.*, vol. 17, pp. 273-278, 2002.
- [34] S. Kamboj and R. Dahiya, "Evaluation of DTLR of power distribution line from sag measured using GPS," in *Int. Conf. on Energy, Automation, and Signal*, 2011.
- [35] S. M. Mahajan and U. M. Singareddy, "A Real-Time Conductor Sag Measurement System Using a Differential GPS," *IEEE Trans. Power Del.*, vol. 27, pp. 475-480, 2012.
- [36] Lindsey Manufacturing, "Dynamic Real Time Transmission Line Monitoring, Online, Available: <http://www.lindsey-usa.com/newProduct.php>.
- [37] W. de Villiers, J. H. Cloete, L. M. Wedepohl, and A. Burger, "Real-Time Sag Monitoring System for High-Voltage Overhead Transmission Lines Based on Power-Line Carrier Signal Behavior," *IEEE Trans. Power Del.*, vol. 23, pp. 389-395, 2008.
- [38] P. Schell, B. Godard, H. M. Nguyen, J. L. Lilien, "Using Dynamic Line Rating to minimize Curtailment of Wind power connected to rural
-

- power networks," in *11th Wind Integration Workshop*, Aarhus, Denmark, 2011.
- [39] I. Albizu, E. Fernandez, P. Eguia, E. Torres, and A. J. Mazon, "Tension and Ampacity Monitoring System for Overhead Lines," *IEEE Trans. Power Del.*, vol. 28, pp. 3-10, 2013.
- [40] Nexans. (2013, 04/11/2013). *CAT-1 Transmission Line Monitoring System*. Available: [http://www.nexans.us/eservice/US-en\\_US/navigatepub\\_0\\_-17373\\_1673\\_40\\_4932/CAT\\_1\\_Transmission\\_Line\\_Monitoring\\_System.html](http://www.nexans.us/eservice/US-en_US/navigatepub_0_-17373_1673_40_4932/CAT_1_Transmission_Line_Monitoring_System.html)
- [41] H. M. Nguyen, P. Schell, J.-L. Lilien, "Dynamic Line Rating and Ampacity Forecasting as the Keys to Optimise Power Line Assets with the Integration of RES. The European Project Twenties Demonstration Inside Central Western Europe" in *22nd Int. Conf. on Electricity Distribution*, Stockholm, 2013.
- [42] P. Schell, B. Godard, J.-L. Lilien, H.-M. Nguyen, V. De Wilde, O. Durieux, *et al.*, "Large penetration of distributed productions: Dynamic line rating and flexible generation, a must regarding investment strategy and network reliability," in *CIREN 2012 Workshop on Integration of Renewables into the Distribution Grid*, 2012.
- [43] J. A. Carta, P. Ramírez, and C. Bueno, "A joint probability density function of wind speed and direction for wind energy analysis," *Energy Conversion and Management*, vol. 49, pp. 1309-1320, 6// 2008.
- [44] A. Michiorri, P. C. Taylor, and S. C. E. Jupe, "Overhead line real-time rating estimation algorithm: description and validation," *IMechE Part A: J. Power and Energy*, vol. 224, pp. 293-304, 2009.
- [45] A. Michiorri, "Power system real-time thermal rating estimation," in *Doctoral Thesis*, Durham: Durham University, 2010.
- [46] D.M. Greenwood, J.P. Gentle, K.S. Myers, P.J. Davison, I. J. West, G.L. Ingram, *et al.*, "A Comparison of Real Time Thermal Rating Systems in the U.S. and the UK," *IEEE Trans. Power Del.*, 2014.
- [47] J. Gentle, K. S. Myers, T. Baldwin, I. West, B. Savage, M. Ellis, P. Anderson, "Concurrent Wind Cooling in Power Transmission Lines," in *Western Energy Policy Research Conf.*, Boise, Idaho, 2012.
- [48] A. R. Gravdahl, Harstveit, K., "WindSim - Flow Simulations in Complex Terrain," in *5th German Wind Energy Conf.*, Wilhelmshaven, 2000.
- [49] J. Hosek, P. Musilek, E. Lozowski, and P. Pytlak, "Effect of time resolution of meteorological inputs on dynamic thermal rating

- calculations," *IET Generation, Transmission & Distribution*, vol. 5, pp. 941-947, 2011.
- [50] N. D. Sadanandan and A. H. Eltom, "Power donut system laboratory test and data analysis," in *IEEE Southeastcon '90. Proc.*, 1990, pp. 675-679 vol.2.
- [51] F. Kreikebaum, D. Das, Y. Yang, F. Lambert, and D. Divan, "Smart Wires: A distributed, low-cost solution for controlling power flows and monitoring transmission lines," in *IEEE PES Innovative Smart Grid Technologies Conf. Europe*, 2010.
- [52] S. A. Gal, M. N. Oltean, L. Brabete, I. Rodean, and M. Opincaru, "On-line monitoring of OHL conductor temperature; live-line installation," in *IEEE PES 12th Int. Conf. on Transmission and Distribution Construction, Operation and Live-Line Maintenance*, 2011.
- [53] I. Albizu, Ferna, x, E. ndez, Mazo, x, *et al.*, "Influence of the conductor temperature error on the overhead line ampacity monitoring systems," *IET Generation, Transmission & Distribution*, vol. 5, pp. 440-447, 2011.
- [54] A. Popelka, Jurik, D., Marvan, P., "Actual line ampacity using PMU," in *21st Int. Conf. on Electricity Distribution*, Frankfurt, 2011.
- [55] L. Yuan, "Power transmission line parameter estimation and optimal meter placement," in *IEEE SoutheastCon 2010 (SoutheastCon), Proceedings of the*, 2010, pp. 250-254.
- [56] Schneider Electric, ONLINE, 2011. Available: [http://www.global-download.schneider-electric.com/85257849002EB8CB/all/EABB9772C45B1B3285257885006D39DD/\\$File/nrjed111058en\\_lr.pdf](http://www.global-download.schneider-electric.com/85257849002EB8CB/all/EABB9772C45B1B3285257885006D39DD/$File/nrjed111058en_lr.pdf)
- [57] A. Michiorri, R. Currie, P. C. Taylor, F. Watson, D. Macleman, "Dynamic Line Rating Deployment On The Orkney Smartgrid," in *21st Int. Conf. on Electricity Distribution*, Frankfurt, 2011.
- [58] T. Yip, A. Chang, G. Lloyd, M. Aten, and B. Ferri, "Dynamic line rating protection for wind farm connections," in *CIGRÉ/IEEE PES Joint Symposium on Integration of Wide-Scale Renewable Resources Into the Power Delivery System*, 2009.
- [59] M. Aten, R. Ferris, T. Yip, C. An, G. Lloyd, "Field measurements analysis for dynamic line rating," in *21st Int. Conf. on Electricity Distribution*, Frankfurt, 2011.
- [60] T. Yip, C. An, G. J. Lloyd, P. Taylor, A. Michiorri, S. Jupe, *et al.*, "Dynamic thermal rating and active control for improved distribution network utilisation," in *10th IET Int. Conf. on Developments in Power System Protection: Managing the Change*, 2010.

- 
- [61] T. Yip, C. An, G. J. Lloyd, M. Aten, R. Ferris, and G. Hagan, "Field experiences with dynamic line rating protection," in *10th IET Int. Conf. on Developments in Power System Protection: Managing the Change*, 2010.
- [62] Ofgem, Kema, "TSORG - Licensee action summary and review," 2008.
- [63] S.C.E. Jupe, P.C. Taylor, and A. Michiorri, "Coordinated output control of multiple distributed generation schemes," *IET Renewable Power Generation*, vol. 4, pp. 283-297, 2010.
- [64] S.C.E. Jupe and P. C. Taylor, "Distributed generation output control for network power flow management," *IET Renewable Power Generation*, vol. 3, pp. 371-386, 2009 2008.
- [65] L. F. Ochoa, L. C. Cradden, and G. P. Harrison, "Demonstrating the capacity benefits of dynamic ratings in smarter distribution networks," in *Innovative Smart Grid Technologies*, 2010.
- [66] R. Stelmak, "Increasing system reliability/availability and reducing congestion with real time line ratings," in *IEEE PES General Meeting*, 2005, pp. 2626-2634 Vol. 3.
- [67] D. T. C. Wang, L. F. Ochoa, and G. P. Harrison, "DG Impact on Investment Deferral: Network Planning and Security of Supply," *IEEE Trans. Power Syst.*, vol. 25, pp. 1134-1141, 2010.
- [68] S. Blake, P. J. Davison, P. C. Taylor, D. Miller, and A. Webster, "Use of real time thermal ratings to support customers under faulted network conditions," in *22nd Int. Conf. on Electricity Distribution*, Stockholm, 2013.
- [69] A. Michiorri and P. C. Taylor, "Forecasting real-time ratings for electricity distribution networks using weather forecast data," in *20th Int. Conf. on Electricity Distribution*, Prague, 2009.
- [70] B. Adam, "Weather-based and conductor state measurement methods applied for dynamic line rating forecasting," in *Int. Conf. on Advanced Power System Automation and Protection*, 2011, pp. 762-765.
- [71] S. S. Soman, H. Zareipour, O. Malik, and P. Mandal, "A review of wind power and wind speed forecasting methods with different time horizons," in *North American Power Symposium*, 2010.
- [72] B. Banerjee, D. Jayaweera, and S. M. Islam, "Impact of wind forecasting and probabilistic line rating on reserve requirement," in *IEEE Int. Conf. on Power System Technology*, 2012.
- [73] J. Black, S. Connor, and J. Colandairaj, "Planning network reinforcements with Dynamic Line Ratings for overhead transmission lines," in *45th In.t Universities Power Engineering Conf.*, 2010.
-

- 
- [74] A. K. Kazerooni, J. Mutale, M. Perry, S. Venkatesan, and D. Morrice, "Dynamic thermal rating application to facilitate wind energy integration," in *IEEE Int. Conf. on Power System Technology*, Trondheim, 2011.
- [75] P. F. Ribeiro, H. Polinder, and M. J. Verkerk, "Planning and Designing Smart Grids: Philosophical Considerations," *Technology and Society Magazine, IEEE*, vol. 31, pp. 34-43, 2012.
- [76] H. Mori and T. Yoshida, "Probabilistic distribution network expansion planning with multi-objective Memetic Algorithm," in *IEEE Canada Electric Power Conference*, 2008.
- [77] H. M. Nguyen, P. Schell, J.L. Lilien, "Quantifying the limits of weather based dynamic line rating methods," in *CIGRÉ Canada Conference on Power Systems*, Halifax, Canada, 2011.
- [78] L. Shuang, F. Mingtian, and Y. Fan, "Research on security standards of power supply in China and UK," in *Int. Conf. on Power System Technology, 2010*, 2010.
- [79] North American Electricity Reliability Corporation, 2012, 16/04/2013). Available: <http://www.nerc.com/>
- [80] M. A. Rios, D. S. Kirschen, D. Jayaweera, D. P. Nedic, R. N. Allan, "Value of Security: Modeling Time-Dependent Phenomena and Weather Conditions," *IEEE Trans. Power Syst.*, vol. 17, pp. 543-548, 2002.
- [81] M. Papic, K. Awodele, R. Billinton, C. Dent, D. Eager, G. Hamoud, *et al.*, "Overview of Common Mode outages in power systems," in *IEEE Power and Energy Society General Meeting*, 2012, San Diego, California, USA.
- [82] B. Stott, O. Alsac, A. J. Monticelli, "Security analysis and optimization," *Proc. IEEE*, vol. 75, pp. 1623-1644, 1987.
- [83] D. T.-C. Wang, L. F. Ochoa, G. P. Harrison, "DG Impact on Investment Deferral: Network Planning and Security of Supply," *IEEE Trans. on Power Syst.*, vol. 25, pp. 1134-1141, 2010.
- [84] T. E. Dugan, T. E. McDermott, G. J. Ball, "Planning for distributed generation," *IEEE Ind. Appl. Mag.*, vol. 7, pp. 80-88, 2001.
- [85] V. H. Mendez, Rivier, J., de ka Feunte, J. I., Gomez, T., Arceluz, J., Marin, J., Madurga, A., "Impact of distributed generation on distribution investment deferral," *Int. J. Electric Power and Energy Systems* vol. 28, pp. 244-252, 2006.

- 
- [86] H. A. Gil, G. Joos, "On the quantification of the network capacity deferral value of distributed generation," *IEEE Trans. Power Syst.*, vol. 21, pp. 244-252, 2006.
- [87] G. P. Harrison, A. Piccolo, P. Siano, A. R. Wallace, "Exploring the trade-offs between incentives for distributed generation developers and DNOs," *IEEE Trans. on Power Syst.*, vol. 22, pp. 821-828, 2007.
- [88] National Grid, "Electricity Transmission Cost Study: How does the independent report compare to National Grid's view?," 2012.
- [89] *Security of Supply*, ENA ER P2/6, 2006.
- [90] G. Strbac, R. Moreno, D. Pudjianto, and M. Castro, "Towards a risk-based network operation and design standards," in *IEEE PES General Meeting*, 2011.
- [91] R. N. Allan, P. Djapic, and G. Strbac, "Assessing the Contribution of Distributed Generation to System Security," in *Int. Conf. on Probabilistic Methods Applied to Power Systems*, 2006, pp. 1-6.
- [92] Z. Zhu, J. Zhou, C. Yan, and L. Chen, "Power System Operation Risk Assessment Based on a Novel Probability Distribution of Component Repair Time and Utility Theory," in *Power and Energy Engineering Conference (APPEEC), 2012 Asia-Pacific*, 2012, pp. 1-6.
- [93] Y. Yi, R. G. Harley, D. Divan, and T. G. Habetler, "Overhead conductor thermal dynamics identification by using Echo State Networks," in *Int. Joint Conf. on Neural Networks*, 2009, pp. 3436-3443.
- [94] N. Hung Khanh, J. B. Song, and H. Zhu, "Demand side management to reduce Peak-to-Average Ratio using game theory in smart grid," in *IEEE Conference on Computer Communications Workshops*, 2012, pp. 91-96.
- [95] M. Bertinat, "Re-appraisal of ACE 104 - Stage 2: Methodology for determining probabilistic distribution ratings based on present load profiles," ea Technology, 2014.
- [96] A. Agüera-Pérez, J. C. Palomares-Salas, J. J. González de la Rosaa, and A. Moreno-Muñoz, "Spatial persistence in wind analysis," *J. Wind Engineering and Industrial Aerodynamics*, vol. 119, pp. 48-52, 2013.
- [97] P. Torres, J. van Wingerden, and M. Verhaegen, "Modeling of the flow in wind farms for total power optimization," in *9th IEEE Int. Conf. on Control and Automation*, 2011, pp. 963-968.

- 
- [98] S. Al-Yahyai, Y. Charabi, and A. Gastli, "Optimal micro-siting of small wind turbine using numerical simulation," in *7th IEEE GCC Conf. and Exhibition 2013*, pp. 28-32.
- [99] J. M. L. M. Palma, F. A. Castro, L. F. Ribeiro, A. H. Rodrigues, and A. P. Pinto, "Linear and nonlinear models in wind resource assessment and wind turbine micro-siting in complex terrain," *Journal of Wind Engineering and Industrial Aerodynamics*, vol. 96, pp. 2308-2326, 12// 2008.
- [100] A. Makridis and J. Chick, "Validation of a CFD model of wind turbine wakes with terrain effects," *J. Wind Engineering and Industrial Aerodynamics*, vol. 123, pp. 12-29.
- [101] L. Landberg, L. Myllerup, O. Rathmann, E. L. Petersen, B. H. Jørgensen, J. Badger, *et al.*, "Wind Resource Estimation—An Overview," *Wind Energy*, vol. 6, pp. 261-271, 2003.
- [102] E. Davakis, Varvayanni, P., Catsaros, N., "Diagnosis of wind flow and dispersion over complex terrain based on limited meteorological data," *Environmental Pollution*, vol. 103, 1998.
- [103] S. Mathew, *Wind energy: fundamentals, resource analysis and economics*: Springer-Verlag New York, 2006.
- [104] J.-F. Sini, S. Anquetin, and P. G. Mestayer, "Pollutant dispersion and thermal effects in urban street canyons," *Atmospheric Environment*, vol. 30, pp. 2659-2677, 8// 1996.
- [105] J. R. Garratt, *The Atmospheric Boundary Layer*: Cambridge University Press, 1992.
- [106] R. B. Stull, *An Introduction to Boundary Layer Meteorology*: Springer Netherlands, 1988.
- [107] D. M. Hargreaves and N. G. Wright, "On the use of the k- $\epsilon$  model in commercial CFD software to model the neutral atmospheric boundary layer," *J. of Wind Engineering and Industrial Aerodynamics*, vol. 95, pp. 355-369, 2007.
- [108] B. B. S. Massey and A. A. J. Ward-Smith, *Mechanics of Fluids*: Taylor & Francis, 2012.
- [109] J. H. Ferziger and M. Perić, *Computational methods for fluid dynamics*, Springer Berlin, 1996.
- [110] I. Troen and E. Lundtang Petersen, "European wind atlas," 1989.
- [111] J. Sumner, C. S. Watters, and C. Masson, "CFD in wind energy: the virtual, multiscale wind tunnel," *Energies*, vol. 3, pp. 989-1013, 2010.

- 
- [112] H.-G. Kim and V. C. Patel, "Test of turbulence models for wind flow over terrain with separation and recirculation," *Boundary-Layer Meteorology*, vol. 94, pp. 5-21, 2000.
- [113] H. G. Kim, V. C. Patel, and C. M. Lee, "Numerical simulation of wind flow over hilly terrain," *J. wind engineering and industrial aerodynamics*, vol. 87, pp. 45-60, 2000.
- [114] S. B. Pope, *Turbulent flows*: Cambridge university press, 2000.
- [115] U. Piomelli, "Wall-layer models for large-eddy simulations," *Progress in aerospace sciences*, vol. 44, pp. 437-446, 2008.
- [116] D. G. Blumberg and R. Greeley, "Field studies of aerodynamic roughness length," *J. Arid Environments*, vol. 25, pp. 39-48, 7// 1993.
- [117] H. Schlichting, K. Gertsen, *Boundary Layer Theory*, Springer, 2000.
- [118] B. Blocken, T. Stathopoulos, and J. Carmeliet, "CFD simulation of the atmospheric boundary layer: wall function problems," *Atmospheric Environment*, vol. 41, pp. 238-252, 1// 2007.
- [119] A. M. Endalew, M. Hertog, M. A. Delele, K. Baetens, T. Persoons, M. Baelmans, *et al.*, "CFD modelling and wind tunnel validation of airflow through plant canopies using 3D canopy architecture," *Int. J. Heat and Fluid Flow*, vol. 30, pp. 356-368, 4// 2009.
- [120] J. C. Lopes da Costa, F. A. Castro, J. M. L. M. Palma, and P. Stuart, "Computer simulation of atmospheric flows over real forests for wind energy resource evaluation," *J. Wind Engineering and Industrial Aerodynamics*, vol. 94, pp. 603-620, 8// 2006.
- [121] D. Hertwig, G. C. Efthimiou, J. G. Bartzis, and B. Leitl, "CFD-RANS model validation of turbulent flow in a semi-idealized urban canopy," *J. Wind Engineering and Industrial Aerodynamics*, vol. 111, pp. 61-72, 12// 2012.
- [122] N. Cressie and C. K. Wikle, *Statistics for Spatio-Temporal Data*, Wiley, 2011.
- [123] *WAsP – the Wind Atlas Analysis and Application Program*. Available: <http://www.wasp.dk/>, Accessed 08/10/2012
- [124] W. Weng, P. A. Taylor, and J. L. Walmsley, "Guidelines for airflow over complex terrain: model developments," *J. Wind Engineering and Industrial Aerodynamics*, vol. 86, pp. 169-186, 2000.
- [125] *ATmospheric, Meteorological and Environmental Technologies*. Available: <http://www.atmet.com/>, Accessed 08/10/2012.
-

- 
- [126] C. Meissner, K. Vogstad, A. Energi and U. W.-S. Horn, "Park optimization using IEC constraints for wind quality," in *EWEA Annual Event*, Brussels, Belgium, 2011.
- [127] *Ansys FLUENT*. Available: <http://www.ansys.com/Products/Simulation+Technology/Fluid+Dynamics/ANSYS+Fluent>, Accessed 08/10/2012.
- [128] D. Cabezon, Iniesta, A., Ferrerm E., Marti, I., "Comparing WASP and FLUENT for highly complex terrain and wind prediction," *Wind Energy*, Springer Berlin Heidelberg, 2007.
- [129] W. Pattanapol, S.J. Wakes, M.J. Hilton and K. J. M. Dickinson, "Modeling of Surface Roughness for Flow over a Complex Vegetated Surface," *World Academy of Science, Engineering and Technology*, vol. 32, pp. 273-281, 2007.
- [130] Astrium Geo-Information Services, 2014, *LiDAR Acquisition*. Available: <http://www.astrium-geo.com/sg/3254-lidar>, Accessed 04/02/2014
- [131] W. F. Chen, *Handbook of structural engineering*, CRC Press, 1997.
- [132] R. Peyret, *Handbook of computational fluid mechanics*, Elsevier Academic Pr, 1996.
- [133] P. J. Richards and R. P. Hoxey, "Appropriate boundary conditions for computational wind engineering models using the k- $\epsilon$  turbulence model," *J. Wind Engineering and Industrial Aerodynamics*, vol. 47, pp. 145-153, 1993.
- [134] P. J. Richards and S. E. Norris, "Appropriate boundary conditions for computational wind engineering models revisited," *J. Wind Engineering and Industrial Aerodynamics*, vol. 99, pp. 257-266, 2011.
- [135] Ansys, "ANSYS FLUENT 12.0 User's Guide," ed, 2009.
- [136] J. B. A. Bechmann, M.S. Courtney, H.E. Jørgensen, J. Mann and N.N. Sørensen., "The Bolund Experiment: Overview and Background.," Risø DTU, National Laboratory for Sustainable Energy Roskilde, Denmark, 2009.
- [137] J. Berg, J. Mann, A. Bechmann, M. Courtney, and H. Jørgensen, "The Bolund Experiment, Part I: Flow Over a Steep, Three-Dimensional Hill," *Boundary-Layer Meteorology*, vol. 141, pp. 219-243, 2011.
- [138] A. Bechmann, N. Sørensen, J. Berg, J. Mann, and P. E. Réthoré, "The Bolund Experiment, Part II: Blind Comparison of Microscale Flow Models," *Boundary-Layer Meteorology*, vol. 141, pp. 245-271, 2011.

- 
- [139] D. E. Weir, C. Meissner, A. R. Gravdahl, "CFD Validation: A Simple Approach," in *EWEA Annual Event*, Brussels, 2011.
- [140] P. A. Taylor and H. W. Teunissen, "The Askervein Hill project: Overview and background data," *Boundary-Layer Meteorology*, vol. 39, pp. 15-39, 1987.
- [141] National Grid, "Development near overhead lines," 2008.
- [142] UK Meteorological Office, "MIDAS land surface station data," 2006, available:  
[http://badc.nerc.ac.uk/view/badc.nerc.ac.uk\\_ATOM\\_dataent\\_ukmo-midas](http://badc.nerc.ac.uk/view/badc.nerc.ac.uk_ATOM_dataent_ukmo-midas).
- [143] G. Murphy, "Implementation of Real-Time Thermal Ratings," Scottish Power Energy Networks, 2013, available:  
[http://www.spenergynetworks.co.uk/userfiles/file/Final\\_Close\\_Down\\_Report\\_09-10-2013.pdf](http://www.spenergynetworks.co.uk/userfiles/file/Final_Close_Down_Report_09-10-2013.pdf).
- [144] *Loading and strength of overhead transmission lines*, IEC Standard 60826, 1991.
- [145] B. P. Hayes, I. Ilie, A. Porpodas, S. Z. Djokic, and G. Chicco, "Equivalent power curve model of a wind farm based on field measurement data," in *IEEE PowerTech*, 2011, Trondheim
- [146] F. E. Croxton, D. J. Cowden, and S. Klein, *Applied General Statistics*, Pritman, 1968.
- [147] D. M. Greenwood, G. L. Ingram, P. C. Taylor, S. C. Brown, and A. Collinson, "Network Planning Case Study Utilising Real-Time Thermal Ratings and Computational Fluid Dynamics," in *22<sup>nd</sup> Int. Conf. on Electricity Distribution*, Stockholm, 2013.
- [148] R. A. F. Currie, G. W. Ault, R. W. Fordyce, D. F. MacLeman, M. Smith, and J. R. McDonald, "Actively Managing Wind Farm Power Output," *IEEE Trans. Power Syst.*, vol. 23, pp. 1523-1524, 2008.
- [149] R. Billinton and R. N. Allan, *Reliability evaluation of power systems*: Pitman Advanced Publishing Program, 1984.
- [150] R. Billinton and L. Gan, "A Monte Carlo simulation model for adequacy assessment of multi-area generating systems," in *Third Int. Conf. on Probabilistic Methods Applied to Power Systems*, 1991, pp. 317-322.
- [151] A. Sankarakrishnan and R. Billinton, "Sequential Monte Carlo simulation for composite power system reliability analysis with time varying loads," *IEEE Trans. Power Syst.*, vol. 10, pp. 1540-1545, 1995.

- 
- [152] R. Billinton, R. Karki, G. Yi, H. Dange, H. Po, and W. Wangdee, "Adequacy Assessment Considerations in Wind Integrated Power Systems," *IEEE Trans. Power Syst.*, vol. 27, pp. 2297-2305, 2012.
- [153] W. Wangdee and R. Billinton, "Bulk electric system well-being analysis using sequential Monte Carlo simulation," *IEEE Trans. Power Syst.*, vol. 21, pp. 188-193, 2006.
- [154] G. Celli, E. Ghiani, G. G. Soma, and F. Pilo, "Active distribution network reliability assessment with a pseudo sequential Monte Carlo method," in *IEEE Int. Conf. on Power System Technology*, Trondheim, 2011.
- [155] Y. Gao and R. Billinton, "Adequacy assessment of generating systems containing wind power considering wind speed correlation," *IET Renewable Power Generation*, vol. 3, pp. 217-226, 2009.
- [156] R. Billinton, H. Chen, and R. Ghajar, "Time-series models for reliability evaluation of power systems including wind energy," *Microelectronics Reliability*, vol. 36, pp. 1253-1261, 1996.
- [157] D. C. Hill, D. McMillan, K. R. W. Bell, and D. Infield, "Application of Auto-Regressive Models to U.K. Wind Speed Data for Power System Impact Studies," *IEEE Trans. on Sustainable Energy*, vol. 3, pp. 134-141, 2012.
- [158] C. I. F. Agreira, S. M. F. de Jesus, S. L. de Figueiredo, C. M. Ferreira, J. A. D. Pinto, and F. P. M. Barbosa, "Probabilistic Steady-State Security Assessment of an Electric Power System Using A Monte Carlo Approach," in *Proc. 41st Int. Universities Power Engineering Conf.*, 2006, pp. 408-411.
- [159] H. Yu-Qing, P. Jian-Chun, S. Li, X. Chao, and L. Jing-Jing, "Reliability evaluation of electrical distribution system considering the random energy output of wind power generators," in *China Int. Conf. on Electricity Distribution*, 2012, pp. 1-8.
- [160] J. He, Y. Sun, D. S. Kirschen, C. Singh, and L. Cheng, "State-space partitioning method for composite power system reliability assessment," *IET Generation, Transmission & Distribution*, vol. 4, pp. 780-792, 2010.
- [161] Z. Kai, A. P. Agalgaonkar, K. M. Muttaqi, and S. Perera, "Distribution System Planning With Incorporating DG Reactive Capability and System Uncertainties," *IEEE Trans. Sustainable Energy*, vol. 3, pp. 112-123, 2012.
- [162] J. Mitra and X. Xufeng, "Composite system reliability analysis using particle swarm optimization," in *11th Int. Conf. on Probabilistic Methods Applied to Power Systems*, 2010, pp. 548-552.

- 
- [163] K. Moslehi and R. Kumar, "Smart Grid - a reliability perspective," in *Innovative Smart Grid Technologies*, 2010.
- [164] H. Wan, J. D. McCalley, and V. Vittal, "Increasing thermal rating by risk analysis," *IEEE Trans. Power Syst.*, , vol. 14, pp. 815-828, 1999.
- [165] G. Bowden, P. Barker, V. Shestopal, and J. Twidell, "The Weibull distribution function and wind power statistics," *Wind Engineering*, vol. 7, pp. 85-98, 1983.
- [166] L. Guo, C. X. Guo, W. H. Tang, and Q. H. Wu, "Evidence-based approach to power transmission risk assessment with component failure risk analysis," *IET Generation, Transmission & Distribution*, , vol. 6, pp. 665-672, 2012.
- [167] R. Billinton, R. Ghajar, F. Filippelli, and R. Del Bianco, "Transmission equipment reliability using the Canadian Electrical Association information system," in *Second Int. Conf. on the Reliability of Transmission and Distribution Equipment*, 1995, pp. 13-18.
- [168] R. Billinton, S. Kumar, N. Chowdhury, K. Chu, K. Debnath, L. Goel, *et al.*, "A reliability test system for educational purposes-basic data," *IEEE Trans. Power Syst., actions on*, vol. 4, pp. 1238-1244, 1989.
- [169] F. Miao, V. Vittal, G. T. Heydt, and R. Ayyanar, "Probabilistic Power Flow Studies for Transmission Systems With Photovoltaic Generation Using Cumulants," *IEEE Trans. Power Syst.*, vol. 27, pp. 2251-2261, 2012.
- [190] G. H. Golub and C. F. Van Loan, *Matrix Computations*, Johns Hopkins University Press, 1996.
- [171] S. C. E. Jupe, A. K. Kazerooni, G. Murphy, "De-Risking the Implementation of Real-Time Thermal Ratings," in *22nd Int. Conf. on Electricity Distribution*, Stockholm, 2013.
- [172] E. Cloet and J. I. Lilien, "Upgrading Transmission Lines through the use of an innovative real-time monitoring system," in *IEEE PES 12th Int. Conf. on Transmission and Distribution Construction, Operation and Live-Line Maintenance*, 2011.
- [173] S. Abbott, S. Abdelkader, L. Bryans, and D. Flynn, "Experimental validation and comparison of IEEE and CIGRE dynamic line models," in *45th Int. Universities Power Engineering Conference*, 2010.
- [174] F. Milano, "An Open Source Power System Analysis Toolbox," *IEEE Trans. Power Syst.*, vol. 20, pp. 1199-1206, 2005.
- [175] S.R. Blake, P.J. Davison, P.C. Taylor, D. Miller, and A. Webster, "Use of Real-Time Thermal Ratings to Increase Network Reliability under

- 
- Faulted Conditions," in CIGRÉ Regional South-East European Conf., Sibiu, Romania, 2012.
- [176] UKCP09 Climate Projections, 2011, UKCP09. Available: <http://ukclimateprojections.defra.gov.uk/> Accessed 20/02/2014
- [177] L. C. Cradden and G. P. Harrison, "Adapting overhead lines to climate change: Are dynamic ratings the answer?," *Energy Policy*, vol. 63, pp. 197-206, 2013.
- [178] D. M. H. Sexton and J. Murphy, "UKCP09: Probabilistic projections of wind speed," UKCP09 Climate Projections, 2010.
- [179] H. Hueging, R. Haas, K. Born, D. Jacob, and J. G. Pinto, "Regional Changes in Wind Energy Potential over Europe Using Regional Climate Model Ensemble Projections," *J. of Applied Meteorology & Climatology*, vol. 52, 2013.
- [180] D. J. Brayshaw, A. Troccoli, R. Fordham, and J. Methven, "The impact of large scale atmospheric circulation patterns on wind power generation and its potential predictability: A case study over the UK," *Renewable Energy*, vol. 36, pp. 2087-2096, 2011.
- [181] S. C. Pryor and R. J. Barthelmie, "Climate change impacts on wind energy: A review," *Renewable and sustainable energy reviews*, vol. 14, pp. 430-437, 2010.
- [182] E. Valor, V. Meneu, and V. Caselles, "Daily air temperature and electricity load in Spain," *J. applied Meteorology*, vol. 40, pp. 1413-1421, 2001.
- [183] A. Pardo, V. Meneu, and E. Valor, "Temperature and seasonality influences on Spanish electricity load," *Energy Economics*, vol. 24, pp. 55-70, 2002.
- [184] G. Franco and A. H. Sanstad, "Climate change and electricity demand in California," *Climatic Change*, vol. 87, pp. 139-151, 2008.
- [185] D. Coumou and S. Rahmstorf, "A decade of weather extremes," *Nature Climate Change*, vol. 2, pp. 491-496, 2012.
- [186] R. Billinton and J. R. Acharya, "Weather-based distribution system reliability evaluation," *IEE Proc. Generation, Transmission and Distribution*, vol. 153, pp. 499-506, 2006.
- [187] N. C. Abi-Samra, K. R. Forsten, and R. Entriken, "Sample Effects of extreme weather on power systems and components, part I: Sample effects on distribution systems," in *IEEE PES General Meeting*, 2010, 2010.

- [188] T. H. Mehr, M. A. S. Masoum, and N. Jabalameli, "Grid-connected Lithium-ion battery energy storage system for load leveling and peak shaving," in Australasian Universities Power Engineering Conf., 2013.
- [189] R. E. Kalman, "A new approach to linear filtering and prediction problems," J. basic Engineering, vol. 82, pp. 35-45, 1960.
- [190] J. W. Bialek, "Why has it happened again? Comparison between the UCTE blackout in 2006 and the blackouts of 2003," in IEEE Int. Conf. on Power System Technology, Lausanne, 2007, pp. 51-56.

Chapter 2,3,4,5,6,7,8 Cover Images Copyright <http://etc.usf.edu/clipart/>

## Appendix 1: CIGRÉ Ratings Code

```

function [ratings]=CIGRÉ_rating(Ws,Wd,T,Qsm,samples)

%Set Global Parameters
g = 9.807;
Dc=0.01953;
dw=0.00279;
R = 0.0001576;
TDesign = 50;
Dinner = 0.00837;
Douter = 0.01953;
Kr = 2;
Delta = 0.01;
a = 0.00403;
e = 0.9;
s = 5.6697 * 10 ^ -8;
Prandlt = 0.707625;
Densr = 0.998840672539926;
ni = 1.60025E-05;
l = 0.026324;
y=10;
alpha=0.5;

%Main Loop
for i=1:samples
    Idiff=1;
    Iass=100;
    Ta=T(i);
    v=Ws(i);
    SR=Qsm(i);
    tetag=Wd(i);
    %Set temperatures to K
    Ta=Ta+273.15;
    Tc=TDesign+273.15;
    Ts=Tc-10;
    while abs(Idiff) >= 0.1

        %Set conductor temperature limit
        Tf = ((Ta-273.15) + (Tc-273.15)) / 2;

        ni = 1.32e-5 + 9.5e-8 * (Tf);

        Prandlt = 0.715 - 2.5e-4 * (Tf);

        Densr = exp(-1.16e-4 * y);

        Rf = dw / (2 * (Dc - 2 * dw));
        l = 2.42e-2 + 7.2e-5 * (Tf);

        %Calculate Solar Heating
        Qs = alpha * SR * Douter;

        x=0;
        while abs(Ts-x)>0.01
            x = Ts;
            %Calculate Resistance

```

---

```

        Ts = Tc - ((Qs + (Iass ^ 2 * R * (1 + 0.00403 * ((Tc +
x)/2 - 293) / 2))) / (2 * pi * Kr)) * (0.5 - (Dinner ^ 2 / (Douter ^ 2
- Dinner ^ 2)) * log(Douter / Dinner));

end

Rt = R * (1 + a * ((Tc + Ts)/2 - 293));

%Calculate Radiative Cooling
Qr = pi * Douter * e * s * ((Ts)^4 - (Ta)^4);

%Calculate Convective Cooling
%Calculate Nusselt Number

tetar = tetag*pi/180;

        %Nusselt Natural
Gr = Douter ^ 3 * (Ts - Ta) * g / ((Tf+273) * ni ^ 2);
Pe = Prandlt * Gr;
    if Pe < 10 ^ 4
        A2 = 0.85;
        m2 = 0.188;
    else
        A2 = 0.48;
        m2 = 0.25;
    end
    NuNat = A2 * Pe ^ m2;

        %Nusselt Forced
if abs(sin(tetar))<0.406737
    A1 = 0.42;
    B2 = 0.68;
    m1 = 1.08;
else
    A1 = 0.42;
    B2 = 0.58;
    m1 = 0.9;
end

    Kangle = A1 + B2 * abs(sin(tetar)) ^ m1;

%reynolds
Re = Densr * v * Douter / ni;

    if Re < 2650
        B1 = 0.641;
        n = 0.471;
    else
        if Rf <= 0.05
            B1 = 0.178;
            n = 0.633;
        else
            B1 = 0.048;
            n = 0.8;
        end
    end

    NuForce = B1 * Re ^ n;
    NuAngle = NuForce * Kangle;

```

---

```

if v==0
    Nusselt=NuNat;
elseif v>=0.5
    Nusselt=NuAngle;
else
    %Nusselt Mixed

    tetag = 45;
    tetar = 0.785398163;

    A1 = 0.42;
    B2 = 0.58;
    m1 = 0.9;

    Kangle = A1 + B2 * sin(tetar) ^ m1;

    % reynolds
    Re = Densr * v * Doutr / ni;

    if Re < 2650
        B1 = 0.641;
        n = 0.471;
    else
        if Rf <= 0.05
            B1 = 0.178;
            n = 0.633;
        else
            B1 = 0.048;
            n = 0.8;
        end
    end
end

Nusselt = B1 * Re ^ n;

Nu45 = Nusselt * Kangle;
NuCor = NuAngle*0.55;

if NuCor<Nu45
    NuInterim = Nu45;
else
    NuInterim = NuCor;
end

if NuInterim <=NuNat
    NuMixed = NuNat;
else
    NuMixed = NuInterim;
end

Nusselt=NuMixed;

end

Qc = pi * l * (Ts - Ta) * Nusselt;
Idc = ((Qc + Qr - Qs) / Rt) ^ 0.5;
Iac = Idc / (1.0045 + 0.09e-6 * Idc) ^ 0.5;

```

```
        Idiff = Idc - Iass;  
        Iass = Idc;  
    end  
    ratings(i)=Iac;  
end  
end
```

## Appendix 2: Table of Confidence Values

		Persistence Time (Hours)															
		1	2	3	4	5	6	12	24	36	48	72	96	120	144	168	
<b>0%</b>	97.37%	97.29%	97.21%	97.07%	96.99%	96.86%	96.28%	94.46%	93.27%	91.40%	87.98%	83.75%	81.86%	79.93%	75.99%		
<b>10%</b>	94.35%	94.16%	93.92%	93.76%	93.49%	93.08%	91.56%	87.45%	85.05%	80.95%	73.81%	68.37%	61.54%	56.90%	50.78%		
<b>20%</b>	89.93%	89.41%	89.06%	88.59%	87.99%	87.46%	85.17%	79.33%	74.15%	67.99%	59.13%	51.13%	41.84%	36.04%	30.40%		
<b>30%</b>	83.96%	83.43%	82.77%	82.15%	81.41%	80.66%	77.15%	67.92%	61.74%	55.26%	45.24%	36.20%	26.17%	18.85%	14.70%		
<b>40%</b>	76.80%	76.19%	75.35%	74.57%	73.62%	72.96%	68.00%	57.97%	50.47%	43.67%	31.71%	21.66%	13.72%	9.25%	8.34%		
<b>50%</b>	68.77%	67.95%	67.13%	66.20%	65.40%	64.43%	58.49%	46.94%	37.94%	30.93%	20.28%	12.87%	9.77%	6.76%	6.36%		
<b>60%</b>	59.77%	59.05%	58.05%	57.02%	55.94%	54.97%	48.16%	35.61%	28.12%	22.22%	13.54%	9.33%	6.26%	5.46%	5.48%		
<b>70%</b>	51.12%	50.26%	49.32%	48.07%	46.94%	46.04%	39.43%	28.47%	22.26%	16.00%	8.81%	5.57%	4.30%	3.89%	3.93%		
<b>80%</b>	42.61%	41.81%	40.98%	39.81%	38.69%	37.82%	31.51%	22.77%	16.45%	12.19%	6.61%	4.71%	3.18%	3.16%	2.69%		
<b>90%</b>	35.24%	34.43%	33.48%	32.47%	31.57%	30.82%	25.33%	17.21%	12.42%	8.65%	4.88%	3.50%	2.31%	1.56%	1.08%		
<b>100%</b>	28.00%	27.33%	26.55%	25.61%	24.94%	24.01%	19.13%	12.50%	8.76%	5.18%	3.27%	2.76%	1.89%	1.55%	1.08%		

Table A2.1: Confidence values corresponding to varying Tm and Contribution to Security

## Appendix 3: Risk and Confidence Analysis Method

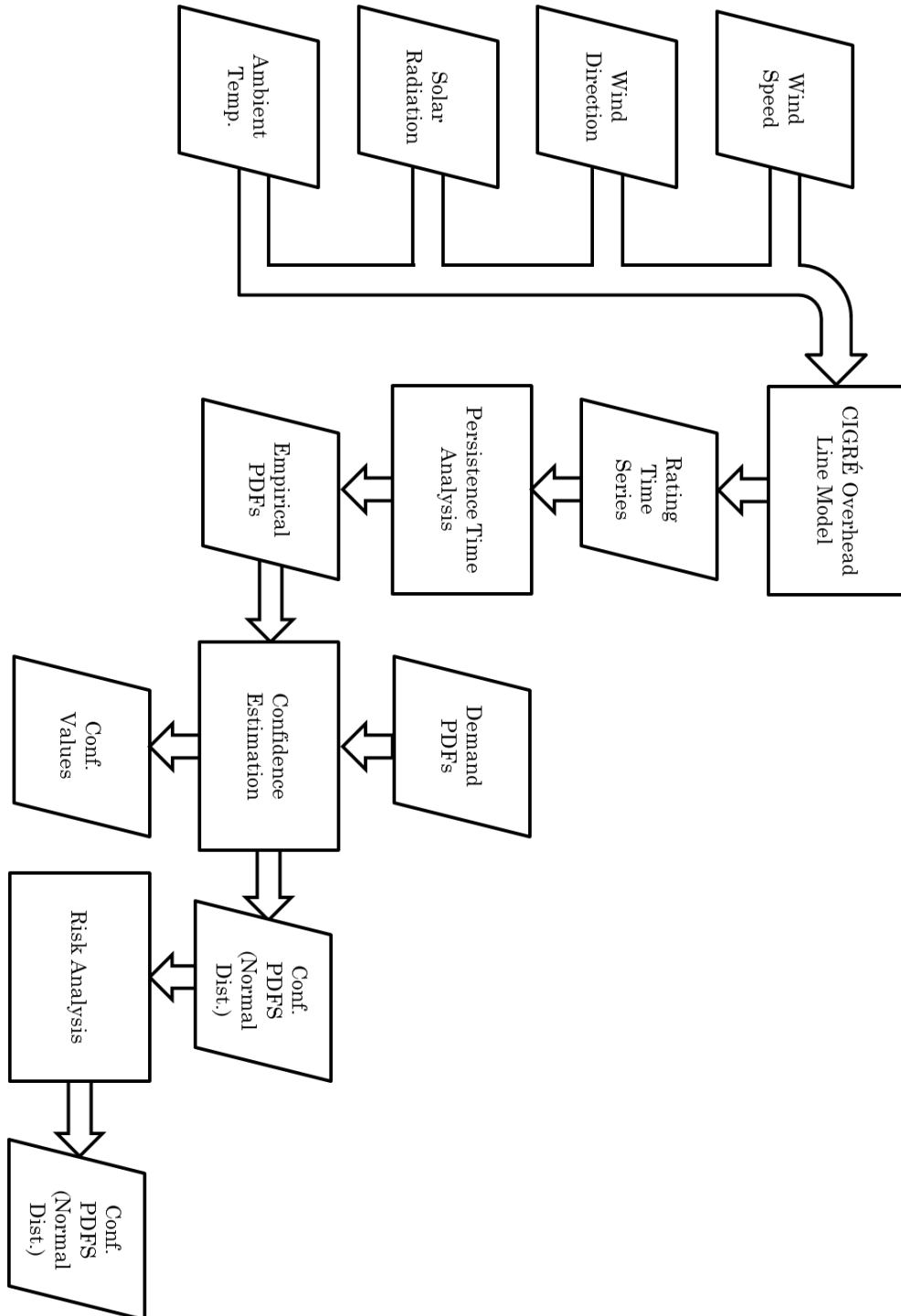


Figure A3.1: A flow chart showing the details of the data and analysis used to calculate the confidence and risk values in Chapter 3